U.S. DEPARTMENT OF COMMERCE
National Technical Information Service

PB-284 828

Evaluating and Optimizing Electron Microscope Methods for Characterizing Airborne Asbestos

IIT Research Inst, Chicago, Ill

Prepared for

Environmental Sciences Research Lab, Research Triangle Park, N C

Jun 78

EPA-600/2-78-038
June 1978

PB 284 828

Environmental Protection Technology Series

EVALUATING AND OPTIMIZING ELECTRON MICROSCOPE METHODS FOR CHARACTERIZING AIRBORNE ASBESTOS

REPRODUCED BY
NATIONAL TECHNICAL
INFORMATION SERVICE
U. S. DEPARTMENT OF COMMERCE
SPRINGFIELD, VA. 22161

Environmental Sciences Research Laboratory
Office of Research and Development
U.S. Environmental Protection Agency
Research Triangle Park, North Carolina 27711

193

RESEARCH REPORTING SERIES

Research reports of the Office of Research and Development, U S. Environmental Protection Agency, have been grouped into nine series. These nine broad categories were established to facilitate further development and application of environmental technology. Elimination of traditional grouping was consciously planned to foster technology transfer and a maximum interface in related fields. The nine series are:

1. Environmental Health Effects Research
2. Environmental Protection Technology
3. Ecological Research
4. Environmental Monitoring
5. Socioeconomic Environmental Studies
6. Scientific and Technical Assessment Reports (STAR)
7. Interagency Energy-Environment Research and Development
8. "Special" Reports
9. Miscellaneous Reports

This report has been assigned to the ENVIRONMENTAL PROTECTION TECHNOLOGY series. This series describes research performed to develop and demonstrate instrumentation, equipment, and methodology to repair or prevent environmental degradation from point and non-point sources of pollution. This work provides the new or improved technology required for the control and treatment of pollution sources to meet environmental quality standards.

This document is available to the public through the National Technical Information Service, Springfield, Virginia 22161.

TECHNICAL REPORT DATA
(Please read Instructions on the reverse before completing)

1. REPORT NO.
EPA 600/2-78-038

2.

3. RECIPIENT'S ACCESSION NO.
PB284828

4. TITLE AND SUBTITLE
EVALUATING AND OPTIMIZING ELECTRON MICROSCOPE
METHODS FOR CHARACTERIZING AIRBORNE ASBESTOS

5. REPORT DATE
June 1978

6. PERFORMING ORGANIZATION CODE

7. AUTHOR(S)
A.V. Samudra, F.C. Bock, C.F. Harwood, and J.D. Stockham

8. PERFORMING ORGANIZATION REPORT NO.

9. PERFORMING ORGANIZATION NAME AND ADDRESS
IIT Research Institute
10 West 35th Street
Chicago, Illinois 60616

10. PROGRAM ELEMENT NO.
1AD712 BA-14 (FY-77)

11. CONTRACT/GRANT NO.
68-02-2251

12. SPONSORING AGENCY NAME AND ADDRESS
Environmental Sciences Research Laboratory - RTP, NC
Office of Research and Development
U. S. Environmental Protection Agency
Research Triangle Park, N. C. 27711

13. TYPE OF REPORT AND PERIOD COVERED
Final Report 6/75-6/77

14. SPONSORING AGENCY CODE
EPA/600/09

15. SUPPLEMENTARY NOTES
This report complements EPA Report 600/2-77-178 entitled "Electron Microscope Measurement of Airborne Asbestos Concentrations -- A Provisional Methodology Manual"

16. ABSTRACT

Evaluation of EM methods for measuring airborne asbestos fiber concentrations and size distributions was carried out by studying a large number of variables and subprocedures in a five-phase program using elaborate statistically designed experiments. Observations were analyzed by advanced regression techniques to evaluate the effects of independent variables and subprocedures. It was shown that the optimized method for estimating airborne chrysotile should have the following features: (a) collecting an air sample on Nuclepore filter; (b) coating the Nuclepore filter with carbon; (c) transferring the particulate deposit to a 200-mesh electron microscope grid using chloroform in a modified Jaffe-wick washer; (d) examining the grid at about 10,000 x magnification (20,000 x for counting very fine fibers); (e) counting fibers using a field of view method; and (f) identifying the type of asbestos from morphology and selected area electron diffraction.

A provisional manual of instructions was prepared (EPA Report 600/2-77-178) and six independent laboratories participated in an interlaboratory test of the proposed method using two air samples. One of these was prepared at IITRI from pure aerosolized UICC chrysotile, and the other was an ambient air sample collected by IITRI personnel in a factory processing asbestos. Intercomparison of the results from the separate laboratories yielded some preliminary estimates of the precision and accuracy of the provisional method.

17. KEY WORDS AND DOCUMENT ANALYSIS

a. DESCRIPTORS		b. IDENTIFIERS/OPEN ENDED TERMS	c. COSATI Field/Group
*Air pollution	*Electron microscopy	Chrysotile	13B
*Asbestos	*Electron diffraction		08G
*Serpentine			11E
*Amphiboles			14B
Measurement			

18. DISTRIBUTION STATEMENT RELEASE TO PUBLIC	19. SECURITY CLASS *(This Report)* UNCLASSIFIED	21. NO. OF PAGES 198
	20. SECURITY CLASS *(This page)* UNCLASSIFIED	22. PRICE PCA09 / MF A01

EPA Form 2220-1 (Rev. 4-77) PREVIOUS EDITION IS OBSOLETE

EPA 600/2-78-038
June 1978

EVALUATING AND OPTIMIZING ELECTRON MICROSCOPE METHODS FOR CHARACTERIZING AIRBORNE ASBESTOS

by

A.V. Samudra, F.C. Bock, C.F. Harwood, and J.D. Stockham
IIT Research Institute
Chicago, Illinois 60616

Contract No. 68-02-2251

Project Officer

Jack Wagman
Director, Emissions Measurement and Characterization Division
Environmental Sciences Research Laboratory
Research Triangle Park, North Carolina 27711

ENVIRONMENTAL SCIENCES RESEARCH LABORATORIES
OFFICE OF RESEARCH AND DEVELOPMENT
U. S. ENVIRONMENTAL PROTECTION AGENCY
RESEARCH TRIANGLE PARK, N. C. 27711

1b

DISCLAIMER

This report has been reviewed by the Environmental Sciences Research Laboratory, U. S. Environmental Protection Agency, and approved for publication. Approval does not signify that the contents necessarily reflect the views and policies of the U. S. Environmental Protection Agency, nor does mention of trade names or commercial products constitute endorsement or recommendation for use.

FOREWARD

The occurrence of asbestos or asbestiform minerals as pollutants in the ambient air and in supplies of food and drinking water has caused considerable concern because occupational exposures to these fibrous materials have been found to induce mesothelioma of the pleura and peritoneum, as well as cancer of the lung, esophagus, and stomach, after latent periods of about 20 to 40 years.

Electron microscopy is currently the principal technique used to identify and characterize asbestos fibers in ambient air and water samples. Because of the poor sensitivity and specificity of conventional bulk analytical methods, electron microscopy is also being used for routine measurement of airborne or waterborne asbestos concentrations. The several laboratories that perform such analyses generally have reasonable internal self consistency. However, interlaboratory comparisons have shown that the results obtained by the separate laboratories are often widely different.

In recognition of this problem, the Environmental Sciences Research Laboratory, U. S. Environmental Protection Agency, initiated a comprehensive two-year study (June 1975 - June 1977) through EPA Contract No. 68-02-2251 to evaluate the various electron microscope procedures currently used for the measurement of airborne asbestos concentrations. The scope of work included the development of an optimum procedure incorporating the best features of current methods together with whatever improvements in sample collection, specimen preparation, and electron microscope examination that seem desirable for enhancement of accuracy and precision and for reduction of analysis time and cost.

A manual entitled "Electron Microscope Measurement of Airborne Asbestos Concentrations -- A Provisional Methodology Manual" describing an optimized method resulting from this study has been published as EPA Report 600/2-78-178 (August 1977). This final report contains a detailed account of the investigation and the experimental data supporting the provisional methodology.

Jack Wagman
Project Officer

A. Paul Altshuller
Director

Environmental Sciences
Research Laboratory
Research Triangle Park, N.C.

ABSTRACT

Electron microscopy is currently the principal technique used to identify and characterize asbestos* fibers** in ambient air and water samples. Variations in instrument capabilities, operator proficiency, and the myriad of techniques used in microscopy laboratories have resulted in wide data scatter. Under Contract No. 68-02-2251, a research program was initiated to evaluate the electron microscope methods and subprocedures currently in use at different laboratories to measure airborne asbestos fiber concentrations and develop a composite procedure that would minimize the variability of results.

Other objectives of the program were to provide a handbook describing the optimized method and to test the ruggedness of the optimized method through interlaboratory analyses.

A five-phase program of statistically designed experiments was used to evaluate 19 major independent variables and 50 subprocedures (or variable levels). The data from transmission and scanning electron microscopy examination were analyzed by statistical techniques to evaluate the effects of the independent variables and subprocedures on two major dependent variables, asbestos fiber number and mass concentrations. Multiple criteria were used to select the independent variable levels for the optimized procedure.

The optimized method for estimating the concentration of asbestos fibers in ambient air samples has the following features:

1. Use polycarbonate membrane filters to collect ambient air samples.
2. Coat the polycarbonate filter with a thin layer of carbon to lock-in the collected fibers.

---

* Asbestos is used as a collective term for the six minerals: chrysotile, amosite, crocidolite, and the asbestiform varieties of anthophyllite, actinolite, and tremolite.

** The term fiber is used for a particle with an aspect ratio of 3:1 or greater, and with substantially parallel sides.

3. Transfer the collected fibers to 200 mesh electron microscope grids in a modified Jaffe washer using chloroform to dissolve the filter.

4. Examine the grids in a transmission electron microscope (TEM) at a screen magnification of 16,000X.

5. Identify and characterize each fiber from its morphology and selected-area electron diffraction (SAED) pattern. Place the fibers into three categories: chrysotile, amphibole, and non-asbestos.

6. Enumerate the number of asbestos fibers using the field-of-view method. If mass concentration information is needed, measure the length and width of each fiber and compute the mass from the fiber volume and density data.

A manual describing the optimized method was prepared and reviewed by six independent laboratories. The manual was subsequently published as Environmental Protection Agency Technology Series Document EPA-600/2-77-178, "Electron Microscope Measurement of Airborne Asbestos Concentrations - A Provisional Methodology Manual", August, 1977.

The ruggedness of the optimized method was tested by the six laboratories. These laboratories used the method to analyze two filters upon which airborne asbestos fibers had been deposited and were carbon coated to prevent loss of the fibers. One sample was prepared by sampling pure UICC chrysotile that was aerosolized into a large chamber. The second sample was collected from the air inside an industrial plant processing asbestos. These samples were labeled "Lab" and "Field" sample, respectively.

The interlaboratory studies showed the average precision of chrysotile fiber concentration estimates, as determined by the ratio of the standard error of the mean to the mean expressed as a percentage, was about 21% for both the lab and field samples. The average precision of chrysotile mass concentration estimates was 22% for the lab sample and 44% for the field sample when ashing of the filter was used as a subprocedure. When ashing was not used, the average precision for the field sample was 54%. The lower precision of the chrysotile mass concentration estimates for the field sample is attributed to the presence of a few large bundles of fibers. These few bundles do not affect the number concentration estimates but significantly influence mass estimates. As a result, it is suggested that fiber bundles greater than 1 μm^3 should be reported separately.

The accuracy of the transmission electron microscope procedure for estimating the mass concentration of chrysotile was determined by comparing the computed mass from fiber volume and density data with the computed mass calculated from the magnesium concentration obtained by x-ray fluorescence spectrometry (XRF). A chrysotile fiber density of 2.6 g/cm^3 was used to compute fiber mass from size data. A factor of 3.8 times the magnesium concentration was used to determine chrysotile fiber mass by XRF. For the lab sample, the mass estimates for chrysotile agreed within 10%. For the field sample, the mass estimate obtained by electron microscopy was a factor 4.2 less than that obtained by XRF. The difference is attributed to the presence of fiber bundles and other sources of magnesium in the field sample.

Testing of the subprocedure that incorporates ashing, resuspension, ultrasonification, and refiltering of the lab and field samples gave inconclusive results. The mean fiber lengths were decreased by the ashing subprocedure and fiber concentration estimates were significantly increased (4-8 times higher for ashed sample than the unashed). The data cannot resolve whether the apparent increase in fiber concentration in the ashed sample results from fiber breakage or results from less interference in observing and identifying small fibrils in the diluted ashed sample. It is suggested that the ashing subprocedure should be used only when the direct transfer method is not suitable.

This report is submitted in fulfillment of EPA Contract No. 68-02-2251, IITRI Project No. C6351, by IIT Research Institute under sponsorship of the Environmental Protection Agency. This report covers the period July, 1975, to June, 1977.

CONTENTS

Foreword iii
Abstract iv
Figures ix
Tables xii
Acknowledgments xv

1. Introduction 1
2. Conclusions 3
3. Recommendations. 6
4. Scope of the Work 8
    Introduction 8
    Strategy 9
5. Statistically Designed Experimental Plans 17
    Introduction 17
    Five phase program. 18
6. Experimental Work. 28
    The preparation of laboratory filters of controlled asbestos loading in Phase 1 28
    Sample preparation for TEM 34
    Examining samples in transmission electron microscope 34
    Data recording 36
    Experimental work in Phase 2: Study of fiber identification method. 36
    Experimental work in Phase 3: Evaluating a TEM and an SEM . . 37
    Experimental work in Phase 4: Ashing and sonification 40
    Experimental work in Phase 5: Study of direct drop method . . 44
7. Results and Discussion of Phase 1 45
    Introduction 45
    Criteria selected 45
    Summary of Phase 1 results 45
    Statistical distribution tests 47
    Mass concentration estimates 67
8. Results and Discussion of Phases 2, 3, 4 and 5 70
    Phase 2 results 70
    Results and discussion of Phase 3 87
    Phase 4 results 90
    Statistical analysis of Phase 5 data 104
9. Provisional Optimized Method and Round-Robin Testing 109
    Preparing calibration filters 109
    Final choice of samples for round-robin test 110
    Independent estimate of chrysotile mass concentrations 111

CONTENTS (continued)

10. Results and Discussion of Round-Robin Tests 113
  - Poisson distribuiton tests 113
  - General procedures 115
  - Interlaboratory comparisons 121
  - Graphical representation of results 125
  - Accuracy and precision of estimates 125
  - Effect of ashing, ultrasonification, and reconstitution 137
  - Conclusions 145

References 147

Appendices

A. The Experiment Design for Phase 1 152
B. Regression Analysis 157
C. Poisson Distribution Tests 166
D. Optimized Method for Measurement of Airborne Asbestos Concentrations 175
E. Estimating Chrysotile Mass on Air Filters Using Neutron Activation Technique 177
F. X-Ray Fluorescence Analysis of Standard Samples of Chrysotile . . . 179

FIGURES

Number		Page
1	Flow chart of electron microscope procedures for estimating size distribution and concentration of airborne asbestos	10
2	(a) Top view and size view of aerosol chamber showing location of apparatus. (b) Flow diagram of aerosol generator	30
3	Graphical presentation of performance equation 9 in Phase 1. Net contribution to square root of fiber concentration (no. of all fibers/cm^3 of air).	59
4	Graphical presentation of performance equation 9 in Phase 1. Net contribution of square root of fiber concentration (no. of all fibers/cm^3 of air).	60
5	Graphical presentation of performance equation 10 in Phase 1. Net contribution to natural log of mass concentration of all fibers, $\mu g/m^3$ of air.	61
6	Graphical presentation of performance equation 10 in Phase 1. Net contribution to natural log of mass concentration of all fibers, $\mu g/m^3$ of air.	62
7	Estimated number concentration of chrysotile fibers in the nine Phase 2 samples (standard classification method), with 95% confidence intervals	82
8	Estimated mass concentration of chrysotile fibers in Phase 2 (standard and alternative classification methods) in relation to filter composition, transfer method, and identification technique, with 90% confidence intervals.	83
9	Estimated geometric mean length of chrysotile fibers in Phase 2 (standard classification method) in relation to filter composition and transfer method, with 90% confidence intervals.	84
10	Estimated percent of all Phase 2 fibers that were exceptional (ambiguous or other by the standard classification method) in relation to transfer method and identification technique, with 90% confidence intervals.	85
11	Graphical presentation of performance equation 6 in Phase 4. Net contribution to square root of fiber concentration, $10^6/cm^2$ of filter.	97

FIGURES (continued)

Number		Page
12	Graphical presentation of performance equation 9 in Phase 4. Net contribution to mean log of fiber length (μm)	98
13	Graphical presentation of performance equation 1 in Phase 5. Net contribution to square root of fiber concentration (10^6 fibers/cm^2) .	108
14	90% confidence intervals (inner) and 95% confidence intervals on the mean fiber number concentration	117
15	95% confidence intervals about the means in laboratory air sample 154 (see Tables 42 and 45).	126
16	95% confidence intervals about the means in field air sample 661 (see Tables 43 and 46), ashed samples only	127
17	95% confidence intervals about the means in field air sample 661 (see Tables 44 and 47), unashed samples only	128

TABLES

Number Page

1 Procedural Variables of Electron Microscope Method. 11

2 Independent Variables Selected for Evaluation in This Study 15

3 Representative Dependent Variables in Phase 1 19

4 Independent Variables, Phase 1. 20

5 Phase 1 Experiment Design (Compact Notation). 21

6 Phase 1 Experimental Plant (Long Notation). 22

7 Phase 2 Experiment Design 24

8 Phase 3 Experiment Design 25

9 Phase 4 Experiment Design 26

10 Phase 5 Experiment Design 27

11 Experimental Scheme for Simulated Air Samples for Phase 1 35

12 Scheme of Electron Microscope Parameters for Fiber Identification Methods in Phase 2. 38

13 Details of the Ashing Parameters Used in Phase 4. 42

14 Summary of Phase 1 Data 46

15 Tests for Applicability of the Poisson Distribution to Number of Fibers Per Field. 48

16 Variable Level Frequency Distribution in Two Groups 50

17 Precision in Fiber Count Per Field as a Criterion for Optimizing. . . 53

18 Variable Level Frequency Distribution in Two Group. 54

19 Dependent Variables, Phase 1. 57

20 Signs of Coefficients of Independent Variables in Performance Equations, Phase 1. 58

TABLES (continued)

Number Page

21 Optimization of Variable Levels According to Four Different Criteria 66

22 Estimates of Number and Mass Concentration of All Fibers Per Unit Volume of Air, Phase 1 68

23 Numbers of Fibers Observed and Classified, Phase 2 Samples 72

24 Concentrations of Chrysotile Fibers, Phase 2 Samples 73

25 Size Distributions of Chrysotile Fibers, Phase 2 Samples 74

26 Concentrations of All Fibers and of Fibers of "Ambiguous" and "Other" Categories, Phase 2 Samples 75

27 Phase 2 Regression Equations 78

28 Properties of Phase 2 Regression Equations 79

29 Summary of Phase 3 Data 88

30 Difference in Number of Chrysotile Fibers Counted When Same Grid Openings are Observed Under SEM and Convensional TEM Mode in JEOL 100C 91

31 Estimating Chrysotile Asbestos in Phase 4 Samples (Ashing and Sonification Experiments) 92

32 Size Distribution Characteristics of Chrysotile Fibers in Phase 4 Samples (Ashing and Sonification Experiments) 93

33 Values of Dependent Variables in Phase 4 95

34 Means and Standard Deviations of Dependent Values in Phase 4 96

35 Regression Equations in Phase 4 96

36 Characteristics of Fiber Length in Cumulative Distribution in Phase 4 100

37 Characteristics of Fiber Width in Cumulative Distribution in Phase 4 101

38 Values of Dependent Variables in Phase 5 105

39 Fiber Number and Mass Concentration in Phase 5 106

40 Tests for Applicability of the Poisson Distribution to Number of Fibers Per Field 114

TABLES (continued)

Number Page

41 Mean Values and Lower and Upper Limits of Fiber Concentration Estimate According to Poisson Distribution. 116

42 Summary of Round-Robin Test Results on Air Sample 154 118

43 Summary of Round-Robin Test Results on Field Sample 661 (All Samples Ashed). 119

44 Summary of Round-Robin Test Results on Field Sample 661 (All Samples Analyzed Without Ashing). 120

45 95% Confidence Intervals on the Mean Estimates for Individual Operators in Air Sample 154 (See Table 42). 122

46 95% Confidence Intervals on the Mean Estimates for Individual Operators in Field Air Sample 661 (See Table 42) (Ashed Samples Only) 123

47 95% Confidence Intervals on the Mean Estimates for Individual Operators in Field Air Sample 661 (See Table 44) (Unashed Samples Only) 124

48 Precision of Fiber Concentration Estimates on Laboratory Air Sample 154. 130

49 Precision of Fiber Concentration Estimates of Field Sample 661 (All Samples Ashed). 132

50 Precision of Fiber Concentration Estimates of Field Sample 661 (Unashed) 133

51 Precision of Different Measurements in the Two Samples. 134

52 Effect of a Few Large Bundles on Number Concentration and Mass Concentration of Chrysotile in Field Sample 661 136

53 Effect of Low Temperature Ashing and Reconstitution of Fiber Concentration Estimates 138

54 Effect of Low Temperature Ashing and Reconstitution of Mean Fiber Dimensions. 139

55 Length Distribution in Ashed and Unashed Samples, Data from Operator Number 2 141

56 Length Distribution in Ashed and Unashed Samples, Data from Operator Number 4 142

TABLES (continued)

Number Page

57 Length Distribution in Ashed and Unashed Samples, Data from Operator Number 5 143

58 Length Distribution in Ashed and Unashed Samples, Data from Operator Number 6 144

ACKNOWLEDGMENTS

The authors gratefully acknowledge the expert technical support of several colleagues. Meticulous work in preparing simulated air samples in our laboratory by Mr. David R. Jones deserves a special mention. The assistance of Mr. Jones and Mr. George Yamate in electron microscopy work is also acknowledged. Prompt secretarial effort of Miss Elaine Brown and Miss Bonnie Fitzpatrick is duly acknowledged.

Acknowledgments are also due to Dr. Philip Cook of EPA, Duluth, MN, Mr. J. M. Long of EPA, Athens, GA, Mr. John Miller of EPA, Research Triangle Park, NC, Dr. Ralph Zumwalde of NIOSH, Cincinnati, OH, Dr. Edward Peters of A.D. Little, Cambridge, MA, and Miss Wendy Dicker of Ontario Ministry of Environment, Toronto, Canada, for reviewing the methodology manual and for participating in the round-robin test of air samples.

Finally, the authors thank Dr. Jack Wagman of the Environmental Protection Agency, Research Triangle Park, NC, for his continued interest and encouragement.

SECTION 1

INTRODUCTION

The association of asbestos microfibers with adverse health effects prompted various governmental agencies and private industries to consider the electron microscope for characterizing microfibers in air. The choice of the electron microscope is ideal because of its ability to detect very fine fibers, estimate the size and shape, and identify each fiber from morphology and electron diffraction supplemented, in some instances, by energy-dispersive X-ray analysis. No other instrument matches the modern analytical electron microscopes in overall capabilities. The information gained on the quantity of fibers and their characteristics in given localities can be utilized to understand the significance of fiber exposure in terms of health hazard.

Unfortunately, because of the recent and rapid utilization of electron microscopes for quantifying fiber concentration levels, there is no standard methodology. In general, many different techniques and procedures have been used to collect samples, prepare samples for electron microscopy, examine the samples in the electron microscope, and interpret and evaluate the results. As a consequence, the various laboratories performing the asbestos characterization in air samples have reasonable intralaboratory agreement; but, interlaboratory agreement is totally unacceptable. This wide variability in results of electron microscope studies makes the technique unacceptable in a court-of-law, and the electron microscope results are generally treated as order-of-magnitude estimates for broad comparisons only. Since this is a serious limitation on a powerful tool, it is very important to understand the sources of this variation and minimize or eliminate the variation by appropriate optimization.

The U.S. Environmental Protection Agency realized the need for the development of an optimum methodology, particularly with respect to asbestos in air because of its known association with cancer. The present study at IIT Research Institute, directed at developing an optimum analytical methodology for determining asbestos* fibers** in the ambient air, uses statistically designed experimental techniques for simultaneous evaluation of a large number of independent variables and subprocedures. As stated in the scope of work, the investigation included "the development of an electron microscope procedure incorporating the best features of the current methods together with whatever improvements in sample collection, specimen preparation, and electron microscope examination seem desirable for enhancement of accuracy and precision and reducing analysis time and cost." The optimum procedure sought in this study is one that yields maximum information on asbestos fiber characteristics in the airborne state (from studying fibers collected on suitable filters), including fiber count and size distribution, as well as mass concentration.

---

* Asbestos is used as a collective term for the six minerals: chrysotile, amosite, crocidolite, anthophyllite, actinolite, and tremolite.

** The term fiber is used for a particle with an aspect ratio of 3:1 or greater, and with substantially parallel sides.

SECTION 2

CONCLUSIONS

The major conclusions drawn from the statistically designed experiments and the interlaboratory investigations are itemized below.

1. The optimized method for characterizing the asbestos levels in ambient air samples by electron microscopy is summarized as follows:

    a. Collect ambient air samples for asbestos analysis on 0.4 μm pore size polycarbonate membrane filters.

    b. Secure the collected fibers to the filter as soon as possible after collection by vapor depositing a 40 nm thick layer of carbon on the filter.

    c. Transfer the collected fibers to an electron microscope grid by dissolving the filter in a Jaffe washer using chloroform as a solvent.

    d. Place the electron microscope grid in a transmission electron microscope (TEM) and observe the fibers at a magnification of 20,000X (screen magnification 16,000X). A lower magnification, about 10,000X, is adequate for samples containing predominently amphibole asbestos fibers or where the aim is to assess the total mass of the asbestos fibers and the detection of very small fibers is unimportant.

    e. Identify and characterize the observed fibers by their morphology and selected area electron diffraction pattern. Use energy dispersive X-ray spectroscopy, if available, to aid in the classification of fibers not classified by SAED. The ED X-ray technique is particularly useful for characterizing amphibole asbestos minerals that exhibit indistinguishable electron diffraction patterns.

    f. Enumerate the asbestos fibers using the field-of-view method for medium and high fiber loading levels and the full-grid opening method for low loading levels. If mass concentration data are needed, measure the length and width of each fiber and compute the mass from the fiber volume and density.

2. The identification of fibers based on morphology and electron diffraction, as proposed by the optimized method, is adequate for classifying fibers into three categories: chrysotile, amphibole asbestos,

and other minerals. This identification scheme provides the largest amount of information for the analysis time; it is 2 to 3 times faster than methods involving X-ray analysis. Thus, the proposed methodology is cost effective.

3. The subprocedure of ashing, ultrasonification, and refiltration of the collected material is not recommended despite the lack of strong evidence to show the subprocedure is detrimental. Ashing decreases the fiber lengths. This should result in an increase in the number of fibers; but, the fiber number concentrations of ashed and unashed samples were statistically equivalent in Phase 4 data. In the interlaboratory tests, however, ashing subprocedure gave decreased fiber length and increased fiber number concentration, as compared with the unashed sample. The data could not resolve whether the apparent increase in fiber number concentration in the ashed sample resulted from fiber breakage or from reduced interference in detecting and identifying small fibrils of chrysotile. It is suggested that ashing be reserved for those instances where the TEM grids prepared by the optimized method are unsuited for analysis. These instances include those where fiber loadings are high and dilution is necessary and where the presence of organic matter obscures the observation of the fibers.

4. The presence of a few large bundles of fibers strongly influence mass concentration estimates but has no significant effect on number concentration estimates. To circumvent the effect of bundles, it is suggested that bundles greater than 1 μm^3 be counted as single entities. These bundles should be reported separately and, if mass information is needed, a significant number of bundles should be counted and sized.

5. The conventional transmission electron microscope is superior to the scanning electron microscope for detecting and identifying chrysotile fibrils. The superiority results from the higher resolution and the stationary image in the TEM.

6. Samples of airborne chrysotile prepared in the laboratory and analyzed by several laboratories using the optimized procedure showed good precision and accuracy. The ratio of the spread between the 95% confidence limits to the mean value was about 0.48 for chrysotile fiber number concentration and about 0.40 for chrysotile mass concentration. The mass concentration computed from size and density data compared favorably with the mass estimate obtained by X-ray fluorescence.

7. Samples of air collected in a plant handling asbestos materials give less precision and accuracy than the pure chrysotile sample prepared in the laboratory. When ashing was used as a subprocedure, the ratio of the spread between the 95% confidence limits to the mean value was about 0.49 for the chrysotile fiber concentration estimates and about 1.57 for the chrysotile mass concentration estimates. Without ashing, the corresponding values were 0.62 and 2.34. The mass estimates based on size and density were a factor of 4.2 less than the mass obtained by X-ray fluorescence. The lower precision estimate of the field sample is due to the

presence of a few large fiber bundles and to the possible presence of sources of magnesium other than chrysotile. These factors combine to underestimate the chrysotile mass obtained by electron microscope and overestimate the chrysotile mass obtained by X-ray fluorescence.

SECTION 3

RECOMMENDATIONS

The following recommendations are made to further the development and acceptance of the optimized method for characterizing airborne asbestos by electron microscope.

1. Sampling and collection methods were only briefly addressed in the present study. Further study in five areas is recommended. First, the deployment of polycarbonate filters in the field presents handling problems. Field investigators prefer the cellulose ester filters. While cellulose ester filter deposits can be transferred to electron microscope grids in a Jaffe washer using acetone, the microscopist prefers the clarity of the transferred deposit from polycarbonate filters. Therefore, a technique for transferring the deposit from cellulose ester filters to polycarbonate filters needs development. Secondly, the effect of face velocity on the collection of fibers needs clarification. Personal samplers, with 1/5 the face velocity of high-volume samplers, gave higher fiber count estimates. Thirdly, a method for securing the deposit to the filter substrate at the collection site needs to be devised. Fourthly, the rearrangement or loss of fibers on the filter due to handling and transportation of the sample to the laboratory needs to be determined. And, fifthly, the collection efficiencies of the polycarbonate and cellulose ester filters for small filters need evaluation.

2. Computer programs for the quantitative identification of asbestos minerals from energy-dispersive X-ray spectra need to be developed. At present, the method is only semiquantitative. A quantitative method should allow obtaining proportions of the various elements or their oxides and comparing them with standard reference spectra stored in a computer memory. A search technique should use reiterative techniques to narrow the choice among the possible reference spectra and the unknown by assigning probabilities to the degree of match between the spectra. Some preliminary work along these lines is reported by Millette and McFarren.[47]

3. The modifications suggested in this report for dealing with fiber bundles need to be tested. New and improved methodology, such as stratified analyses, needs to be investigated. These modifications should improve the reliability of the fiber mass concentration data computed from fiber size and density estimates.

4. Further work is needed to determine the effect of the total area

scanned, i.e., the number of fibers counted, on the reliability of the fiber concentration estimate.

5. The present study produced inconclusive results for a few subprocedures. More definitive studies are suggested to clarify the importance of these subprocedures. The effects of low temperature ashing, diluent and dispersant selection, and ultrasonic treatment should be isolated.

6. Intralaboratory reproducibility should be determined. Duplicate samples should be exposed at different times to the entire sequence of processing steps from collection to TEM examination.

7. Additional round-robin tests are suggested to obtain a complete picture of interlaboratory variability.

8. Techniques, other than electron microscopy, should be sought to assess the mass of asbestos minerals present in ambient air samples.

SECTION 4

SCOPE OF THE WORK

INTRODUCTION

Although asbestos fibers are a definite health hazard [1-27], the effects of low-dosage, chronic inhalation exposures from natural and occupational environments have not been defined [23-27]. It is believed that fiber characteristics and size distribution are important parameters in addition to the amount of asbestos in the inhaled air [21,22]. There are several methods available for determining the mass of asbestos [27-39]. X-ray diffraction [31-35], X-ray fluorescence, differential thermal analysis [36], infrared spectroscopy [37-39], neutron activation analysis [28], and atomic absorption cannot distinguish fibrous from non-fibrous minerals and cannot give fiber size distribution data. Optical and electron microscope methods allow the size distribution data to be obtained. The main limitations of the optical microscope methods are the inability to detect fibers smaller than about 0.2 μm diameter. Electron optical instruments allow much better resolution and facilitate recognition of asbestos from non-asbestos minerals from studying morphological features [15-17,30,40-43]. Further authentic identification is possible using electron diffraction data obtained with a transmission electron microscope [44-48] and by using X-ray emission spectroscopy data in electron-probe instruments or scanning electron microscopes [35,42-44,47-49]. New analytical electron microscopes are now available which allow all three types of data (morphological, electron diffraction, and X-ray spectroscopy) on individual fibers for unique and fullest characterization of particles [47-49]. However, because of the rapid acceptance and utilization of electron optical instruments, there is no standard methodology available. Several laboratories perform the analysis of airborne asbestos fibers and while they claim a reasonable internal consistency, the results obtained by separate laboratories are often widely different. The purpose of this study was to evaluate the methods and subprocedures currently in use in different laboratories, and to select and develop a composite procedure which will minimize the variability of results. The second objective of the program was to prepare a detailed handbook describing the optimized method without ambiguity. The third objective was to test this optimized method by several independent laboratories in a round-robin test and evaluate the results and to further improve it.

STRATEGY

A strategy to five tasks was planned for evaluating and optimizing a large number of important procedures, subprocedures, or variables.

Task 1: Literature Search and Survey of EM Procedures

Published Work and Experience of Analytical Laboratories--

A reference library containing over a thousand articles on asbestos-related topics was compiled. Several prominent investigators were contacted and asked to supply details of their methods for estimating asbestos. Selected laboratories were visited to study first-hand the different aspects of specimen collection, specimen preparation and examination, and evaluation of the data. The laboratories visited were:

(a) Dow Chemical Laboratory, Midland, MI; Dr. Don Beamon

(b) Battelle Memorial Institute, Columbus, OH; Dr. Heffelfinger

(c) Atomic Energy Research Establishment, Harwell, England; Dr. A. E. Morgan

(d) Pneumoconiosis Research Institute, Penarth, Wales; Dr. V. Timbrell

(e) Franklin Research Institute, Philadelphia, PA; Dr. A. Pattnaik

(f) Naval Research Laboratory, Washington, DC; Dr. L. S. Birks

(g) Mount Sinai Laboratory, New York, NY; Dr. Arthur Langer

(h) McCrone Associates, Chicago, IL; Dr. I. Stewart

(i) National Institute for Occupational Safety and Health, Cincinnati, OH; Dr. Ralph Zumwalde

List of Possible Variables--

The electron microscope method involves several steps such as sample collection, sample preparation, sample examination, and interpretation of results. A generalized scheme for quantitative characterization of asbestos is illustrated in Figure 1. Table 1 lists the various steps and subprocedures which may be

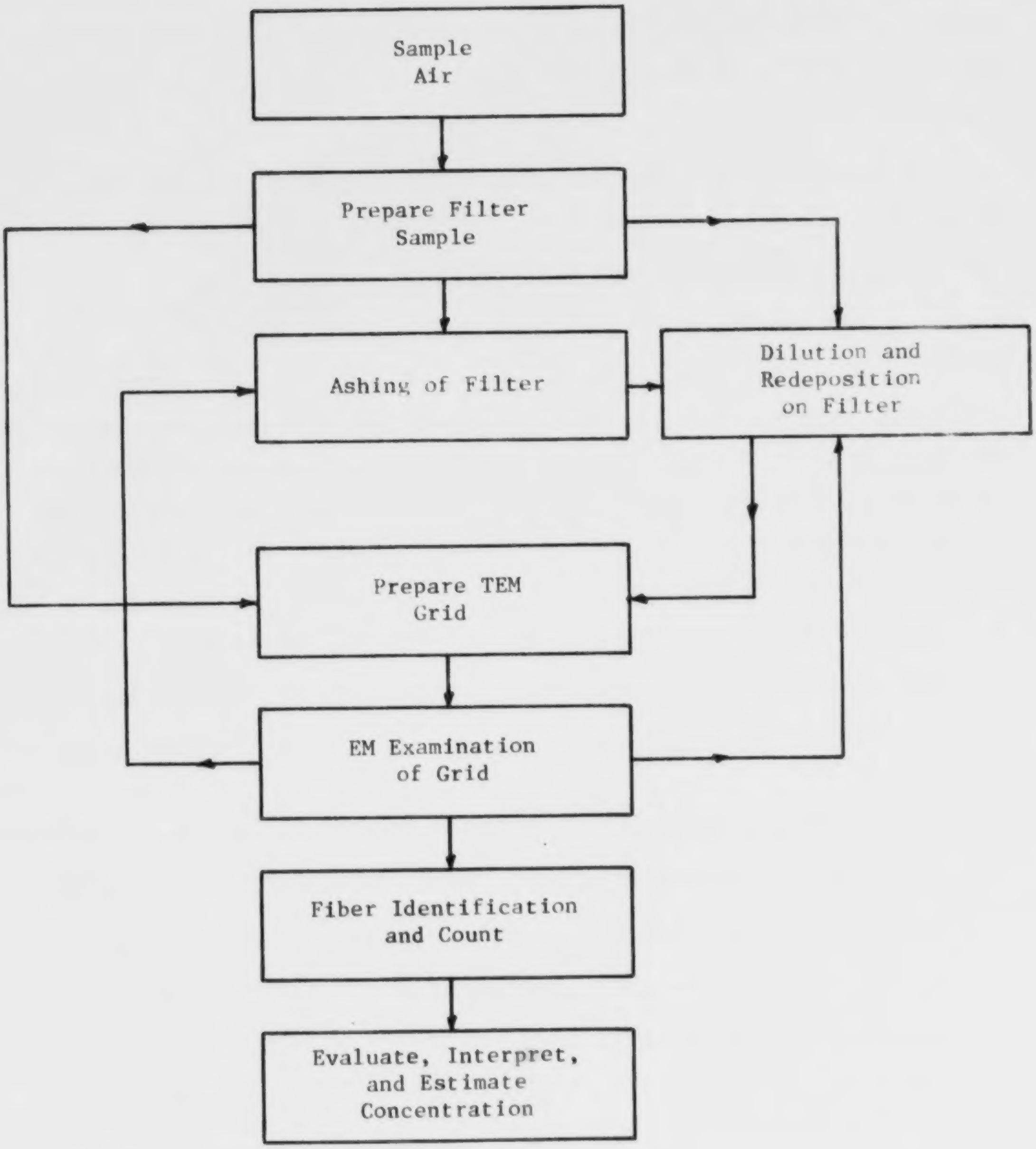

Figure 1. Flow chart of electron microscope procedures for estimating size distribution and concentration of airborne asbestos.

Table 1

PROCEDURAL VARIABLES OF ELECTRON MICROSCOPY METHOD

Variable	Variable Label	Levels
	Sampling Variables	
1	Asbestos Source Type and Time	(1) raw fiber (2) cement industry (3) plastics industry
2	Distance from Source	(1) point (2) near point (3) ambient
3	Sampler Type	(1) personal (2) hi-vol
4	Volume Sampled	(1) small (2) medium (3) large
5	Filter Type	(1) cellulose acetate (2) polycarbonate
6	Pore Size	(1) 0.2 μm (2) 0.4 μm (3) 0.8 μm
7	Locking of Particulates to Filter	(1) none (2) carbon coating (3) gelatinizing
	Filter Examination Variables	
8	Location on Filter	(1) center (2) mid-radius (3) periphery
9	Magnification, nominal	(1) 5,000X (2) 10,000X (3) 20,000X
10	Measurement Method	(1) ruler (2) eyeball using micrograph (3) eyeball using fluorescent screen
11	Examiner	(1) #1 (2) #2 (3) #3
	Ashing Variables	
12	Portion of Original Filter Used for Ashing	(1) pieshape #1 (2) pieshape #2 (3) pieshape #3
13	Ignition Before Ashing	(1) none (2) yes

Table 1 (continued)

Variable	Variable Label	Levels
14	Ashing	(1) low temperature (2) high temperature
15	Duration of Ashing	(1) short (2 hrs) (2) long (24 hrs)
	Suspension and Redeposition	
16	Dilution Medium	(1) Toluene (2) Aerosol O.T. 0.1% (3) Aerosol O.T. 0.2%
17	Sonification	(1) none (2) low energy (3) high energy
18	Duration of Sonification	(1) short (2) medium (3) long
19	Type of Redeposition Filter	(1) cellulose acetate (2) polycarbonate
	Grid Preparation Variables	
20	3 mm Sample Location	(1) center (2) mid-radius (3) periphery
21	Deposition Method	(1) cold finger soxhlet extraction (short duration) (2) Soxhlet extraction (long duration) (3) Jaffe-Method
22	Type of EM Grid	(1) copper (2) nickel
23	Mesh Size of the EM Grid	(1) 200-mesh (2) 400-mesh
24	Filter Side During Washing	(1) particle side up (2) particle side down
	Grid Examination Variables	
25	Fiber Identification Method	(1) TEM-Morphology (2) TEM-Morphology plus diffraction (3) TEM-Morphology plus chemistry (4) TEM-Morphology plus diffraction plus chemistry (5) SEM-Morphology (6) SEM-Morphology plus chemistry
26	Grid Opening	(1) center (2) mid-radius (3) periphery

Table 1 (continued)

Variable	Variable Label	Levels
27	Field Selection	(1) random (2) consecutive (3) full grid opening
28	Magnification	(1) 5,000X (2) 10,000X (3) 20,000X
29	Operator	(1) #1 (2) #2 (3) #3
30	Experience of Operator	(1) short (2) long

important. The list is by no means complete. One can extend it further.

It is clear that a large number of steps are involved in following any of the several possible paths. At each step, a multitude of choices is possible. There is no apriori way of choosing a particular level or a step on a rational basis. Therefore, one must evaluate these and provide a rational basis for selection of a step and selection of the proper level in each variable.

Task 2: Selection of Procedures or Subprocedure Variables and Experimental Plan

The number of possible variables listed in Table 1 is large and evaluating all of them would mean spreading the experimental effort too thinly over too large an area. To avoid this and to achieve meaningful estimates, the choice was narrowed down to 19 as shown in Table 2. In view of this large number of variables, it was necessary to adopt a multiphase approach, each phase utilizing a statistically designed experimental plan. This approach yields a maximum of information with a high degree of statistical significance for a given experimental effort.

A highly fractionated factorial design was used. Independent variables were controlled simultaneously according to a predetermined experimental scheme. Each of the tests (or set of data) represented a unique combination of several independent variables.

Task 3: Statistical Evaluation of the Variables

The results obtained from Task 2 were evaluated using statistical methods. The data allowed several dependent variables to be studied and explained their relationship with the independent variables.

Task 4: Development of an Optimal Procedure

The evaluation from Task 3 was to lead to selecting those independent variables and their level which gave the least variability of results. One could formulate a combination of these variables into a composite procedure. These subprocedural steps are described in detail in the form of a manual.

Task 5: Statistical Evaluation of the Optimal Method

The performance of this optimized method was evaluated in a round-robin test on the same air samples by independent laboratories.

Table 2

INDEPENDENT VARIABLES SELECTED FOR EVALUATION IN THIS STUDY

	Variable	Levels
X_1	Composition of Sample	(1) #1 100% Chrysotile (2) #2 60% Chrysotile + 40% Amphibole (3) #3 70% Chrysotile + 20% Amphibole + 10% Non-Asbestos Fiber
X_2	Concentration of Sample	(1) Low (2) Medium (3) High
X_3	Sampling Instrument	(1) Hi-Vol (2) Personal
X_4	Filter Type	(1) Nuclepore (polycarbonate) (2) Millipore (cellulose acetate)
X_5	Pore Size, nominal	(1) 0.2 μm (2) 0.4 μm (3) 0.8 μm
X_6	Filter Orientation (Particle Side)	(1) Down (2) Up
X_7	2.3 mm Portion Location	(1) Periphery (2) Mid-radius (3) Center
X_8	Use of Carbon Coating	(1) Yes (2) No
X_9	Transfer Method	(1) Soxhlet Extraction 1 (short) (2) Soxhlet Extraction 2 (long) (3) Jaffe Method
X_{10}	Magnification, nominal	(1) 5,000X (2) 10,000X (3) 20,000X
X_{11}	Grid Opening	(1) Periphery (2) Mid-radius (3) Center
X_{12}	Choice of Fields	(1) Random (2) Consecutive (3) Full Grid Opening
X_{13}	Identification	(1) Morphology plus chemistry (2) Morphology plus diffraction (3) Morphology plus chemistry plus diffraction (4) Morphology alone
X_{14}	Ashing	(1) High Temperature (2) Low Temperature
X_{15}	Sonification	(1) Low Energy (2) Medium Energy (3) High Energy

Table 2 (continued)

	Variable	Levels
X_{16}	Redeposition Filter	(1) Millipore (cellulose acetate) (2) Nuclepore (polycarbonate)
X_{17}	2.3 mm Portion of Redeposition Filter	(1) Periphery (2) Mid-radius (3) Center
X_{18}	Instrument	(1) JSM 50A (2) JEOL 100C
X_{19}	Ignition Before Ashing	(1) No (2) Yes

SECTION 5

STATISTACALLY DESIGNED EXPERIMENTAL PLANS

INTRODUCTION

There are different ways of investigating systems having many independent variables.

Two Extreme Approaches

One approach consists of varying only one variable at a time, holding all others fixed. This is the simplest and most unambiguous way of evaluating each of the variables by itself. However, this approach does not provide information on a variable when other variables are also changed simultaneously. At the other extreme, to obtain all possible combinations of all independent variables and their levels may require an astronomically large experimental effort. For the problem being studied, in which there are 19 independent variables with three possible levels per variable, the number of tests would be 3^{19}, which is an astronomically large number, and it would clearly be impractical to proceed with this complete factorial approach.

Fractional Factorial Designs

This approach allows evaluation of a large number of independent variables with a reasonable experimental effort. It is the best approach for screening the most important variables from other less important ones. These important variables can then be studied in greater detail in subsequent small experiments. A good discussion of the statistical design of experiments may be found in References 50-54.

In this project, fractional factorial experiment designs of a special class were utilized for the investigation and optimization of procedural variables in the electron microscope examination of airborne asbestos. These designs are characterized as having three levels per factor (which can be reduced to two where desired) and being highly efficient in the sense that the number of test combinations is small compared with the number of effects that can be estimated.

The use of properly coded values (linear and quadratic) permits orthogonal estimates of the effects of the independent variables to be computed by multiple regression analysis. These three-level compact orthogonal designs were constructed by extension of the method for constructing similar two-level designs described by Youden [51]. A detailed discussion of the Phase 1 design, as an illustration of the general class, is given in Appendix A.

From the experimental data on each sample, characterizing quantities such as fiber number concentration, fiber mass concentration, mean fiber length, etc., were computed. These measured or estimated quantities are designated as the dependent variables. Some dependent variables were subjected to suitable mathematical transformations for the usual purposes of linearization of the effects of the independent variables, variance stabilization, and normalization of the distribution of residuals. The transformations applied include the logarithmic, the square root, and the arcsine square root [55-57]. Table 3 lists a few representative dependent variables considered in Phase 1.

A stepwide least-square multiple regression method was used to construct the equation relating each chosen dependent variable to the independent variables [58-60]. A detailed discussion of the procedure and resulting equations is given in Appendix B.

FIVE PHASE PROGRAM

We decided to study the selected 19 variables in five phases, each phase using a fractional factorial design.

Phase 1

In this phase, we examined the procedures employed when no ashing and resuspension were undertaken and fibers were identified by morphology alone. Twelve procedural variables (see Table 4) were studied in a plan of 27 tests. The 12 variables comprise five variables of sample collection (X_1-X_5), four variables of sample preparation (X_6-X_9), and three variables of sample examination (X_{10}-X_{12}) in transmission electron microscope. The compact notation of the scheme is shown in Table 5. The 12 independent variables are denoted by X_1-X_{12}. The numbers in each row refer to the variable's value (or level code) for the particular combination. Table 6 shows the same scheme in long notation for easy recognition of variable level combinations.

Table 3

REPRESENTATIVE DEPENDENT VARIABLES IN PHASE 1

Variable	Definition
Y_1	Mean Ln (fiber width, μm)
Y_3	Mean Ln (fiber length, μm)
Y_5	Mean Ln (aspect ratio)
Y_7	Mean Ln (fiber volume, $(\mu m)^3$)
Y_9	Square root (estimated number of fibers per cm^3 of air sampled)
Y_{10}	Ln (estimated mass concentration of fibers in the air, $\mu g/m^3$)
Y_{11}	Square root (estimated number of chrysotile fibers per cm^2 of filter)
Y_{12}	Ln (estimated mass concentration of chrysotile fibers, 10^{-9} gm per cm^2 of filter)

Table 4

INDEPENDENT VARIABLES, PHASE 1

Variable		Levels and Codes			
INDEPENDENT VARIABLES OF FILTER LOADING					
X_1	Composition of Sample in Aerosol Chamber	(1)	100% Chrysotile	$X_1L=-1$	$X_1Q= 1$
		(2)	60% Chrysotile + 40% Amphibole	$X_1L= 1$	$X_1Q= 1$
		(3)	70% Chrysotile + 20% Amphibole + 10% Non-Asbestos Fiber	$X_1L= 0$	$X_1Q=-2$
X_2	Concentration of Sample on Filter	(1)	Light	$X_2L=-1$	$X_2Q= 1$
		(2)	Medium	$X_2L= 0$	$X_2Q=-2$
		(3)	Heavy	$X_2L= 1$	$X_2Q= 1$
X_3	Sampling Instrument	(1)	High Volume	$X_3Q=-2$	
		(2)	Personal	$X_3Q= 1$	
X_4	Filter Type	(1)	Nuclepore	$X_4Q=-2$	
		(2)	Millipore	$X_4Q= 1$	
X_5	Pore Size, nominal	(1)	0.2 µm	$X_5L=-1$	$X_5Q= 1$
		(2)	0.4 µm	$X_5L= 0$	$X_5Q=-2$
		(3)	0.8 µm	$X_5L= 1$	$X_5Q= 1$
INDEPENDENT VARIABLES OF TEM GRID PREPARATION					
X_6	Filter Side	(1)	Particle side down	$X_6Q= 1$	
		(2)	Particle side up	$X_6Q=-2$	
X_7	2.3 mm Portion Location	(1)	Periphery	$X_7L=-1$	$X_7Q= 1$
		(2)	Mid-radius	$X_7L= 0$	$X_7Q=-2$
		(3)	Center	$X_7L= 1$	$X_7Q= 1$
X_8	Use of Carbon Coating	(1)	Yes	$X_8Q=-2$	
		(2)	No	$X_8Q= 1$	
X_9	Transfer Method	(1)	Soxhlet Extraction 1 (short)	$X_9L=-1$	$X_9Q= 1$
		(2)	Soxhlet Extraction 2 (long)	$X_9L= 1$	$X_9Q= 1$
		(3)	Jaffe Method	$X_9L= 0$	$X_9Q=-2$
INDEPENDENT VARIABLES OF TEM EXAMINATION					
X_{10}	Magnification, nominal*	(1)	5,000X (screen mag. 4,000X)	$X_{10}L=-1$	$X_{10}Q= 1$
		(2)	10,000X (screen mag. 8,000X)	$X_{10}L= 0$	$X_{10}Q=-2$
		(3)	20,000X (screen mag. 16,000X)	$X_{10}L= 1$	$X_{10}Q= 1$
X_{11}	Grid Opening Location	(1)	Periphery	$X_{11}L=-1$	$X_{11}Q= 1$
		(2)	Mid-radius	$X_{11}L= 0$	$X_{11}Q=-2$
		(3)	Center	$X_{11}L= 1$	$X_{11}Q= 1$
X_{12}	Choice of Fields	(1)	Random choice of small fields	$X_{12}L=-1$	$X_{12}Q= 1$
		(2)	Small fields, consecutive	$X_{12}L= 1$	$X_{12}Q= 1$
		(3)	Entire grid opening as a field	$X_{12}L= 0$	$X_{12}Q=-2$

---

*The actual magnification at the fluorescent screen is somewhat smaller than the nominal or camera magnification, depending upon the design geometry of each transmission electron microscope.

Table 5

PHASE 1 EXPERIMENT DESIGN (COMPACT NOTATION)

	Factor (Independent Variable)											
Combination	$\underline{X}_1$	$\underline{X}_2$	$\underline{X}_3$	$\underline{X}_4$	$\underline{X}_5$	$\underline{X}_6$	$\underline{X}_7$	$\underline{X}_8$	$\underline{X}_9$	$\underline{X}_{10}$	$\underline{X}_{11}$	$\underline{X}_{12}$
1	1	1	2	2	1	1	3	2	1	2	2	1
2	1	1	2	2	2	1	1	2	2	1	1	3
3	1	1	2	2	3	2	2	1	3	3	3	2
4	1	2	1	1	1	1	1	2	3	2	3	2
5	1	2	1	1	2	1	2	1	1	1	2	1
6	1	2	1	1	3	2	3	2	2	3	1	3
7	1	3	2	2	1	1	2	1	2	2	1	3
8	1	3	2	2	2	1	3	2	3	1	3	2
9	1	3	2	2	3	2	1	2	1	3	2	1
10	2	1	1	2	1	1	3	2	2	3	2	2
11	2	1	1	2	2	2	1	1	3	2	1	1
12	2	1	1	2	3	1	2	2	1	1	3	3
13	2	2	2	2	1	1	1	1	1	3	3	3
14	2	2	2	2	2	2	2	2	2	2	2	2
15	2	2	2	2	3	1	3	2	3	1	1	1
16	2	3	2	1	1	1	2	2	3	3	1	1
17	2	3	2	1	2	2	3	2	1	2	3	3
18	2	3	2	1	3	1	1	1	2	1	2	2
19	3	1	2	1	1	2	3	1	3	1	2	3
20	3	1	2	1	2	1	1	2	1	3	1	2
21	3	1	2	1	3	1	2	2	2	2	3	1
22	3	2	2	2	1	2	1	2	2	1	3	1
23	3	2	2	2	2	1	2	2	3	3	2	3
24	3	2	2	2	3	1	3	1	1	2	1	2
25	3	2	1	2	1	2	2	2	1	1	1	2
26	3	3	1	2	2	1	3	1	2	3	3	1
27	3	3	1	2	3	1	1	2	3	2	2	3

Table 6

PHASE 1 EXPERIMENTAL PLAN (LONG NOTATION)

	Independent Variables											
	X_1	X_2	X_3	X_4	X_5	X_6	X_7	X_8	X_9	X_{10}	X_{11}	X_{12}
Sample	Compo.	Loading	Sampler	NP/MP	Pore Size	Particle Side Down/Up	3 mm Location	C-Coat	Filter Removal	Magnifi. 1,000X	Grid Opening Loc.	Choice of Field
1	1	Low	P	M	0.22	--	Ctr	--	Sox 1	10	MR	Random
2	1	Low	P	M	0.45	--	Peri	--	Sox 2	5	Peri	Full Grid
3	1	Low	P	M	0.8	Up	MR	Yes	J	20	Ctr	Consecutive
4	1	Med	HV	N	0.2	--	Peri	--	J	10	Ctr	Consecutive
5	1	Med	HV	N	0.4	--	MR	Yes	Sox 1	5	MR	Random
6	1	Med	HV	N	0.8	Up	Ctr	--	Sox 2	20	Peri	Full Grid
7	1	High	P	M	0.22	--	MR	Yes	Sox 2	10	Peri	Full Grid
8	1	High	P	M	0.45	--	Ctr	--	J	5	Ctr	Consecutive
9	1	High	P	M	0.8	Up	Peri	--	Sox 1	20	MR	Random
10	2	Low	HV	M	0.22	--	Ctr	--	Sox 2	20	MR	Consecutive
11	2	Low	HV	M	0.45	Up	Peri	Yes	J	10	Peri	Random
12	2	Low	HV	M	0.8	--	MR	--	Sox 1	5	Ctr	Full Grid
13	2	Med	P	M	0.22	--	Peri	Yes	Sox 1	20	Ctr	Full Grid
14	2	Med	P	M	0.45	Up	MR	--	Sox 2	10	MR	Consecutive
15	2	Med	P	M	0.8	--	Ctr	--	J	5	Peri	Random
16	2	High	P	N	0.2	--	MR	--	J	20	Peri	Random
17	2	High	P	N	0.4	Up	Ctr	--	Sox 1	10	Ctr	Full Grid
18	2	High	P	N	0.8	--	Peri	Yes	Sox 2	5	MR	Consecutive
19	3	Low	P	N	0.2	Up	Ctr	Yes	J	5	MR	Full Grid
20	3	Low	P	N	0.4	--	Peri	--	Sox 1	20	Peri	Consecutive
21	3	Low	P	N	0.8	--	MR	--	Sox 2	10	Ctr	Random
22	3	Med	P	M	0.22	Up	Peri	--	Sox 2	5	Ctr	Random
23	3	Med	P	M	0.45	--	MR	--	J	20	MR	Full Grid
24	3	Med	P	M	0.8	--	Ctr	Yes	Sox 1	10	Peri	Consecutive
25	3	High	HV	M	0.22	Up	MR	--	Sox 1	5	Peri	Consecutive
26	3	High	HV	M	0.45	--	Ctr	Yes	Sox 2	20	Ctr	Random
27	3	High	HV	M	0.8	--	Peri	--	J	10	MR	Full Grid

Footnotes:

P = Personal
HV = High-volume

Ctr = Center
Peri = Periphery
MR = Mid-radius

Sox 1 = Short
Sox 2 = Long
J = Jaffe

C-Coat = Carbon Coat
M = Millipore/Cellulose Acetate
N = Nuclepore/Polycarbonate

Phase 2

In phase 2, three variables, X_1, X_9, and X_{13}, were examined in nine tests. The compact notation of the scheme is shown in Table 7. The independent variables, their levels, and coding are also listed in Table 7. The coding is necessary to balance the design and facilitate the regression analysis. Further explanation may be found in Appendix A.

Phase 3

This phase was intended for comparing two instruments used in the secondary electron mode. The JEOL JSM 50A, an excellent scanning electron microscope, and JEOL 100C, the latest scanning-transmission electron microscope, were evaluated in SEM mode using either morphology alone or in conjunction with elemental analysis by X-ray probe. Phase 3 also used nine tests. The scheme is shown in Table 8.

Phase 4

Phase 4 provided data for examining effects of ashing and redeposition procedures. We examined four variables, X_{16}, X_{19}, X_{14}, and X_{15}, in nine tests. The compact designation of the scheme is illustrated in Table 9. The variable names and different levels in each and their coding are also listed in Table 9.

Phase 5

In phase 5, we examined the variables of the direct drop method being followed at a few laboratories. The method uses a liquid suspension (either a water sample or resuspended ash of an air filter). Instead of redepositing the particles onto another filter (see phase 4), a microdrop is withdrawn and deposited directly on a carbon-coated TEM grid and allowed to dry. Two common ways of drying the drop are keeping the drop-side facing up or keeping the drop-side facing down. There have been conflicing reports about the uniformity of deposit on the 3 mm diameter grid. Hence. another variable evaluated in this phase was the grid opening location on TEM grid (X_{11}), i.e., peripheral (level 1), mid-radious (level 2), and central locations (level 3). The scheme for phase 5 experiment and the orthogonal coding are given in Table 10.

Table 7

PHASE 2 EXPERIMENT DESIGN

Sample Description Code*	Factors (Independent Variables)		
	X_1	X_9	X_{13}
2113	1	1	3
2121	1	2	1
2132	1	3	2
2211	2	1	1
2222	2	2	2
2233	2	3	3
2312	3	1	2
2323	3	2	3
2331	3	3	1

Independent Variable Code	Description of Variables	Levels	Codes	
X_1	Composition of Sample	(1) Pure chrysotile	$X_1L=-1$	$X_1Q=1$
		(2) Chrysotile plus amosite	$X_1L=0$	$X_1Q=-2$
		(3) Chrysotile plus crocidolite plus wollastonite	$X_1L=1$	$X_1Q=1$
X_9	Transfer Method	(1) Soxhlet 1	$X_9L=-1$	$X_9Q=1$
		(2) Soxhlet 1 with carbon coating	$X_9L=0$	$X_9Q=-2$
		(3) Jaffe	$X_9L=1$	$X_9Q=1$
X_{13}	Identification Method	(1) Morphology plus chemistry	$X_{13}L=-1$	$X_{13}Q=1$
		(2) Morphology plus electron diffraction	$X_{13}L=0$	$X_{13}Q=-2$
		(3) Morphology plus chemistry plus electron diffraction	$X_{13}L=1$	$X_{13}Q=1$

*First digit in the sample description code shows the phase number; second, third, and fourth digits refer to the levels of independent variable used.

Table 8

PHASE 3 EXPERIMENT DESIGN

Test	Sample Description Code*	Factors (Independent Variables)		
		X_1	X_{13}	X_{18}
1	3142	1	4	2
2	3111	1	1	1
3	3142	1	4	2
4	3212	2	1	2
5	3242	2	4	2
6	3241	2	4	1
7	3341	3	4	1
8	3342	3	4	2
9	3312	3	1	2

Independent Variable Code	Description of Variables	Level
X_1	Composition of Sample	(1) Pure chrysotile (2) Chrysotile plus amosite (3) Chrysotile plus crocidolite plus wollastonite
X_{13}	Identification Method	(1) Morphology plus X-ray analysis (4) Morphology
X_{18}	Analytical Electron Microscope	(1) JSM-50A (2) JEOL 100C

*First digit in the sample description code refers to the phase number; the second, third, and fourth digits refer to the levels of the independent variables used.

Table 9

PHASE 4 EXPERIMENT DESIGN

Sample Number	Sample Description Code*	Factors (Independent Variables)			
		X_{16}	X_{19}	X_{14}	X_{15}
1201	42211	2	2	1	1
1202	41112	1	1	1	2
1203	42213	2	2	1	3
1204	41221	1	2	2	1
1205	42222	2	2	2	2
1206	42123	2	1	2	3
1207	42121	2	1	2	1
1208	42222	2	2	2	2
1209	41223	1	2	2	3

Independent Variable Code	Description of Variables	Levels	Codes	
X_{16}	Filter Type (both primary and secondary)	(1) Millipore (2) Nuclepore	$X_{16}Q=-2$ $X_{16}Q=1$	
X_{19}	Ignition	(1) No (2) Yes	$X_{19}Q=-2$ $X_{19}Q=1$	
X_{14}	Ashing	(1) High temperature (2) Low temperature	$X_{14}Q=-2$ $X_{14}Q=1$	
X_{15}	Sonification	(1) Low energy (2) Medium energy (3) High energy	$X_{15}L=-1$ $X_{15}L=0$ $X_{15}L=1$	$X_{15}Q=1$ $X_{15}Q=-2$ $X_{15}Q=1$

---

*First digit of the sample description code refers to the phase number; second, third, fourth, and fifth digits refer to the levels of the independent variables used.

Table 10

PHASE 5 EXPERIMENT DESIGN

Sample Number	Sample Description Code*	Factors (Independent Variables)	
		X_6	X_{11}
5101	523	2	3
5102	522	2	2
5103	521	2	1
5104	513	1	3
5105	512	1	2
5106	511	1	1

Independent Variable Code	Description of Variables	Levels	Codes	
X_6	Orientation of drop during drying on TEM grid	(1) Drop side up (2) Drop side down	$X_6 = 1$ $X_6 = -1$	
X_{11}	Radial Location of Opening on TEM grid	(1) Center (2) Mid-radius (3) Periphery	$X_{11} L = -1$ $X_{11} L = 0$ $X_{11} L = 1$	$X_{11} Q = 1$ $X_{11} Q = -2$ $X_{11} Q = 1$

*First digit of the sample description code refers to the phase number; second and third digits refer to the levels of the independent variables used.

SECTION 6

EXPERIMENTAL WORK

THE PREPARATION OF LABORATORY FILTERS OF CONTROLLED ASBESTOS LOADING IN PHASE 1

Introduction

Phase 1 of the statistically designed study to evaluate the electron microscope analytical methodology for determining asbestos required that filters be prepared under controlled conditions to obtain three different asbestos concentrations. Both polycarbonate (Nuclepore) and cellulose acetate (Millipore) filters, with pore sizes of 0.2, 0.4, and 0.8 μm, were used and samples were collected using both high volume samplers [61] (with 20 cm x 25 cm filters) and personal samplers [62] (with 3.5 cm diameter filters).

Filters could be prepared in several ways, preferably by simultaneous sampling using different filter types, pore sizes, and samplers. Filters could be prepared by:

- taking samples close to a natural source
- preparing solutions of known asbestos concentration by ultrasonic treatment of water and filtering from liquid suspension
- preparing asbestos aerosols and sampling from an aerosol cloud of calculated concentration

Sampling from a natural asbestos source, for example, an asbestos products factory, would be the most convenient, but unfortunately, it has the serious disadvantage that the concentration of the source is not known.

Filter samples could be prepared from liquid suspension of known concentration of asbestos minerals. However, the disadvantage with this method is that the deposition of fibers from water suspension onto a filter may not be equivalent to that obtained from an aerosol cloud.

Simultaneous sampling from an aerosol cloud of known concentration appears the best since it simulates normal operating conditions while allowing some control of the aerosol concentration.

Experimental

The Aerosol Chamber--

A spherical chamber fabricated from welded steel plate with a diameter of 5.5 m was utilized to obtain an aerosol cloud. The volume of the chamber is 86 m^3. The inside of the chamber is coated with an epoxy-phenolic material (Plasite 7122) to prevent corrosion. The chamber can be cleaned by a hot water spray to wash down the walls, and by a high volume extraction system to purge the chamber through an absolute filter device at the rate of 12 air changes per hour.

Inside the chamber there is a catwalk as shown in Figure 2a. Three high-volume samplers and six personal samplers were mounted on the catwalk. The aerosol cloud entered the chamber from the generator located outside the chamber. A fan inside the chamber circulated the air to ensure a uniformly mixed aerosol.

Ultrasonic Treatment to Break Fibers to a Sufficiently Fine Size--

The UICC asbestos minerals have a very coarse particle size, which is unsuitable for charging in an aerosol cloud. Three ultrasonic devices were tested to determine their efficiency in breaking up asbestos into fibers under 10 μm in length. They were:

• Ultra-Sonic Industries	- System Forty 80 Watts Bath Type
• Polytron Cell Disruptor	- PT10 5000 Watts with High Speed Agitator
• Branson Sonifier	- W 185C 100 Watts Horn Type

Tests were conducted by weighing out a small quantity of asbestos and suspending it in distilled water to give an asbestos concentration of about 0.3% by weight. Aerosol OT was added as a dispersing aid at a concentration of about 0.2%. Ultrasonics were applied for time periods of 5, 10, 20, and 30 minutes. Using each device, the sample was then diluted to a concentration of 0.03% with distilled water.

The Branson Sonifier was the only unit found suitable for achieving small enough fiber lengths in chrysotile asbestos. By varying the time of the ultrasonic treatment, the chrysotile asbestos could be reduced to any fiber length desired. The most satisfactory chrysotile dispersion was produced by giving a

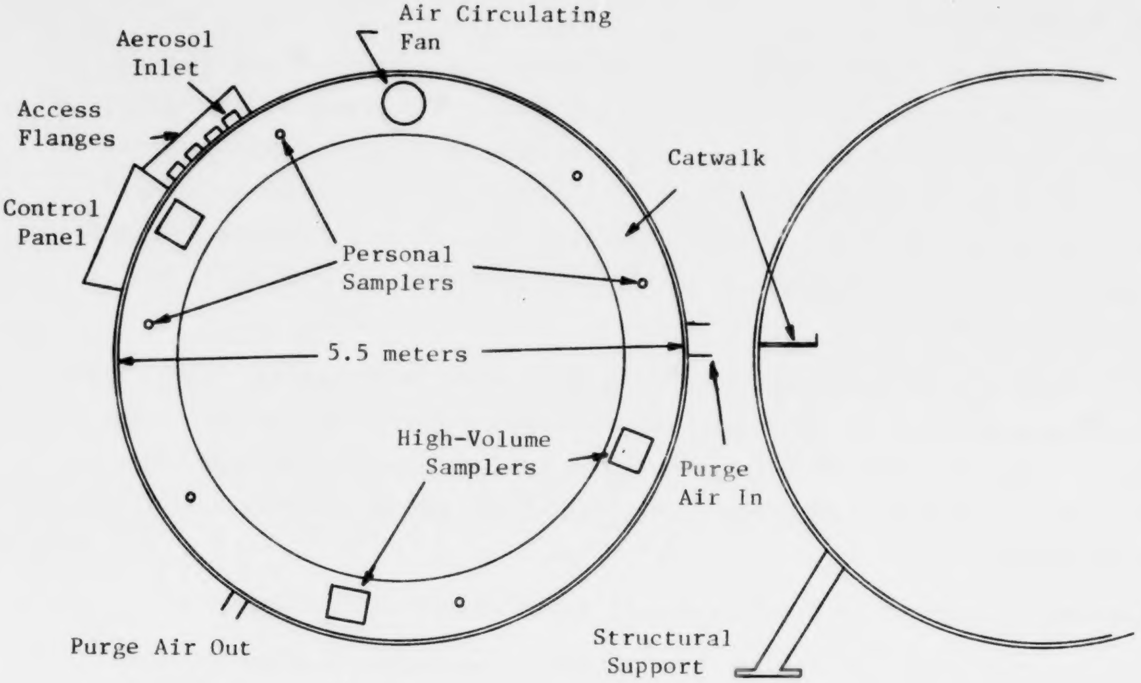

Figure 2a: Top view and side view of aerosol chamber showing location of apparatus.

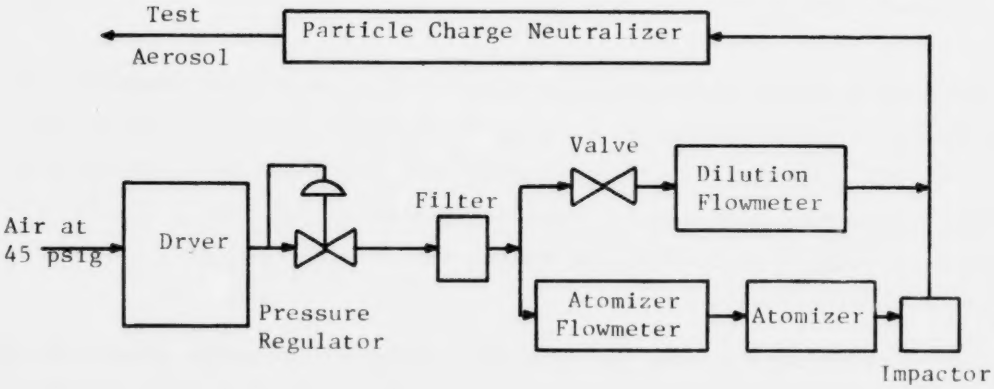

Figure 2b. Flow diagram of aerosol generator

45 minute treatment at 100 watts power to 250 mg of asbestos suspended in 150 ml of water with 2% of Aerosol OT added as a dispersing agent. The results of the treatment were checked by optical and electron microscopes.

The Branson unit was found to be less effective with amosite asbestos and fiber glass. A series of hand-grinding experiments were performed using an agate pestle and mortar. A techniques was developed which les to satisfactory dispersion of both amosite and fiber glass. It consisted of wet hand grinding a 100 mg quantity of fiber in a few drops of 1:1 solution of water and Aerosol OT for 30 minutes.

Aerosol Generation--

The Sierra Instrument Company's Model 133G Fluid Atomization Aerosol Generator utilizes air-blast atomization and inertial impaction to produce aerosols. It could produce particles at rates of up to 10^9 particles per second. The droplet size was variable from 0.03 to 3 μm.

The generator is schematically illustrated in Figure 2b. It consisted of a dryer, a pressure regulator, an absolute filter, an adjustable valve, two precision flowmeters, a fluid atomizer, an impactor, and an ionizer.

High pressure air was supplied to the generator at a minimum pressure of 45 psig. The air passed through a chemical dryer and a pressure regulator which reduced the pressure to 35 psig. The air then flowed through an absolute filter and was subsequently divided into two fractions: the atomizer air and the dilution air.

The atomizer air flowed through a flowmeter and a Collison-type atomizer. As the air passed through the nozzles of the atomizer, it produced a spray of the suspension directed against a baffle. The spray was then carried by the air through an impactor where the large droplets were removed, leaving an aerosol of a narrow size distribution. The remaining droplets then flowed to a mixing tee located upstream of the ionizer.

After flowing through the filter, the dilution air flowed through a manually adjusted valve. It then passed through a flowmeter and into the mixing tee. From the mixing tee, the diluted aerosol flowed into the ionizer where it was mixed with bipolar ions and the solvent evaporated. The aerosol was then exhausted through the outlet located on the side of the generator housing. Care was taken to adjust the fiber concentration to a point where each droplet formed would contain 0 or 1 fiber the vast majority of the times. This precaution is required to minimize agglomeration or clumping of the fibers as the water evaporated. The ionizer employed a radioactive source (1 milli-curie of Krypton 85 gas) to neutralize static charge on the particles.

During preliminary runs, contamination of the aerosol chamber by the high-volume samplers was observed. The requirement that high-volume sampling time be kept below a total of one hour, coupled with the failure of aerosol generators producing larger droplets to provide an adequately dispersed aerosol, led to a modification to the aerosol generator. Provision was made to pump asbestos slurry, whose concentration was adjusted to compensate for the fiber loss and evaporative water loss, in the atomizer unit. The Sierra Atomizer was operated for periods of 16 to 80 hours on a continuous basis using this make-up system.

This method was used since the fiber sizes were small enough to remain in suspension indefinitely with minimal air recirculation. Trial and error tests were necessary to control the desired concentration of fiber loading on the filter. It was found that the Sierra Fluid Atomization Aerosol Generator was not capable of delivering the airborne concentrations required in a few hours.

Experiments to use other aerosol atomizers for obtaining higher concentrations in a short time proved futile because of unpredictable dispersion of fibers. Such air samples would be unsuitable for good electron microscopy work.

The problem remained on how to obtain a reasonably high aerosol concentration in the chamber while at the same time ensuring the quality of the dispersion. We settled upon a procedure that assumed a very low decay constant for the concentration of the aerosol in the chamber and involved operating the Sierra aerosolizer for long periods (up to 95 hours) to build up a suitable concentration. The assumption was deemed reasonable since the gravitational sedimentation of the ultra-fine particles produced was negligible and the large diameter (18 foot) chamber gave a low wall effect. Thus, all the aerosol dispersions were finally made with one instrument, the Sierra Fluid Atomizer.

Details of Experimental Work in Phase 1 Samples Prepared in Chamber

In all, 27 samples were prepared as detailed in Table 6. Each sample was unique and had to be individually prepared.

The effective area of the 37 mm personal samplers was 6.7 cm^2 versus 406.5 cm^2 area of 20 cm x 25 cm filter in high-volume samplers. Also, the difference in flow rates of the two devices was quite significant. The personal samplers were fitted with an adjustable orifice and an excess pumping capacity which gave rise to a constant flow rate of 2.0 liters per minute, irrespective of the filter type, filter pore size, or particle build-up encountered in this program.

The flow rate of the high-volume samplers on the other hand were strongly dependent on both filter type and pore size from the following experimentally measured flow rates*:

FLOW RATES OF HIGH-VOLUME SAMPLERS

Nominal Pore Size	Flow Rate (ℓ/min)	
	Polycarbonate	Cellulose Acetate
0.2	651	396
0.4	708	453
0.8	764	679

Chrysotile asbestos was aerosolized into the chamber to provide concentrations ranging from 0.3 mg/m^3 to 1.8 mg/m^3; sampling times were selected to give nominal deposition levels of:

low level, 0.0014 mg/cm^2

medium level, 0.0054 mg/cm^2

high level, 0.022 mg/cm^2

It was necessary, when operating the high-volume samplers, to compensate for the removal of a significant fraction of the fibers. The chamber was considered to be a well-mixed batch reactor with a first-order reaction occurring. When combined with a mass balance and the assumption of total removal, an exponential decay in concentration results. The approximate validity of the assumption was verified by direct comparison of fiber counts from a high-volume filter membrane and a personal sampler filter membrane prepared during preliminary studies. This approach, and the variation of flow with pore diameter, accounts for the distribution of sampling times seen in Table 11 for the high-volume samplers.

---

*These results are independent of the sampler actually used, and remained constant for every sampling run.

SAMPLE PREPARATION FOR TEM

The sample preparations involved numerous subprocedures as described below.

Carbon Coating

Filters needing carbon coating (independent variable X_8, level 1) were placed in a vacuum evaporator and given a thin (40 nm thick) coating of carbon.

Cutting Out 2.3 mm Diameter Segment

Small discs were cut from each filter according to the variable X_7 (level 1 - peripheral location, level 2 - mid-radius, and level 3 - central location). A standard 2.3 mm punch was used for this purpose.

Particle Transfer Method

Three methods of filter dissolution were used. Variable X_9, level 1 is the Soxhlet Extraction of short duration, level 2 is the Soxhlet Extraction of long duration, and level 3 is the Jaffe method [63]. The solvent used depended on the type of filter; acetone for cellulose acetate and chloroform for polycarbonate. Duration for filter dissolution also depended on type of filter. Short and long durations were four hours and eight hours for the acetone extraction of cellulose acetate and eight hours to 16 hours for the chloroform extraction of polycarbonate filters. The Jaffe method used a 24 hour duration.

Filter Topside (Particle Side) Orientation

Variable X_6 had two possibilities. Levels 1 and 3 refer to particle side down (i.e., during filter dissolution, the particles should be in direct contact with the carbon-coating of the grid) and level 2 referred to keeping particle side up (not in direct contact with the carbon-coating of TEM grid).

EXAMINING SAMPLES IN TRANSMISSION ELECTRON MICROSCOPE

The study of samples in transmission electron microscope involves the following important considerations.

Grid Opening Location

After positioning a grid in the transmission electron microscope, an area of about 2 mm diameter was available for examination. The first step was to

Table 11

EXPERIMENTAL SCHEME FOR SIMULATED AIR SAMPLES FOR PHASE 1

Run No.	Sample No.	Fiber Composition[a]	Sampler Type[b]	Filter Type[c]	Pore Size, μm	Air Volume Filtered, ℓ	Sampling Time, min	Expected Mass Concentration of Fibers on Filter, $\mu g/cm^2$			Anticipated Mass Concentration of Fibers in Chamber, $\mu g/m^3$
								Chrysotile	Amphibole	Fiberglass	
1	1	C	P	M	0.22	32	16	1.385			Chrysotile 290
	2	C	P	M	0.45	32	16	1.385			
	3	C	P	M	0.80	32	16	1.385			
	4	C	Hi-vol	N	0.2	9116	14	6.503			
	5	C	Hi-vol	N	0.4	9200	13	6.563			
	6	C	Hi-vol	N	0.8	8400	11.2	5.993			
	7	C	P	M	0.22	512	256	22.161			
	8	C	P	M	0.45	512	256	22.161			
	9	C	P	M	0.80	512	256	22.161			
2	10	C + A	Hi-vol	M	0.22	2080	5.25	1.484	0.987		Chrysotile 290 Amphibole 193
	11	C + A	Hi-vol	M	0.45	2030	4.5	1.448	0.964		
	12	C + A	Hi-vol	M	0.80	2040	3.0	1.455	0.968		
	13	C + A	P	M	0.22	124	62	5.367	3.572		
	14	C + A	P	M	0.45	124	62	5.367	3.572		
	15	C + A	P	M	0.80	124	62	5.367	3.572		
	16	C + A	P	N	0.2	513	258	22.204	14.777		
	17	C + A	P	N	0.4	513	258	22.204	14.777		
	18	C + A	P	N	0.8	513	258	22.204	14.777		
3	19	C + A + F	P	N	0.2	7.6	3.8	1.406	0.401	0.201	Chrysotile 1240 Amphibole 354 Fiberglass 177
	20	C + A + F	P	N	0.4	7.6	3.8	1.406	0.401	0.201	
	21	C + A + F	P	N	0.8	7.6	3.8	1.406	0.401	0.201	
	22	C + A + F	P	M	0.22	29.2	14.6	5.404	1.543	0.771	
	23	C + A + F	P	M	0.45	29.2	14.6	5.404	1.543	0.771	
	24	C + A + F	P	M	0.80	29.2	14.6	5.404	1.543	0.771	
	25	C + A + F	Hi-vol	M	0.22	7920	20	24.159	6.897	3.448	
	26	C + A + F	Hi-vol	M	0.45	7701	17	23.491	6.706	3.353	
	27	C + A + F	Hi-vol	M	0.80	9167	13.5	27.963	7.983	3.992	

[a] C = chrysotile
C + A = chrysotile + amosite
C + A + F = chrysotile + amosite + fiberglass

[b] P = Personal

[c] M = Millipore
N = Nuclepore

reduce the magnification to a minimum (which was about 90X on the JEOL 100C transmission microscope) and to select a grid opening from central, mid-radius, or peripheral location as called for by the scheme (see Table 6).

Magnification

The required grid opening was brought to the center of the screen and the electron microscope was adjusted to 5,000, 10,000, or 20,000 nominal magnification, again as required by the scheme (see Table 6).

Choice of Fields

In variable X_{12}, the field of view could be chosen as a rectangular area (of the tiltable section) of the fluorescent screen and these fields could be either selected in a random fashion (level 1) or in a consecutive (adjacent) fashion (level 2). Alternately, the entire grid opening could be treated as one single field of view (level 3). For scanning the entire grid, the area was scanned from the top corner sideways until the grid bar was reached. The field was displaced upwards slightly and again scanned sideways until the opposite boundary of the grid opening was reached. This was repeated until the entire grid opening area was scanned. The levels for this variable were explained in the overall scheme (see Table 6).

DATA RECORDING

All particles with an aspect ratio 3:1 and greater and having substantially parallel sides were considered as fibers. The length and width of each fiber were estimated in mm by visual comparison with graduated circles on the fluorescent screen and all fibers visible in each field of view were counted and sequentially numbered. No attempt was made to recognize each type of mineral fibers; only a computed average density was assumed for all fibers in each sample. For fibers extending beyond the perimeter of the field of view, the length within the field of view was estimated and the fiber was treated as a half fiber for fiber concentration estimation.

EXPERIMENTAL WORK IN PHASE 2: STUDY OF FIBER IDENTIFICATION METHOD

The main objective of this phase was to evaluate the three methods of fiber identification; (a) morphology in conjunction with X-ray analysis, (b) morphology in conjunction with electron diffraction, and (c) morphology in conjunction with both electron diffraction and X-ray analysis.

Filter Preparation

Polycarbonate filters of 47 mm diameter and 0.4 µm pore size were used. Known volumes of standard liquid suspensions of UICC asbestos minerals were filtered through these filters. Filter 1 represented only chrysotile. Filter 2 represented a mixture of chrysotile plus an amphibole (amosite). Filter 3 represented a mixture of chrysotile, an amphibole (crocidolite), and a contaminant mineral (wollastonite).

Particle Transfer Method

All methods used chloroform as the solvent for dissolution of the filter. Method 1 consisted of Soxhlet extraction for eight hours of the polycarbonate filter (without carbon-coating). Method 2 consisted of Soxhlet extraction for eight hours of the same polycarbonate filters coated previously with carbon. Method 3 consisted of first carbon-coating the filter and then Jaffe washing for 24 hours.

Since these three methods were applied to the same three initial polycarbonate filters, this scheme was expected to give a close comparison among the methods of particle transfer.

Electron Microscopic Examination

EM Parameter Selection--

On the JEOL 100C electron microscope, the various parameters, such as accelerating voltage, beam spot size, tilt angle, screen magnification, etc., could be adjusted to obtain the best performance for achieving specific information. Morphological examination and electron diffraction analysis were done at 0° tilt angle and 100 kv accelerating voltage, whereas the X-ray analysis was conducted at 40° tilt angle and 40 kv accelerating voltage. The scheme for different microscope parameters is shown in Table 12.

EXPERIMENTAL WORK IN PHASE 3: EVALUATING A TEM AND AN SEM

The main objective of this phase was to compare two electron microscopes used in the secondary electron emission mode.

Preparation of Filters

The filters used in this study were 0.4 µm pore size polycarbonate, prepared by filtering liquid suspension. Sample 1 referred to chrysotile alone, Sample 2 referred to chrysotile plus an amphibole asbestos (amosite), and

Table 12

SCHEME OF ELECTRON MICROSCOPE PARAMETERS FOR FIBER IDENTIFICATION METHODS IN PHASE 2

VARIABLE COMBINATION CODE			MORPHOLOGY				ELECTRON DIFFRACTION				X-RAY FLUORESCENCE			
X_1	X_9	X_{13}	Acc. Volt KV	Beam Spot Size*	Magni-fication	Tilt Angle Degree	Acc. Volt KV	Beam Spot Size*	Camera Length cm	Tilt Angle Degree	Acc. Volt KV	Beam Spot Size*	Magni-fication	Tilt Angle Degrees
1	1	3	100	1	160,000	0	100	1	20	0	40	3	44,000	40
1	2	1	100	1	160,000	0	-	-	-	-	40	3	44,000	40
1	3	2	100	1	160,000	0	100	1	20	0	-	-	-	-
2	1	1	100	1	160,000	0	-	-	-	-	40	3	44,000	40
2	2	2	100	1	160,000	0	100	1	20	0	-	-	-	-
2	3	3	100	1	160,000	0	100	1	20	0	40	3	44,000	40
3	1	2	100	1	160,000	0	100	1	20	0	-	-	-	-
3	2	3	100	1	160,000	0	100	1	20	0	40	3	44,000	40
3	3	1	100	1	160,000	0	-	-	-	-	40	3	44,000	40

* Beam spot size refers to a setting on the JEOL 100C electron microscope. Spot size refers to a large size and spot size 3 refers to a significantly smaller size beam.

Sample 3, to a mixture of chrysotile, amphibole (crocidolite), and a contaminant (wollastonite).

Particle Transfer Method

All filters were prepared by Soxhlet condensation washing for eight hours using chloroform as a solvent. The carbon-coated TEM grids used were nickel marker (finder) grids to facilitate examining the same grid opening in the two instruments.

EM Instrument Parameters

The electron microscope parameters were chosen such that the highest capability of each instrument was not exceeded. The comparison was done at 10,000X, which represented the highest usable magnification in JSM 50A scanning electron microscope.

Instrument	Identification Method	Accelerating Voltage KV	Tilt Angle degrees	Magnification
JEOL 100C TEM	Morphology	100	0	10,000
	Morphology + X-ray	40	35	10,000
JEOL-JSM 50A SEM	Morphology	40	5	10,000
	Morphology + X-ray	40	20	10,000

Specific grid openings were examined in the two instruments in succession.

Electron Microscope Examination

Morphological identification in secondary electron imaging was based on the fiber dimensions rather than the internal, or surface structure, because of the difficulty in focusing the image. The focusing difficulty was due partly to the movement of fiber images under the beam because the fibers acquired electrical charge. In the JEOL 100C instrument, a tilted specimen was more difficult to focus because of the height differences created by tilting the grid.

The sequential image formation, as observed on the CRT screen in the scanning mode, was strenuous on the eye. Thus, scanning a grid opening while watching the secondary electron image required a meticulous effort to avoid double counting. It was found that the number of fibers recognized in a secondary electron image was smaller than those from a transmission scanning electron image of the same field of view. However, since the scanning transmission mode is not available on most common SEM microscopes, only secondary electron imaging was used for the purposes of comparison between the JSM 50A and JEOL 100C. In the morphological identification method, there were no special differences between amphibole fibers and wollastonite and, hence, this classification was subjective and was based on the observed chunkier appearance of wollastonite.

In the identification based on both morphology and X-ray analysis, emphasis was placed on the X-ray spectrum information. Interpretation was qualitative and, hence, subjective. The presence of Si and Fe was interpreted to mean amosite or crocidolite, while the presence of Si and Ca was interpreted as indicating wollastonite, and the presence of Si and Mg was interpreted as chrysotile. (A rigorous and quantitative analysis should consider the relative proportion of these elements also as described by Millette [47]). In general, the X-ray count rate was quite small and, hence, the X-ray peaks were also small. Fibers which did not given recognizable X-ray peaks were classified as ambiguous.

The sequence of examining samples was random to avoid bias.

EXPERIMENTAL WORK IN PHASE 4: ASHING AND SONIFICATION

Filter Preparation

Twelve membrane filters, eight polycarbonate, 0.2 μm pore size, and four cellulose acetate, 0.45 μm pore size, were used separately to filter a standard chrysotile suspension. The nominal amount of chrysotile (0.13×10^{-6} grams) was deposited by filtering on 37 mm diameter filters (with effective area of 9.6 cm^2) to achieve a calculated chrysotile concentration of 13.5×10^{-9} gm/cm^2. After filtration, the filters were stored in disposable petri dishes and air-dried in the clean work bench.

Six of the polycarbonate and three of the cellulose acetate filters were cut in half for ashing and sonification tests. Samples on polycarbonate membrane and one cellulose acetate membrane were transferred to 200-mesh carbon-coated copper grids to serve as control standards. Transfer to the TEM grids was accomplished using the Jaffe washer method with chloroform (for polycarbonate) or acetone (for cellulose acetate) as solvents.

Ashing and Sonification Procedures

Preignition--

Nine filter samples were rolled and placed with the fiber side facing the wall in 25 mm diameter pyrex test tubes. Preignition of three filters (two polycarbonate and one cellulose acetate) was accomplished by moistening the filters with 95% ethyl alcohol and igniting the filter by heating the pyrex tube (without an open flame on the filter) prior to completion of ashing.

Two more filters (one polycarbonate and one cellulose acetate) were prepared directly (without the ashing step). Details of the scheme for phase 4 samples are summaried in Table 13.

Ashing--

Three different ashing techniques were used:

1. Three samples, including the preignited cellulose acetate, placed in separate 25 mm diameter pyrex test tubes and placed in a muffle furnace at room temperature. The temperature was then slowly raised to 500°C and held overnight.

2. Two samples in 25 mm diameter pyrex test tubes were ashed using nascent oxygen generated low-temperature asher (Model 302 LTA supplied by LFE Corporation, Waltham, MA). The asher was operated at 50 watts and ashing continued overnight.

3. The four remaining samples were also ashed in the LTA using a slow start of 25 watts for the first half-hour, and completed by 2½ hours at 50 watts. It was observed that the majority of the membrane was ashed in the first half hour at low power.

Ultrasonic Dispersion--

After the ashing treatments, three different levels of dispersion were applied. In each case, the glass tube containing the ash was filled with distilled water containing 1% Aerosol OT as a dispersion aid.

1. Low energy ultrasonic treatment was applied from a normal laboratory ultrasonic cleaning bath (e.g., Bendix UTL-4B-1). The sample tube was placed in the neck of a 250 ml water filled conical flask such that it was held upright. Ultrasonic energy was applied for 15 minutes to disperse the ash.

2. Medium and high energy ultrasonic dispersion was applied from a Branson Sonifier (Model 200). Fitted with a variable power supply,

Table 13

DETAILS OF THE ASHING PARAMETERS USED IN PHASE 4

Sample Number	Sample Description Code*	Initial Filter	Preignition	Ashing Treatment		Ultrasonic Treatment		Final Filter
1201	42211	NP	No	HT	500°C Overnight	L	Bath 15 min	NP
1202	41112	MP	Yes	HT	500°C Overnight	M	Branson Unit 35 watts-2 min	MP
1203	42213	NP	No	HT	500°C Overnight	H	Branson Unit 65 watts-2 min	NP
1204	41221	MP	No	LT	25 watts-30 min 50 watts-150 min	L	Bath 15 min	MP
1205	42222	NP	No	LT	25 watts-30 min 50 watts-150 min	M	Branson Unit 35 watts-2 min	NP
1206	42123	NP	Yes	LT	25 watts-30 min 50 watts-150 min	H	Branson Unit 65 watts-2 min	NP
1207	42121	NP	Yes	LT	Same as above	L	Bath 15 min	NP
1208	42222	NP	No	LT	25 watts-30 min 50 watts-150 min	M	Branson Unit 35 watts-2 min	NP
1209	41223	MP	No	LT	25 watts-30 min 50 watts-150 min	H	Branson Unit 65 watts-2 min	MP
1210		NP						
1211		MP						

*First digit of the sample description code refers to the phase number; second, third, fourth, and fifth digits refer to the levels of independent variables used.

this unit supplied ultrasonic vibrations at 20,000 cps via a microtip probe which was immersed in the suspension.

3. Medium level energy was applied by using the Branson sonifier (Model 200) (equipped with a microtip probe) at its lowest setting (No. 1) for a period of two minutes. The energy was measured at 35 watts of output power. High energy was applied at the highest allowable setting (No. 7) again for a period of two minutes. The output power was measured at 65 watts.

After the ultrasonics had been applied, the probe was washed and the washings were collected in the sample tube. Between samples, the probe was cleaned by operating it three times in distilled water containing Alconox detergent, then rinsing four times in filtered distilled water.

The sample from each of the dispersion experiments was filtered through a 25 mm filter of the same type and pore size as the starting filter. The filter was dried and stored in a disposable petri dish in a clean work bench.

Particle Transfer Method--

Grid preparation was accomplished using the Jaffe washer method (without carbon-coating of filters) with analytical grade chloroform as the solvent for the Nuclepore membranes and analytical grade acetone for the Millipore membranes. The apparatus arranged in a clean air bench consisted of a glass petri dish containing a stack of five microscope slides with a strip of Whatman filter paper laid over the slides. Solvent was gently poured into the dish to bring the level to the top of the slides.

A 3 mm copper grid, carbon side up, was placed on the Whatman filter. A 3 mm disc cut from the membrane filters could then be gently placed (particle side down) on top of the grid. Solvent was added dropwise to restore the solvent level as required. The filters took 24-72 hours to completely dissolve. The dish was covered.

Transmission Electron Microscopy--

The grids resulting from these experiments were studied using a JEM-7 Transmission Electron Microscope (TEM) operated at 100 kv and at a nominal magnification of 10,000X.

Each sample was mounted and examined using TEM. A number of grids sufficient to exceed a count of 100 fibers were examined. Data taken were the number of grid openings examined and the diameter and length of each fiber observed.

Only undamaged grid openings were counted and each grid opening examined was surveyed completely.

EXPERIMENTAL WORK IN PHASE 5: STUDY OF DIRECT DROP METHOD

The objective of this phase was to study the direct drop method of preparation of TEM grids from liquid suspensions.

Preliminary experiments had shown a 5 μℓ droplet to be of appropriate size for coverage of a standard 200-mesh carbon-coated electron microscope grid, and a suspension was prepared such that a 5 μℓ drop would contain sufficient chrysotile asbestos fibers to give loading equivalent to a 10 nanograms per cm^2 filter loading. The same base chrysotile stock suspension used in phases 2 and 4 was used.

The grids were mounted on a 2.5 cm x 7.5 cm glass microscope slide using double-stick tape. The droplets were applied with a 5 μℓ syringe from the freshly prepared suspension. Four grids were used, two of which were allowed to dry in an inverted position, and two as deposited. The grids were prepared in a clean work bench and were covered during the drying process.

Grid openings located near the center, mid-radius, and periphery of the droplet were examined and fiber counts and size distribution measured using a JEM-7 TEM microscope at the same conditions used in phase 4.

SECTION 7

RESULTS AND DISCUSSION OF PHASE 1

INTRODUCTION

Phase 1 represented the largest body of experimental data in this multiphase program. These data were analyzed in a variety of ways to extract relevant information for evaluating 12 variables. It was necessary to decide on specific criteria to be used in determining which variables were important and which levels were desirable.

CRITERIA SELECTED

The following four criteria were selected:

1. Conformance to the Poisson distribution.
2. Precision in fiber count per field of view.
3. Number concentration of chrysotile fibers per unit volume of air sampled.
4. Mass concentration of chrysotile fibers per unit volume of air sampled.

Criteria 1 and 2 refer to fiber frequency distribution characteristics. Criteria 3 and 4 refer to detection and estimation of number and mass of chrysotile fibers in air samples.

SUMMARY OF PHASE 1 RESULTS

Table 14 summarizes the data from Phase 1. The various entries are as follows:

Column 1 lists the combination code (or sample number)

Colume 2 lists the number of fibers counted

Column 3 lists the number of fields examined

Column 4 lists the mean number of fibers per field of view

Column 5 lists the area of each field of view

Table 14

SUMMARY OF PHASE 1 DATA

1	2	3	4	5	6
Data Base and Sample No.	No. of Fibers Counted	No. of Fields	Mean No. of Fibers/Field	Area of each Field $\times 10^{-6}$ cm^2	No. of Fibers/cm^2 $\times 10^6$
1	144	200	0.72	1.0	0.72
2	211	12	17.55	72.0	0.244
3	164	211	0.78	0.25	3.10
4	223	46	4.85	1.0	4.85
5	201	26	7.72	4.0	1.93
6	178	4	44.50	72.0	0.62
7	269	1	269.0	72.0	3.74
8	237	4	59.3	4.0	14.82
9	221	72	3.06	0.25	12.25
10	60	276	0.216	0.25	0.862
11	203	108	1.88	1.0	1.88
12	210	8	26.25	72.0	0.364
13	695	1	695.0	72.0	9.67
14	139	200	0.695	1.0	0.695
15	208	19	10.95	4.0	2.74
16	218	17	12.8	0.25	51.2
17	218	2	109.0	72.0	1.515
18	200	7	28.5	4.0	7.12
19	196	15	13.06	72.0	0.181
20	24	280	0.086	0.25	0.344
21	26	200	0.13	1.0	0.13
22	34	200	0.17	4.0	0.042
23	227	4	56.8	72.0	0.79
24	201	186	1.08	1.0	1.08
25	169	204	0.827	4.0	0.207
26	205	140	1.462	0.25	5.86
27	249	7	35.6	72.0	0.494
41 (Replicate of 1)	215	75	2.86	1.0	2.86
34 (Duplicate of 4)	200	39	5.12	1.0	5.12
44 (Replicate of 4)	206	21	9.8	1.0	9.8
36* (Duplicate of 6)	64	200	0.32	0.25	1.28
120 (Duplicate of 20)	33	220	0.15	0.25	0.60
121 (Duplicate of 21)	35	221	0.158	1.0	0.158

* Small fields of view were chosen in a consecutive sequence.

Column 6 lists the number of fibers per square cm of the filter

STATISTICAL DISTRIBUTION TESTS

Distribution of Fibers in a Microscopic Field of View

Since, in an electron microscope method, only a very small area of the sample is examined and an assumption is made that the area examined is representative of the entire sample for computing the average fiber concentration and fiber characteristics, it is important to check whether this assumption is statistically sound. This is done by comparing the variation of fiber distribution with a Poisson distribution model.

Poisson Distribution Tests

An analysis of the Phase 1 data was performed to determine whether the variation in the observed numbers of fibers per field in the various samples was in accordance with the Poisson distribution, and if not what the nature of the departure was. The Poisson sequence for the expected numbers of fields containing 0, 1, 2, . . . fibers is

$$(F)(e^{-\lambda})(1, \lambda, \lambda^2/2!, \lambda^3/3!, . . .)$$

where F is the total number of fields and λ is the mean number of fibers per field. It is considered desirable that the Poisson model hold, since this is an indication of truly random sampling, and simple methods of establishing confidence intervals for the mean number of fibers per unit volume of air can be applied.

To investigate this question, 21 statistical tests were made, as summarized in Table 15. The data for each test consisted of the fiber counts per field that were recorded during the EM examination of a particular Phase 1 sample or, in three instances, a duplicate pair of samples. The duplicate pairs of samples were: 4 and 34; 20 and 120; 21 and 121. A pair consisted of different 2.3 mm diameter portions of the same filter. It was shown that the two samples of each pair were in good agreement, and therefore the counts were combined for the present purpose.

Each set of test data was analyzed by means of computer program POISSON-1 written at IIT Research Institute for the purpose of determining the goodness of fit of the distribution. The listing of this program is given in Appendix C. The printouts for two illustrative samples, 1 and 26, and presented in Appendix C.

Table 15

TESTS FOR APPLICABILITY OF THE POISSON DISTRIBUTION TO NUMBER OF FIBERS PER FIELD

Test	Samples in Data Base	Size of Field cm² x 10^{-6}	No. of Fields, F	No. of Fibers	Mean No. Fibers per Field, λ	Degrees of Freedom	Chi-Square	Probability	Good Fit to Poisson
1	1	1.0	200	144	0.72	2	30.54	.001>P	
2	2	72.0	12	210	17.50	1	7.69	.01>P>.001	(*)
3	3	0.25	211	164	0.78	2	11.84	.001>P	
4	4 & 34 †	1.0	85	423	4.98	7	21.83	.01>P>.001	(*)
5	5	4.0	26	201	7.73	4	1.45	.9>P>.8	*
6	9	0.25	72	221	3.07	5	120.33	.001>P	
7	10	0.25	276	60	0.22	1	16.19	.001>P	
8	11	1.0	108	203	1.90	4	8.81	.10>P>.05	*
9	14	1.0	200	139	0.70	2	137.02	.001>P	
10	15	4.0	19	208	10.95	2	2.46	.3>P>.2	*
11	16	0.25	17	218	12.82	3	1.95	.7>P>.5	*
12	19	72.0	15	196	13.07	2	3.35	.2>P>.1	*
13	20 & 120 †	0.25	498	57	0.11	1	26.80	.001>P	
14	21 & 121 †	1.0	420	61	0.15	1	6.72	P = .01	(*)
15	22	4.0	200	34	0.17	1	35.46	.001>P	
16	24	1.0	188	201	1.07	3	7.61	.10>P>.05	*
17	25	4.0	203	169	0.83	2	114.44	.001>P	
18	26	0.25	140	205	1.46	3	3.23	.5>P>.3	*
19	36	0.25	215	64	0.30	1	10.73	P = .001	
20	41 (Repl.of 1)	1.0	75	215	2.87	5	16.75	.01>P>.001	(*)
21	44 (Repl.of 4)	1.0	21	206	9.81	2	6.89	.05>P>.02	(*)

† Combined data from original and duplicate 3-mm filter portions.
* Conform to Poisson.
(*) Borderline conformation to Poisson.
Absence of * signifies poor agreement to Poisson.

Presented in Table 15 are the results of all 21 goodness-of-fit tests. The EM field size is specified and the following quantities from the computer analysis of the data are given: the number of fields (F), the number of fibers, the mean number of fibers per field (λ), the degrees of freedom for assessing the goodness of fit of the Poisson distribution, and the total Chi-square value. The range within which the probability, P, lies is given in the last column, determined as a function of Chi-square and the degrees of freedom from a standard table IV in reference 55.

A number of tests revealed good agreement between the observed numbers of fibers per field and the numbers computed from the Poisson model of random variation, while other tests revealed poor agreement. The samples in which the fit was particularly good are 5, 11, 15, 16, 19, 24, and 26. In these seven instances, the probability of a worse fit due purely to accidents of sampling was less than 1 in 1,000. In the remaining five instances (samples 2, 4 and 34 combined, 21 and 121 combined, 41, and 44), the probability values are greater than 1 in 1,000 but less than 1 in 20.

For the purpose of analyzing the EM procedural factors in relation to compliance and non-compliance with the Poisson distribution, the samples in Table 15 were assigned to two categories: those with $P \leq 0.001$ and those with $P > 0.001$.

The cases conforming definitely to Poisson distribution are denoted by asterisks and those borderline cases are shown by bracketted asterisks in Table 15.

Tendency Towards Poisson Distribution as a Criterion for Optimizing Variable Levels

It is interesting to understand why 12 cases tend to follow Poisson distributions whereas the remaining nine cases do not. The frequency of variable-levels among the cases in each class can be examined. The variable-levels were studied for each variable and the frequency distribution of these levels is summaried in Table 16.

For example, consider the variable X_4, the filter-type. Of the 12 cases conforming to Poisson distribution, six had Nuclepore filters and the other six had Millipore filters. Of the nine cases not conforming to Poisson, two had Nuclepore filters and seven had Millipore filters. For another example, consider variable X_9, the method of filter dissolution. Of the 12 cases conforming to

Table 16

VARIABLE LEVEL FREQUENCY DISTRIBUTION IN TWO GROUPS

		Group 1	Group 2	Remarks On
Variable	Level	12 Tests Conforming to Poisson Distribution	Nine Tests Not Conforming	Best Choice to Achieve Maximum Frequency in Conforming and Minimal Frequency in Nonconforming
X_1 Composition	1	5	4	
	2	3	2	
	3	4	3	
X_2 Loading	L	5	4	
	M	[5]	[3]	Best Choice
	H	2	[2]	
X_3 Sampler	Hi-Vol	5	[2]	
	Personal	[7]	7	
X_4 Filter	NP	[6]	[2]	Best Choice
	MP	6	7	
X_5 Pore Size	0.2	[5]	4	
	0.4	4	[2]	
	0.8	3	3	
X_6 Particle Side	Down	[10]	[3]	Best Choice
	Up	2	6	
X_7 2.3 mm Location	Peri	4	3	
	MR	3	3	
	Ctr	5	3	
X_8 Carbon Coat	Yes	5	[1]	
	No	[7]	8	
X_9 Transfer Method	Sox 1	3	4	
	Sox 2	3	4	
	Jaffe	[6]	[1]	Best Choice
X_{10} Magnification	5	4	2	
	10	[6]	[2]	Best Choice
	20	2	5	
X_{11} Grid Opening Location	Peri	5	3	
	MR	3	1	
	Ctr	4	5	
X_{12} Choice of Field	Random	[7]	3	
	Consecutive	3	6	
	Full Grid Opening	2	[0]	

[] indicates the highest frequency in Group 1 and the lowest frequency in Group 2.

Poisson distribution, three were prepared by Soxhlet method 1, three by Soxhlet method 2, and six by Jaffe method. Among the nine cases deviating from Poisson distribution, four were prepared by Soxhlet method 1, four by Soxhlet method 2, and only one by Jaffe.

If we now hypothesize that the variable levels should be chosen which are conducive to Poisson distribution (i.e., maximum frequency among the levels), then we can make a clear-cut choice in some variables. For example, in variable X_6, particle side down is definitely preferable to particle side up. Similarly, in variable X_9, the filter dissolution method, the Jaffe method has the maximum frequency and hence is conducive to obtaining Poisson distribution in fibers.

However, it is difficult to make a clear-cut choice in some cases. For example, in variable X_4, the frequency is 6 for Millipore and 6 for Nuclepore. In order to avoid such indecisive cases, one may look into another group (those deviating from Poisson's distribution) and select the variable level which is the least conducive to deviation from Poisson distribution (i.e., select the least frequency). For example, in variable X_4, Nuclepore filter with a low frequency 2 is preferred to Millipore with frequency of 7.

Thus, a choice of variable level should be such that it corresponds to the maximum frequency in the group conforming to Poisson distribution and also to the least frequency in the group deviating from Poisson distribution.

Following such a criterion, variables X_2, X_4, X_6, X_9, and X_{10} give a definitive choice in variable level. In variables X_3, X_5, X_8, and X_{12}, a compromise has to be made. In the remaining cases of variables, X_1, X_7, and X_{11}, the choice is not governed by the variable levels. The best choices in the levels in the nine out of 12 variables studied are indicated in Table 16.

Most of the choice can be explained rationally. It should be noted that compliance with Poisson distribution is one of the many rational criteria that can be used in selecting variable levels. Other criteria, such as least variability in electron microscopy results, are applied in the next step of statistical analysis.

Precision in Fiber Counts per Field as a Criterion for Optimizing Independent Variables

In a manner similar to that discussed in the previous section, one can also use the precision in fiber counts per field as a criterion for optimizing independent variables.

Table 17 lists for each sample (Column 1) the mean (Column 2), the standard error of the mean (Column 3), and the ratio of standard error to the mean (Column 4). These statistical quantities are based on each field as a unit of analysis. The relative standard error (i.e., R.S.E. = standard error of mean/mean) has been chosen as a measure of the precision. A value of 0.10 and less has been arbitrarily chosen to indicate good precision and higher values to indicate high variability or poor precision. The categories of good and poor precision are denoted in the remarks column.

It is found that our of a total of 28 cases, 12 have been classified as having good precision and 16 as having poor precision. Following the same form of analysis as was explained earlier for compliance with Poisson distribution, the frequency distributions in the variable levels have been developed. Selecting the variable levels with the highest frequency in the good precision group and the least frequency in the poor precision group indicates definite trends as noted in Table 18.

It is interesting to compare these trends with those according to the criterion of compliance with Poisson distribution. A comparison between the two criteria (see Tables 16 and 18) shows that in the majority of cases, the choice of the best variable level is identical in two criteria. In a few cases, the best choice in one does not match with the best choice in the other. For example, in variable X_9, the Jaffe method appeared the best in the criterion of compliance with Poisson distribution. However, in the best precision criterion, Soxhlet method 1 appeared quite comparable with the Jaffe method.

Consideration of Fiber Characteristics

In the discussion so far, we had referred to only the frequency distribution of fibers. Now we consider the other characteristics of the sample, namely, the size distribution of length, width, aspect ratio, volume, and mass of chrysotile fibers. These quantities are termed statistical descriptors.

Statistical Descriptors of the Observed Fibers on a Per-Sample Basis

Included in the Phase 1 data base is a unit record for each of the almost 8,000 fibers observed under the electron microscope. A table was prepared by computer from the fiber records of each sample separately containing summary

Table 17

PRECISION IN FIBER COUNT PER FIELD AS A CRITERION FOR OPTIMIZING

1	2	3	4	5	6
Sample	Mean	Std. Error of Mean	Std. Error/Mean	Remarks R.S.E.*≤0.1	R.S.E.>0.1
1	0.72	0.0787	0.10	good	
2	17.50	4.8218	0.27		poor
3	0.7773	0.0699	0.08	good	
4 + 34	4.9765	0.3036	0.06	good	
5	7.7308	0.4659	0.06	good	
6	44.50	18.3416	0.41		poor
7	(Not Enough Data)**				
8	59.25	16.25	0.27		poor
9	3.0694	0.5029	0.16		poor
10	0.2174	0.0335	0.15		poor
11	1.8796	0.1353	0.07	good	
12	26.25	4.7650	0.18		poor
13	(Not Enough Data)**				
14	0.6950	0.2184	0.31		poor
15	10.9474	1.6463	0.15		poor
16	12.8235	0.9044	0.07	good	
17	109.0	9.0	0.08	good	
18	28.5714	2.0914	0.07	good	
19	13.0667	0.9282	0.07	good	
20 + 120	0.1145	0.0176	0.15		poor
21 + 121	0.1452	0.0221	0.15		poor
22	0.1700	0.0572	0.33		poor
23	56.75	11.2129	0.19		poor
24	1.0691	0.0896	0.08	good	
25	0.8325	0.1676	0.20		poor
26	1.4643	0.1108	0.07	good	
27	35.5714	6.6471	0.18		poor
36	0.2977	0.0580	0.19		poor
41	2.8667	0.2556	0.08	good	
44	9.8095	1.1436	0.11		poor

---

* R.S.E. stands for relative standard error.

** Only one full grid opening was examined and was considered as a unit of analysis. Therefore, the data are inadequate for estimating the precision from one field to the next.

Table 18

VARIABLE LEVEL FREQUENCY DISTRIBUTION IN TWO GROUPS

Variable	Level	Group 1 12 Tests Showing Good Precision	Group 2 16 Tests Showing Poor Precision	Remarks
X_1 Composition	1	5	6	
	2	4	4	
	3	3	6	
X_2 Loading	L	5	5	
	M	3	7	
	H	4	4	
X_3 Sampler	Hi-Vol	4	5	
	Personal	8	11	
X_4 Filter	N.P.	[8]	[3]	Better Choice
	M.P.	4	13	
X_5 Pore Size	0.2	[5]	[4]	Best Choice
	0.4	4	5	
	0.8	3	7	
X_6 Particle Side	Down	8	10	
	Up	4	6	
X_7 3 mm Location	Peri	3	6	
	MR	3	5	
	Ctr	[6]	[5]	Best Choice
X_8 Carbon Coat	Yes	[7]	[0]	Better Choice
	No	5	16	
X_9 Transfer Method	Soxhlet 1	[5]	[4]	Best Choice
	Soxhlet 2	2	7	
	Jaffe	5	5	(close 2nd best)
X_{10} Magnification	5,000	3	6	
	10,000	[6]	[4]	Best Choice
	20,000	3	6	
X_{11} Grid Opening Loc.	Peri	3	6	
	MR	[5]	[5]	Best Choice
	Ctr	4	5	
X_{12} Choice of Field	Random	[6]	[4]	Best Choice
	Consecutive	4	6	
	Full Grid	2	6	

statistics. A typical printout for sample 1 is shown in Table A-4 of Appendix A. The total number of fibers that did not extend beyond the EM field were noted. Values of the following variables were first found on a per-fiber basis within each sample:

V_1 - Fiber width in micrometers (considered as diameter)

V_2 - Fiber length in micrometers (that portion of the fiber within the EM field in the case of a fiber that crossed the boundary of the field)

V_3 - Aspect ratio, $V_3 = V_2/V_1$

V_4 - Fiber volume in cubic micrometers, $(\pi/4)\ (V_1)^2\ (V_2)$

V_{11} - Natural logarithm of V_1

V_{21} - Natural logarithm of V_2

V_{31} - Natural logarithm of V_3

V_{41} - Natural logarithm of V_4

The following statistical descriptors for the designated variables were then computed from the individual fiber values: the total, the mean, the standard deviation, the standard error of the mean, the variance, the minimum value, and the maximum value. The variables for which these quantities are given are:

V_4 - Over all fibers

V_{11} - Over all fibers

V_{21} - Over fibers lying wholly within their fields

V_{31} - Over fibers lying wholly within their fields

V_{41} - Over fibers lying wholly within their fields

The total fiber volume of the sample is required for estimating the mass concentration of fibers in the atmosphere. A log-normal model of random variation among fibers is considered appropriate for width (or diameter), length, aspect ratio, and volume [56].

Statistical Analysis of Phase 1 Fractional Factorial Experiment

For evaluating the effects of independent variables on the statistical descriptors (or dependent variables), we used a regression analysis technique [59,60].

Dependent Variables--

Certain of the sample descriptors (or measured response) were analyzed in relation to the 12 controlled factors (or independent variables) of the Phase 1 experiment design by constructing performance equations with the descriptors as the dependent variables. The dependent variables chosen are listed in Table 19. These are the dependent variables, or observed responses, of the experiment. A square root transformation is appropriate in response to Y_9 because it involves number count [56]. In all other responses, designated Y_1 through Y_{10}, natural logarithmic transformations are appropriate [57].

Regression Analysis--

Regression equations were constructed to express each dependent variable in terms of the coded independent variables. The best values of the coefficients were determined by statistical regression methods using the stepwise regression program BMDO2R from the BMD library of statistical programs [59].

The signs of the coefficients of independent variables in regression equations are listed in Table 20. A positive sign in this table means that the dependent variable increases in value as one increases the coded value of the independent variable. A negative sign represents a decreasing trend and an absence of any sign means that the dependent variable is not significantly affected. This is easy to visualize for the linear components. For the quadratic components and for a combination of linear and quadratic components, the effects associated with the different levels of the experimental factors can be clearly displayed in the form of plots. If the magnitude of the effect was not statistically significant, it was dropped from further consideration. A complete treatment of the method is illustrated in Appendix B.

The results of the analyses for Y_9 and Y_{10} are given in detail in Tables B-1 through B-4 and summarized in Figures 3 through 6 for a quick comparison. Fiber count concentration Y_9 and fiber mass concentration estimates Y_{10} are the most commonly considered responses for quantitative EM work. Other responses, Y_1 through Y_8, are of secondary importance and such detailed analyses of these are not presented.

Discussion of Main Effects

In this section, we discuss separately the effect of each variable on the two dependent variables, namely, the fiber count estimate (Y_9) and the mass concentration estimate (Y_{10}). Rational explanations are offered where possible.

Table 19

DEPENDENT VARIABLES, PHASE 1

Variable	Definition*
Y_1	Mean Ln (fiber width, micrometers)
Y_2	Standard error of Y_1
Y_3	Mean Ln (fiber length, micrometers)
Y_4	Standard error of Y_3
Y_5	Mean Ln (aspect ratio)
Y_6	Standard error of Y_5
Y_7	Mean Ln (fiber volume, micrometers^3)
Y_8	Standard error of Y_7
Y_9	Square root (estimated number of fibers per cm^3 of atmosphere)
Y_{10}	Ln (estimated mass concentration of fibers in the atmosphere, micrograms per cubic meter)

* The unit of observation for these variables is a combination as specified in the experiment design. All logarithms are to base e.

Table 20

SIGNS OF COEFFICIENTS OF INDEPENDENT VARIABLES IN PERFORMANCE EQUATIONS, PHASE 1

Independent Variable Code*			Dependent Variables(1)									
			Y_1	Y_2	Y_3	Y_4	Y_5	Y_6	Y_7	Y_8	Y_9	Y_{10}
1.	X_1L	Composition			+		+				+	+
2.	X_1Q	Composition	—	—		—		—		—	+	
3.	X_2L	Concentration	—	—	—	—		—	—	—	—	—
4.	X_2Q	Concentration									+	
5.	X_3Q	Sampler type			+		+			+	+	
6.	X_4Q	Filter type	+			—		—				+
7.	X_5L	Pore size										
8.	X_5Q	Pore size										—
9.	X_6Q	Filter side									+	
10.	X_7L	Location on filter		—	—		—	—		—		—
11.	X_7Q	Location on filter										
12.	X_8Q	Carbon coating		+	—	+	—	+	—	+	—	—
13.	X_9L	Transfer method	+		+		+		+		—	
14.	X_9Q	Transfer method	—		+		+	+			—	—
15.	$X_{10}L$	Magnification	—		—	+	—		—	+	+	+
16.	$X_{10}Q$	Magnification			—		—				+	—
17.	$X_{11}L$	Grid opening loc.										
18.	$X_{11}Q$	Grid opening loc.							+		+	
19.	$X_{12}L$	Choice of fields										
20.	$X_{12}Q$	Choice of fields	—	+		+		+	—	+	+	+

---

(1) For explanation of dependent variables, please see Table 19.

* Independent variables designated X_1-X_{12} are the same as described in Table 4. Each of these have linear (L) and quadratic (Q) components. A complete description of these is given in Appendix A.

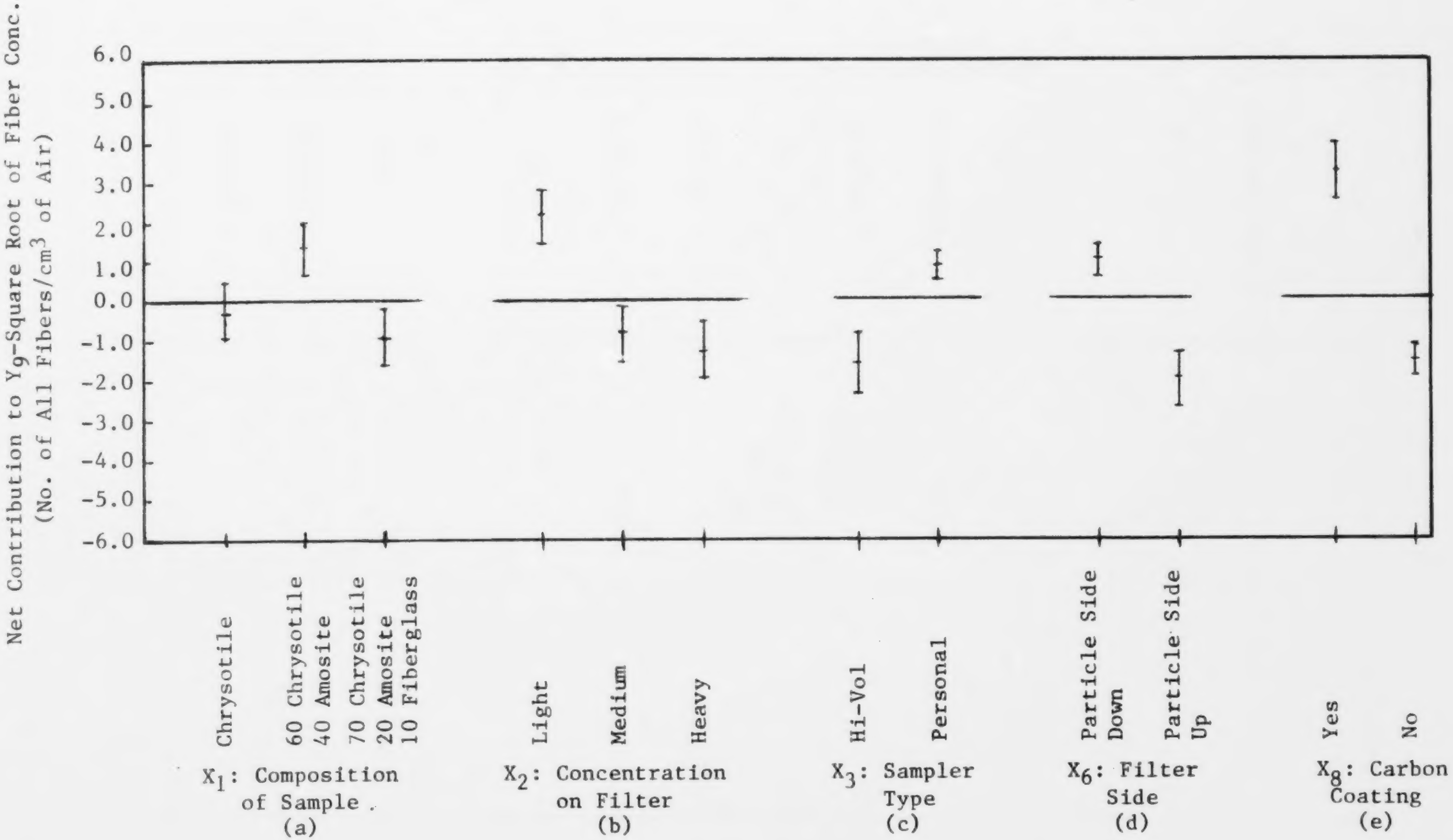

Figure 3. Graphical presentation of performance equation 9 in Phase 1. Net contribution to square root of fiber concentration (no. of all fibers/cm^3 of air).

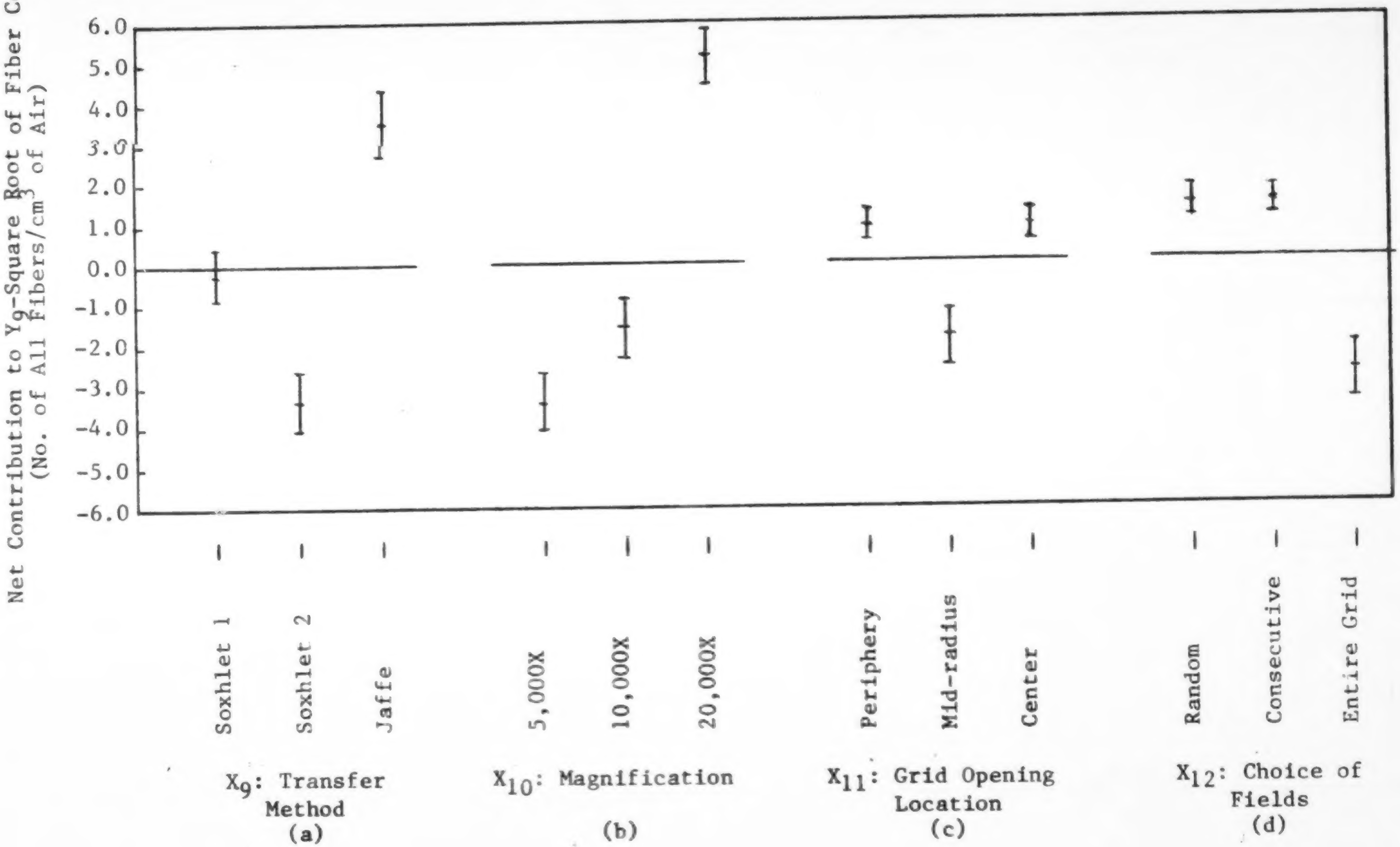

Figure 4. Graphical presentation of performance equation 9 in Phase 1. Net contribution to square root of fiber concentration (no. of all fibers/cm^3 of air).

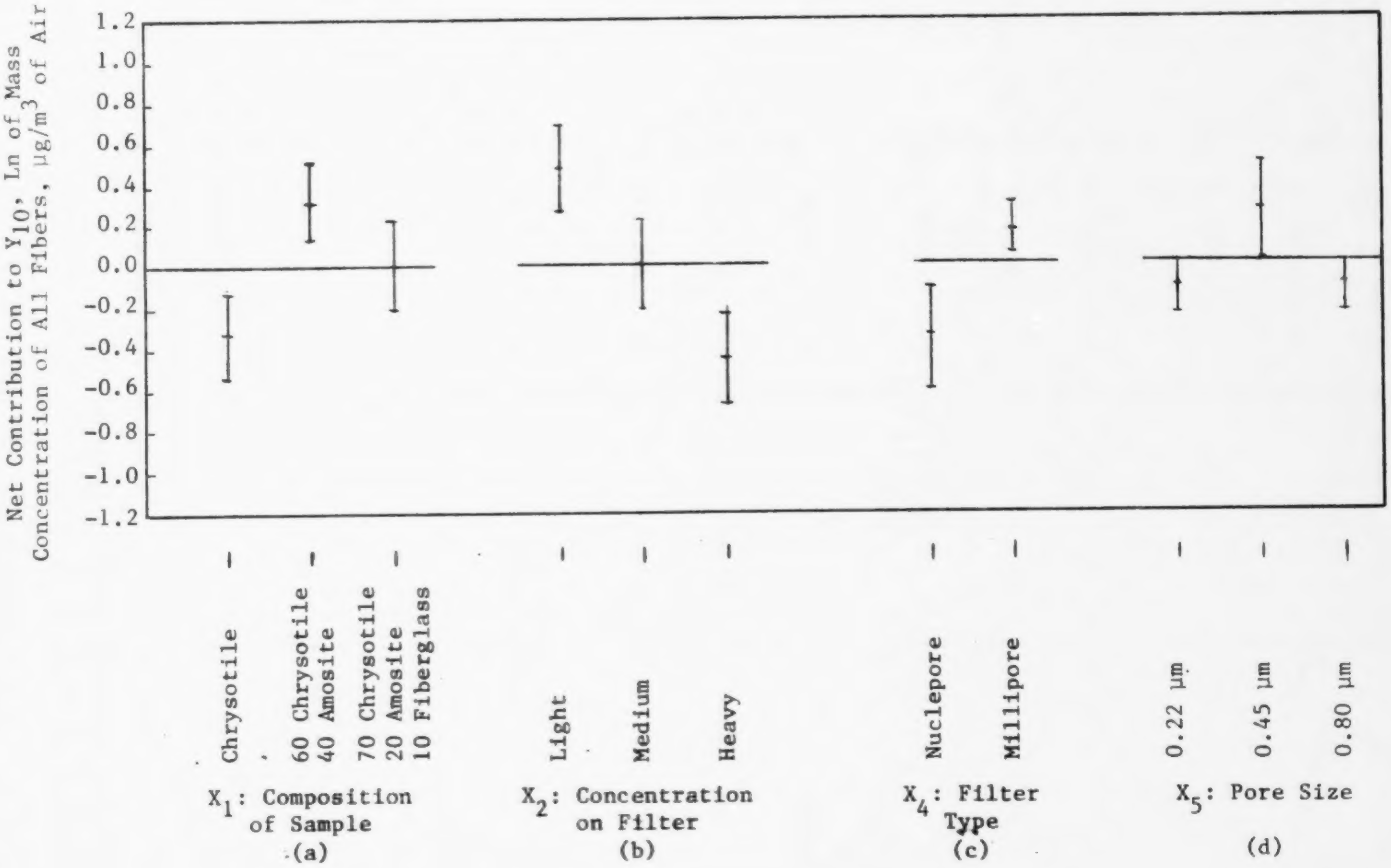

Figure 5. Graphical presentation of performance equation 10 in Phase 1. Net contribution to natural log of mass concentration of all fibers, µg/m^3 of air.

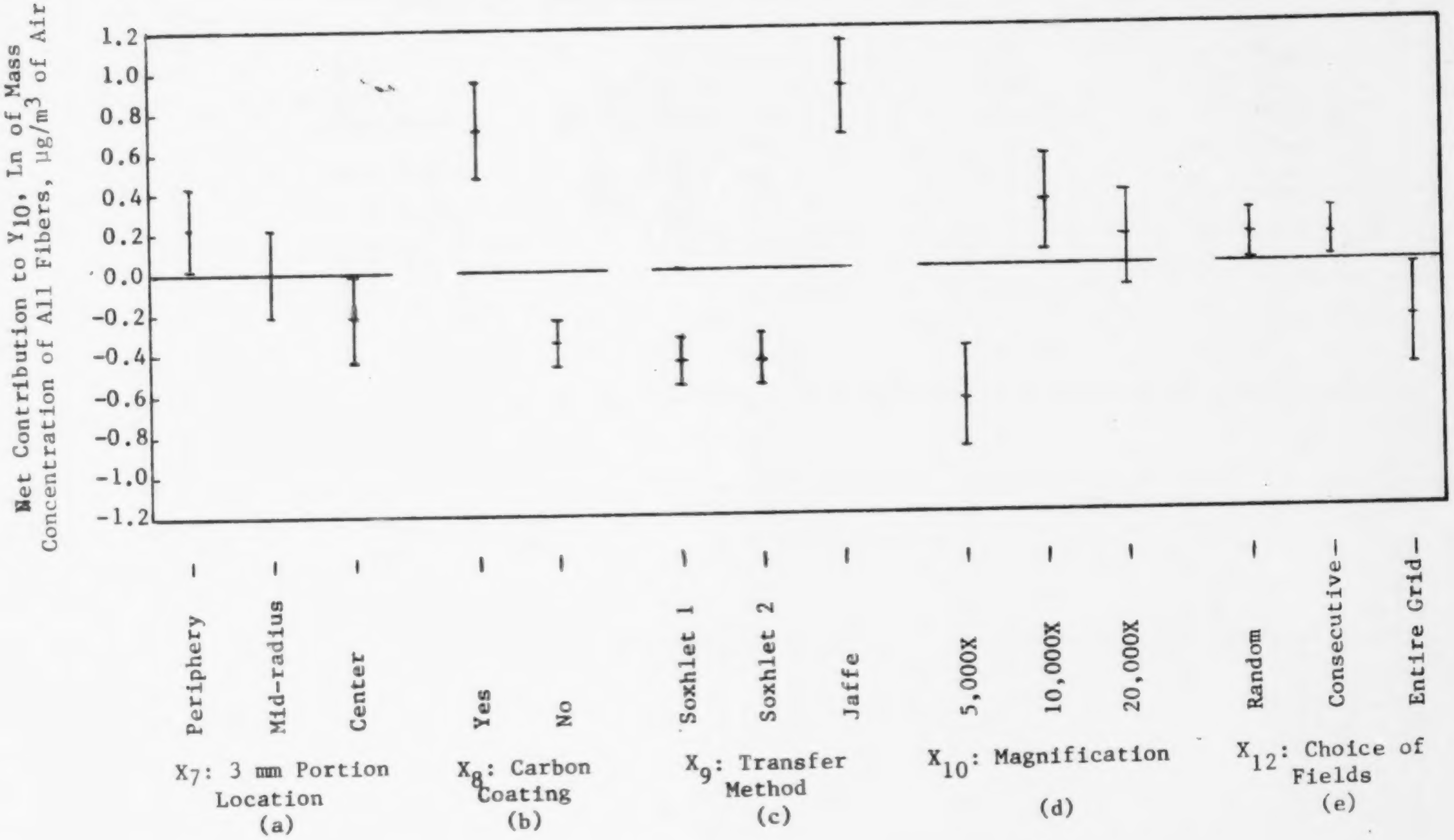

Figure 6. Graphical presentation of performance equation 10 in Phase 1. Net contribution to natural log of mass concentration of all fibers, µg/m^3 of air.

X_1 Composition of Sample: This variable affects the total fiber count estimate. The composition level 2 (viz, 60% chrysotile plus 40% amosite) gives a higher value than either the composition 1 or the composition 3. The variable X_1 also affects the mass concentration estimates, the composition 2 shows higher value than compositions 3 and 1. The probable reason for this is that the amosite fibers are generally blocky, whereas we assume a cylindrical geometry for computing the volume. This assumption of cylindrical shape tends to over-estimate the volume of amosite fibers.

X_2 Concentration on Filter: Light concentration gives the highest relative value for fiber count estimates and the heavy concentration gives the lowest relative value. Exactly the same trend is apparent for the mass concentration estimates. The most probable explanation of this is the possibility of aggregation of fibers in heavy concentration samples, leading to a failure to count all fibers.

X_3 Sampler Type: Personal sampler appears to give a higher value of fiber counts than the high-volume sampler. This variable has no significant effect on mass concentration estimates. One plausible explanation may be that the face velocity of particles in a personal sampler is 1/5th that in the high-volume sampler.

X_4 Filter Type: Millipore filters appear to give slightly higher mass concentration estimates than the Nuclepore; however, the filter type does not significantly affect the fiber count estimate.

X_5 Pore Size: Pore size between 0.2 and 0.8 μm does not significantly affect the fiber count estimate; on the other hand, the 0.4 μm filters appear to yield the highest mass concentration estimates.

X_6 Filter Side on Grid: Keeping the particle side up results in significantly lower fiber count estimate, but does not affect the mass concentration estimate. A probable explanation is that only the very small and fine fibers tend to be washed away and their mass is not appreciable. Keeping particle side down is the best method to avoid this type of fiber loss.

X_7 2.3 mm Portion Location: This variable has no significant effect, either on the fiber count estimate or the mass concentration estimate.

X_8 Carbon Coating: Carbon coating of the filter very definitely gives a higher value of fiber count estimate and also a higher value of the mass concentration estimate. These data give credence to the theory that the carbon coating locks the fibers in place and prevents their washing away.

X_9 Filter Transfer Method: The Jaffe method of filter dissolution gives the highest value of the fiber count estimate and also the highest value of the mass concentration estimate. Thus, these data bear out the contention of the advocates of the Jaffe method that the method is very gentle and slow and, hence, does not wash away any fibers. The Soxhlet method 2 gives the lowest value of fiber count estimate, presumably because of fiber loss due to extended duration of washings.

X_{10} Magnification: 20,000X magnification gives the highest value of the fiber count estimate, but the effect is very slight on the mass concentration estimate. The explanation is that with higher magnification, more fine and short fibers are visible; however, their volume contribution is quite small.

X_{11} Grid Opening Location: A mid-radius location gives low values of fiber count estimate, but does not significantly affect the mass concentration estimate. Presumably, small fibers may migrate from the center of the filter towards the periphery -- if it is not carbon coated, the effect being most noticeable at the mid-radius.

X_{12} Choice of Fields: Random and consecutively selected fields give similar values of the fiber count estimate and significantly higher values of the estimate than those for the entire grid opening. The same trend also holds for the mass concentration estimate. One possible explanation is that the operator may be unknowingly skipping empty fields (with no fibers), thus introducing a bias. Another possible explanation is that a full grid opening examined required a long time for fiber counting and often caused operator fatigue, which could have resulted in lower fiber count.

Optimum Choice of Variable Levels

It is a reasonable assumption that variable levels which give the highest values of the fiber count estimates (Y_9) and/or the mass concentration estimates (Y_{10}) are the optimum levels. (There is no reason to suspect external contamination, which could increase the fiber count or the mass concentration estimates. If fiber migration occurred, there will be some areas with higher true concentration but other areas will be lower in concentration.) Thus, high values are associated with efficiency of fiber retention, fiber recognition, counting, and sizing, and low values are associated with fiber loss, inefficient technique, etc.

Based on these assumptions, the best choices of variable levels for maximizing (Y_9 and Y_{10}) are summarized in Table 21. These choices are also compared with those based on the earlier chosen criteria of compliance with Poisson distribution and with the internal precision of fiber counts per field.

Though the optimum choice is somewhat dependent on the criterion chosen, many very remarkable trends emerge.

The variables X_3, X_4, and X_5 (air sampling variables) do not affect responses Y_9 and Y_{10}. However, considerations of Poisson distribution and better precision allow choice to be NP over MP as indicated in Table 21. Variable X_1 is not generally within one's control. Variable X_2 (concentration on filter) should be kept low (in practical ambient air monitoring applications this would not be a problem).

Among the variables of TEM grid preparation, variable X_7 (2.3 mm portion location) appears immaterial. Still, it is recommended to cut 2.3 mm portions from widely separated locations for duplicate of triplicate grids. Variable X_8 offers a clear-cut choice. Carbon-coating of filters is recommended for preserving the particulate integrity and distribution. Variable X_6 again offers a clear-cut choice. For transferring particles to carbon substrate, the particle side of the filter should be kept facing down, i.e., in contact with the carbon substrate. In variable X_9, the filter transfer method, the Soxhlet method 2 should be eliminated. Indications suggest the superiority of the Jaffe method and this is reinforced by the fact that it is less susceptible to operator technique.

Among the variables of TEM examination, variable X_{11}, the grid opening location of preference, is in the center or the peripheral regions. The variable X_{10}, the magnification, appears to give a clear choice of 10,000X. However, if we assume that the criterion of maximizing the fiber counts is more important than the mass concentration and the other criteria, then the choice is 20,000X. From a practical standpoint, higher resolution and higher magnifications are important for detecting the very fine fibers [46] which may have a greater chance of remaining airborne. Therefore, we recommend a magnification of 20,000X be used for fiber counting, sizing, and studying morphology. For cases

Table 21

OPTIMIZATION OF VARIABLE LEVELS ACCORDING TO FOUR DIFFERENT CRITERIA

Variable	Level	Sq. Root of Est. No. of Fibers/cm^3	Ln Est. Mass Conc. µg/m^3	Poisson-Distr. Compliance	Precision in Fiber count/field	Remarks
X_1 Composition	1					
	2	Highest	Highest			
	3					
X_2 Loading	L	Highest	Highest			A low loading level is certainly preferable. However, this requires covering several grid openings for counting enough number of fields.
	M			Best		
	H					
X_3 Sampler	Hi-Vol					Variable X_3 is probably insignificant.
	Personal	Higher				
X_4 Filter Type	N.P.			Better	Better	Nuclepore appears a better choice.
	M.P.		Higher			
X_5 Pore Size	0.2				Best	Pore size smaller or equal to 0.4 µm is preferable.
	0.4		Highest			
	0.8					
X_6 Particle Side	Down	[Higher]	[Higher]	[Better]		Keeping particle side down is definitely better and must be adopted for transferring fibers to carbon substrates.
	Up					
X_7 3 mm Portion Loc.	Peri		Highest			Variable X_7 is probably insignificant. Duplicate grids should be prepared from different locations.
	MR					
	Ctr				Best	
X_8 Carbon Coating	Yes	[Higher]	[Higher]		[Better]	Carbon coating of filter is certainly better and should form a necessary step in sample processing.
	No					
X_9 Filter Transfer	Soxhlet 1	(2nd Highest)			Best	More work needed for deciding between Soxhlet 1 and Jaffe. Soxhlet 2 should be eliminated.
	Soxhlet 2					
	Jaffe	[Highest]	[Highest]	[Best]	(2nd Best)	
X_{10} Magnification	5,000					5,000X is too low to give reliable EM estimates. While 10,000X appears best overall, 20,000X is preferred when fiber count concentration and detection of small fibers is more important than mass concentration estimate.
	10,000		Highest	Best	Best	
	20,000	Highest	(2nd Highest)			
X_{11} Grid Opening Loc.	Peri					Variable X_{11} is probably insignificant. Grid openings should be chosen from all locations with equal frequency.
	MR	Low			Best	
	Ctr					
X_{12} Choice of Fields	Random	[High]	[High]		[Best]	Though random choice of small fields is best, in practice, it is easier to use full grid opening, which eliminates the fibers crossing the field of view.
	Consecutive	High	High			
	Full Grid	Low	Low			

[ ] Best Choice, ( ) 2nd Best Choice

where majority of fibers are of amphibole asbestos, a lower magnification (e.g., 10,000X) may be sufficient.

Variable X_{12}, the choice of fields, appears to give the random choice of small fields as the best in all respects. However, in practice, this can cause problems in counting fibers longer than the field of view and also fibers extending beyond the perimeter of the field of view. Also, the operator unknowingly may tend to skip empty fields, thereby introducing a bias. These difficulties can be avoided by using full grid opening as one field. If the fiber concentration is low enough, there will be no operator fatigue.

MASS CONCENTRATION ESTIMATES

In addition to fiber number concentration, the mass concentration of asbestos in air may be an important parameter. Table 22 lists the details of the air sampling parameters, namely, the effective filter area (Column 2), the volume of air filtered in leters (Column 3), the air volume filtered per cm^2 of the filter (Column 4). It also lists the total area examined in the EM (Column 5), the observed fiber counts (Column 6), the estimate of fibers per ml of air (Column 7), the total volume over all fibers observed (Column 8), fiber density (weighted average) (Column 9), and estimated mass concentration $\mu g/m^3$ in air (Column 10).

Comparison of Observed Mass Concentrations with Those Expected

When we compare the estimated mass concentration values from Table 22 with those from Table 11 as expected from the aerosol generation parameters, we find there is a substantial difference. The EM estimates are smaller by a factor of 100-300 in samples 1 to 18 and by a factor of 300-1,000 in samples 19 to 27.

Sample 11 gives a substantially larger value than all the rest. This is explained by the fact that a few very large fibers were detected in this sample, as listed below. The 203 fibers counted had a total volume of 11.19 μm^3. The three large fibers listed below account for 7.5 μm^3 of the volume (see p. 69).

The detection of these large fibers indicates that the large fraction of the total mass is accounted for by a few large fibers in the aerosol chamber. It is likely that these large fibers have settled by gravity rather than being drawn onto the filter by the air sampler's suction. Another possible explanation is that the air circulating fan might have acted as an impactor and removed

Table 22

ESTIMATES OF NUMBER AND MASS CONCENTRATION OF ALL FIBERS PER UNIT VOLUME OF AIR, PHASE 1

Samples	Filter Area, cm^2	Air Vol. Filtered, liters	Air Vol. per Unit Area, 1/cm^2	Area Scanned, 10^{-6}cm^2	Obs. Fiber Count	Est. Fibers per cm^3 of Air	Obs. Fiber Volume, μm^3	Fiber Density,* g/cm^3	Est. Mass Concentration, All Fibers, μg/m^3
1	6.7	32	4.78	200	144	151	0.383	2.43	0.974
2	6.7	32	4.78	864	210	51	1.726	2.43	1.016
3	6.7	32	4.78	53	164	647	0.470	2.43	4.508
4 & 34	406.5	9116	22.43	85	423	222	1.302	2.43	1.660
5	406.5	9200	22.63	104	201	85	0.422	2.43	0.436
6	406.5	8400	20.66	288	178	30	0.507	2.43	0.207
7	6.7	512	76.42	72	269	49	2.472	2.43	1.092
8	6.7	512	76.42	16	237	194	1.386	2.43	2.754
9	6.7	512	76.42	18	221	161	0.436	2.43	0.770
10	406.5	2080	5.12	69	60	170	0.167	2.58	1.220
11	406.5	2030	4.99	108	203	377	11.194	2.58	53.590
12	406.5	2040	5.02	576	210	73	1.057	2.58	0.943
13	6.7	124	18.51	72	695	521	2.285	2.58	4.424
14	6.7	124	18.51	200	140	38	3.844	2.58	2.679
15	6.7	124	18.51	76	208	148	1.121	2.58	2.056
16	6.7	513	76.57	4.25	218	670	0.348	2.58	2.759
17	6.7	513	76.57	144	218	19.8	0.751	2.58	0.176
18	6.7	513	76.57	28	200	93	0.678	2.58	0.816
19	6.7	7.6	1.13	1080	196	161	1.778	2.54	3.700
20 & 120	6.7	7.6	1.13	125	57	404	0.093	2.54	1.672
21 & 121	6.7	7.6	1.13	421	61	128	0.241	2.54	1.287
22	6.7	29.2	4.36	800	34	9.7	0.362	2.54	0.264
23	6.7	29.2	4.36	288	227	181	0.492	2.54	0.995
24	6.7	29.2	4.36	186	200	247	0.674	2.54	2.111
25	406.5	7920	19.48	816	169	10.6	0.811	2.54	0.130
26	406.5	7701	18.94	35	205	309	0.587	2.54	2.249
27	406.5	9167	22.55	504	249	21.9	8.383	2.54	1.874

* Fiber density refers to the average density for all mineral fibers considering their weight proportions, in the mixture used.

UNUSUALLY LARGE FIBERS DETECTED
IN SAMPLE 11

Fiber No.	L μm	W μm	Volume (μm)^3
5	9.4*	0.9	6.1
99	5.6*	0.56	1.12
110	1.25*	0.5	0.25

* All of these fibers extended beyond the field perimeter; hence, these lengths represent only underestimates of the true length.

a substantial amount of asbestos from the air in the aerosol chamber. Sample Number 11 was collected on a high-volume sampler with a large surface area (406.5 cm^2). It is only by chance that their presence within the areas randomly selected on the grid was noted. This example points out the large bias introduced by a few large fibers in the estimate of the total volume and, hence, in the total mass concentration.

SECTION 8

RESULTS AND DISCUSSION OF PHASES 2, 3, 4 AND 5

PHASE 2 RESULTS

In the Phase 2 analysis, two types of fiber classification were used. The "standard classification" method allowed six categories, viz, chrysotile, amosite, crocidolite, wollastonite, ambiguous, and other. In the "alternative classification" method, only four categories were allowed, viz, chrysotile, amosite, crocidolite, and wollastonite. This is, in the alternative classification method, the ambiguous and other fibers were assigned to one of the four categories based on the best operator judgment. For example, if a sample was studied using morphology, diffraction, and X-ray, the standard classification was based on all three tests simultaneously. Any fiber not giving a characteristic diffraction pattern or X-ray analysis was classified as ambiguous. In the alternative classification method, such fibers were assigned to the four mineral categories based on other available information. For example, a fiber that did not give a recognizable diffraction pattern, but gave a recognizable X-ray analysis, was classified based on X-ray analysis and/or morphology. Similarly, a fiber that did not give a distinct X-ray analysis was classified based on electron diffraction and/or morphology. The category "other" includes fibers for which X-ray and/or diffraction measurements could not be made.

In the standard classification method, ambiguous and other categories constitute a variable percentage of the fibers. Since the ambiguous and other categories cannot be assigned any fixed density, their mass concentration is subject to error. The difficulty is avoided, although not eliminated, in the alternative classification method, where there are no ambiguous and other categories. The ambiguous and other fibers combined will be designated "exceptional".

Phase 2 Data

Specified properties of the population of individual fibers in each of the nine Phase 2 samples were determined by application of IITRI computer program SIZ1. The results of the data reduction are presented in Tables 23 through 26.

The fiber counts are given in Table 23 for the six fiber categories allowed under the standard classification method and the four categories allowed under the alternative classification method. Additional items of information per sample are: the total fiber count, the area scanned (in units of 10^{-4} cm^2), and the number of grid openings. The area per grid opening was 0.72×10^{-4} cm^2. The area examined in the case of each of the last two samples was a portion of a grid opening. Column 14 lists the total time on TEM for studying each sample.

The estimated number concentration (in units of $10^6/cm^2$ of filter) and mass concentration (units of 10^{-9} gm/cm^2 of filter) are given in Table 24 for fibers classified as chrysotile under the standard and alternative classification methods. The 95% confidence limits for the number concentrations were calculated by the computer program POISSON 2 under the assumption of a Poisson distribution of the fibers. The listing for POISSON 2 is given in Appendix C.

This table also lists the total TEM time for inspecting 100 fibers in each sample, which is a measure of the experimental effort required. It is quite evident that the experimental effort required is substantially dependent on the method of analysis. For example, the method based on morphology and electron diffraction requires the least time and, hence, should be considered preferable among the three methods.

The size distributions of the individual chrysotile fibers within each sample as classified by the two methods, are characterized in Table 25. The properties treated are: fiber length (micrometers), fiber diameter or width (micrometers), and fiber mass (units of 10^{-12} gm). For each quantity, the geometric mean and the mean and standard deviation of the natural logarithms (to the base e) are given.

The estimated number concentration of all fibers combined, and of fibers classified as ambiguous and other under the standard classification method, are listed by sample in Table 26. Also listed are the percentages of the total fibers classified as ambiguous, other, and exceptional (ambiguous and other combined).

Table 23

NUMBERS OF FIBERS OBSERVED AND CLASSIFIED, PHASE 2 SAMPLES

Sample Description Code*	Area Scanned 10^{-4} cm^2	No. Fibers Total	Standard Classification Method						Alternative Classification Method				Total Time on TEM Hrs.
			Chrys-otile	Amo-site	Crocid-olite	Wollas-tonite	Ambig-uous	Other	Chrys-otile	Amo-site	Crocid-olite	Wollas-tonite	
2113	1.44(2)†	149	93	0	0	0	50	6	149	0	0	0	9.0
2121	0.72(1)	114	64	1	0	0	49	0	113	1	0	0	6.0
2132	2.16(3)	228	209	0	0	0	1	18	228	0	0	0	4.0
2211	0.72(1)	137	117	10	0	0	10	0	125	12	0	0	7.0
2222	1.44(2)	287	221	11	0	0	22	33	276	11	0	0	3.5
2233	0.72(1)	227	130	4	0	0	93	0	223	4	0	0	12.0
2312	0.72(1)	398	204	0	43	100	45	6	219	0	56	123	7.0
2323	0.34(1)	188	56	0	38	3	57	34	85	0	94	9	10.5
2331	0.14(1)	176	39	0	61	36	11	29	58	0	72	46	8.0
Combined	8.40(13)	1904	1133	26	142	139	338	126	1476	28	222	178	

* For explanation of the sample description code, see Tables 7 and 12.

† Number in parentheses is number of grid openings.

Table 24

CONCENTRATIONS OF CHRYSOTILE FIBERS, PHASE 2 SAMPLES

Sample Description Code*	Identification Method Used†	Number Concentration Estimate, $10^6/cm^2$ of Filter**	Mass Concentration Estimate, 10^{-9} gm/cm^2 of Filters	TEM Time for Studying 100 Fibers, Hrs.
		STANDARD CLASSIFICATION METHOD		
2113	M+D+X	0.646 (0.521, 0.791)	4.781	6.04
2121	M+X	0.889 (0.684, 1.135)	7.138	5.26
2132	M+D	0.968 (0.841, 1.108)	9.818	1.75
2211	M+X	1.625 (1.344, 1.948)	14.731	5.10
2222	M+D	1.535 (1.339, 1.751)	15.528	1.22
2233	M+D+X	1.806 (1,508, 2.144)	10.742	5.29
2312	M+D	2.833 (2.458, 3.250)	26.008	1.76
2323	M+D+X	1.647 (1.244, 2.139)	25.190	5.59
2331	M+X	2.786 (1.981, 3.808)	35.007	4.54
		ALTERNATIVE CLASSIFICATION METHOD		
2113		1.035 (0.875, 1.215)	6.126	
2121		1.569 (1.293, 1.887)	10.527	
2132		1.056 (0.923, 1.202)	9.959	
2211		1.736 (1.445, 2.069)	14.787	
2222		1.917 (1.697, 2.157)	16.857	
2233		3.097 (2.704, 3.532)	20.586	
2312		3.042 (2.652, 3.472)	29.385	
2323		2.500 (1.997, 3.091)	37.133	
2331		4.143 (3.145, 5.356)	48.340	

* For explanation of the sample description code, see Tables 7 and 12.

** Numbers in parentheses are 95% confidence limits based on the Poisson distribution.

† M+D refers to morphology + electron diffraction,
M+X refers to morphology + X-ray analysis, and
M+D+X refers to morphology + electron diffraction + X-ray analysis.

Table 25

SIZE DISTRIBUTIONS OF CHRYSOTILE FIBERS, PHASE 2 SAMPLES

	Fiber Length, μm			Fiber Width, μm			Fiber Mass, 10^{-12} g		
Sample Description Code*	Geom. Mean	Mean Ln	St. Dev. Ln	Geom. Mean	Mean Ln	St. Dev. Ln	Geom. Mean	Mean Ln	St. Dev. Ln
STANDARD CLASSIFICATION METHOD									
2113	0.7931	-0.2318	0.7899	0.0467	-3.0634	0.4070	0.00354	-5.6557	1.3246
2121	0.8238	-0.1938	0.6754	0.0521	-2.9549	0.3888	0.00456	-5.3896	1.1463
2132	0.8162	-0.2032	0.8270	0.0531	-2.9349	0.3597	0.00471	-5.3589	1.3381
2211	0.7287	-0.3165	0.8657	0.0522	-2.9532	0.3744	0.00405	-5.5090	1.3566
2222	0.7565	-0.2791	0.7700	0.0515	-2.9670	0.4442	0.00409	-5.4991	1.3878
2233	0.7413	-0.2993	0.7387	0.0483	-3.0297	0.3209	0.00354	-5.6448	1.1215
2312	0.8747	-0.1339	0.6119	0.0584	-2.8409	0.3036	0.00609	-5.1017	0.9960
2323	0.9651	-0.0355	0.5990	0.0687	-2.6786	0.3426	0.00929	-4.6789	1.0828
2331	1.0466	0.0456	0.6468	0.0644	-2.7423	0.2696	0.00887	-4.7250	0.8529
ALTERNATIVE CLASSIFICATION METHOD									
2113	0.6780	-0.3886	0.7968	0.0438	-3.1275	0.4200	0.00266	-5.9297	1.3575
2121	0.6996	-0.3573	0.7142	0.0507	-2.9821	0.3929	0.00367	-5.6076	1.1996
2132	0.7587	-0.2761	0.8366	0.0521	-2.9554	0.3600	0.00420	-5.4730	1.3548
2211	0.6737	-0.3590	0.8929	0.0503	-2.9896	0.3962	0.00348	-5.6602	1.4462
2222	0.7028	-0.3527	0.7761	0.0499	-2.9987	0.4337	0.00357	-5.6362	1.3677
2233	0.7254	-0.3210	0.8281	0.0471	-3.0553	0.3547	0.00329	-5.7178	1.2635
2312	0.8467	-0.1664	0.6463	0.0594	-2.8236	0.3151	0.00610	-5.0998	1.0213
2323	0.9912	-0.0088	0.5988	0.0669	-2.7044	0.3611	0.00906	-4.7036	1.0705
2331	0.8214	-0.1967	0.7339	0.0654	-2.7277	0.3296	0.00717	-4.9381	1.0018

---

* First digit of the sample description code refers to the phase number; second, third, and fourth digits refer to the levels of independent variables used. For further explanation of the sample description code, see Tables 7 and 12.

Table 26

CONCENTRATIONS OF ALL FIBERS AND OF FIBERS OF "AMBIGUOUS" AND "OTHER" CATEGORIES, PHASE 2 SAMPLES

	All Fibers	Ambiguous Fibers		Other Fibers		All Exceptional Fibers
Sample Description Code*	Number Concentration Estimate, $10^6/cm^2$ of Filter	Number Concentration Estimate, $10^6/cm^2$ of Filter	Percent of Total Fibers	Number Concentration Estimate, $10^6/cm^2$ of Filter	Percent of Total Fibers	Percent of Total Fibers
2113	1.035	0.347	33.56	0.0416	4.03	37.59
2121	1.583	0.680	42.98	0.0	0.0	42.98
2132	1.056	0.0046	0.44	0.0833	7.89	8.33
2211	1.903	0.139	7.30	0.0	0.0	7.30
2222	1.993	0.153	7.66	0.2291	11.50	19.16
2233	3.153	1.291	40.97	0.0	0.0	40.97
2312	5.528	0.625	11.31	0.0833	1.51	12.81
2323	5.529	1.676	30.32	1.000	18.08	48.40
2331	12.571	0.786	6.25	2.071	16.48	22.73

* First digit of the sample description code refers to the phase number; second, third, and fourth digits refer to the levels of independent variables used. For further explanation, see Tables 7 and 12.

Methods of Data Analysis

Statistical methods applied in the analysis of the Phase 2 data are as follows.

Confidence limits for number concentrations were calculated by IITRI program POISSON 2 (Appendix C) under the assumption of a random distribution of fibers on the grid.

Multiple regression analyses were made on each of the sets of dependent variables defined below by means of a modified version of the stepwise regression program BMDO2R from the BMD package of statistical programs [59]. The data input for each regression analysis included the orthogonally coded values of the independent variables given in Table 7 (X_1L, X_1Q, X_9L, X_9Q, $X_{13}L$, $X_{13}Q$) in addition to the values of the dependent variables.

Regression Equations

The dependent variables for the regression analyses have the following symbols and definitions.

Symbol	Definition
Y_{11}	Square root of the estimated number concentration of chrysotile fibers in units of millions per cm^2 of filter
Y_{12}	Natural logarithm of the estimated mass concentration of chrysotile fibers in units of nanograms per cm^2 of filter
Y_3	Natural logarithm of the geometric mean length of chrysotile fibers in micrometers
Y_1	Natural logarithm of the geometric mean width of chrysotile fibers in micrometers
Y_{14}	Natural logarithm of the geometric mean mass of chrysotile fibers in units of 10^{-12} grams
Y_{15}	Square root of the estimated number concentration of all fibers in units of millions per cm^2 of filter
Y_{13}	Arcsine of the square root of the proportion of all fibers classified as exceptional (ambiguous or other) using the standard classification method

There are nine values of each dependent variable, i.e., one value per Phase 2 sample.

The number concentration estimates were subjected to the square root transformation (Y_{11} and Y_{15}). The mass concentration estimates and the geometric mean fiber lengths, widths, and masses were subjected to the logarithmic transformation (Y_{12}, Y_3, Y_1, and Y_{14}). The exceptional fiber percentages were subjected to the arcsine-square-root transormation (Y_{13}). The selected transformations are often employed in analyzing the effects of independent variables on three kinds of dependent variables by means of analysis of variance or regression analysis [56,57].

The 12 regression equations constructed from the Phase 2 data are given in Table 27. In each equation, only those candidate independent variables appear that have effects that are significant at the 10% probability level. The method of equation construction is described in Appendix B.

Some overall properties of the equations are given in Table 28: the number of residual degrees of freedom, the residual standard deviation, and the degree of determination, R^2. R^2 ranges from 73 to 98% in the group of equations, signifying that the values of the dependent variables are, in general, strongly influenced by the independent variables included in the equations.

The first six equations are based on data in which fibers were classified by the standard method. The next five equations are based on data in which fibers were classified by the alternative method. The final equation refers to the number concentration of all types of fibers combined, and hence the method of fiber classification is not applicable.

Discussion of Phase 2 Results

The results obtained in Phase 2 will be considered in relation to the three factors that were systematically varied in the experiment design: (1) the three different filter preparations; (2) the three transfer methods; and (3) the three techniques of fiber identification, with the further contrast between the standard and alternative methods of classifying fibers.

The Three Filter Compositions--

In the Phase 2 experiment design (Table 7), it was the intent to vary the fiber composition in the preparation of the three filters, with essentially pure chrysotile on the first filter, a mixture of chrysotile plus amosite on the second filter, and a mixture of chrysotile plus crocidolite plus wollastonite on the third filter. The results of EM examination confirm that this aim was achieved (Table 23), the only evidence of contamination being the single amosite fiber in a sample from the first filter, intended to be pure chrysotile (sample 2121). Based on the counts made by the alternative classification method, about

Table 27

PHASE 2 REGRESSION EQUATIONS

STANDARD METHOD OF FIBER CLASSIFICATION

(1) $Y_{11} = 1.247 + 0.318(X_1L)$

(2) $Y_{12} = 2.629 + 0.704(X_1L) + 0.117(X_9L) - 0.174(X_{13}L) - 0.066(X_{13}Q)$

(3) $Y_3 = -0.183 + 0.084(X_1L) + 0.058(X_1Q) + 0.038(X_9L)$

(4) $Y_1 = -2.907 + 0.116(X_1L) + 0.038(X_1Q)$

(5) $Y_{14} = -5.283 + 0.315(X_1L) + 0.134(X_1Q)$

(6) $Y_{13} = 0.523 - 0.062(X_9Q) + 0.103(X_{13}L) + 0.076(X_{13}Q)$

ALTERNATIVE METHOD OF FIBER CLASSIFICATION

(7) $Y_{11} = 1.458 + 0.344(X_1L)$

(8) $Y_{12} = 2.876 + 0.735(X_1L) + 0.219(X_9L)$

(9) $Y_3 = -0.274 + 0.108(X_1L) + 0.041(X_1Q)$

(10) $Y_1 = -2.929 + 0.135(X_1L) + 0.043(X_1Q)$

(11) $Y_{14} = -5.418 + 0.378(X_1L) + 0.126(X_1Q)$

METHOD OF FIBER CLASSIFICATION NOT APPLICABLE

(12) $Y_{15} = 1.791 + 0.824(X_1L)$

Table 28

PROPERTIES OF PHASE 2 REGRESSION EQUATIONS

Equation Number	Method of Fiber Classification	Dependent Variable	Residual Degrees of Freedom	Residual Standard Deviation	R^2 Percent
1	Standard	Y_{11}	7	0.1380	82
2	"	Y_{12}	4	0.1276	98
3	"	Y_3	5	0.0428	92
4	"	Y_1	6	0.0664	80
5	"	Y_{14}	6	0.1679	84
6	"	Y_{13}	5	0.1002	82
7	Alternative	Y_{11}	7	0.1923	73
8	"	Y_{12}	6	0.1099	98
9	"	Y_3	6	0.0705	77
10	"	Y_1	6	0.0683	84
11	"	Y_{14}	6	0.1792	86
12	Inapplicable	Y_{15}	7	0.4487	74

99.8% of the fibers on the first filter were chrysotile; about 95.9% of the fibers on the second filter were chrysotile and about 4.1% were amosite; on the third filter about 47.5% of the fibers were chrysotile, 29.1% were crocidolite, and 23.4% were wollastonite.

The number and mass concentrations of chrysotile fibers on the three filters varied substantially. This is evident from the estimates of these quantities given in Table 24, with concurrence between the standard and alternative classification methods. (Note that the first group of three samples came from the first filter, the second group of three from the second filter, and the third group of three from the third filter.) The pattern is a marked increase in both the number and mass concentrations of chrysotile fibers in the progression from the first to the second to the third filter. This trend is also clearly revealed by equations 1, 2, 7, and 8 (Table 27) in which the linear variable associated with the filter preparations, X_1L, appears with positive coefficients.

The Three Transfer Methods--

The three transfer methods employed in grid preparation were: (1) Soxhlet 1, (2) Soxhlet 1 with carbon coating, and (3) Jaffe, also with carbon coating (Table 7). The candidate coded independent variables representing possible differences in performance of the transfer method are X_9L and X_9Q. The regression analysis revealed significant differences in relation to Y_{12}, i.e., natural logarithm of chrysotile mass concentration. Variable X_9L appears in both equations 2 and 8 with positive coefficients. The indicated effect is an increase in the estimated mass concentration of chrysotile fibers as the transfer method is changed from Soxhlet 1 to Soxlet 1 with carbon coating to Jaffe. The effect is manifest regardless of the method of fiber classification.

Further effects of transfer method are significant in two of the equations based on data in which the standard fiber classification method was employed, i.e., equations 3 and 6 (see Table 27). The dependent variable in equation 3 is Y_3, the natural logarithm of the geometric mean length of chrysotile fibers. The independent variable X_9L is in the equation with a positive coefficient. The effect brought out is a trend in the direction of increasing length of chrysotile fibers in changing from Soxhlet 1 to Soxhlet 1 with carbon coating to Jaffe. The dependent variable in equation 6 is Y_{13}, representing the percentage of fibers classified as exceptional under the standard classification method. In this equation, the independent variable X_9Q (having coded values of 1, -2, and 1) is present with a negative coefficient. The indicated effect is that the percentage of all fibers classified as exceptional tends to be higher when the transfer method is Soxhlet 1 with carbon coating than when the transfer method is either Jaffe or Soxhlet 1 without carbon coating.

The Three Fiber Identification Techniques--

The three techniques employed in identifying fiber types were: (1) morphology plus X-ray fluorescence, (2) morphology plus electron diffraction, and (3) morphology plus X-ray fluorescence plus electron diffraction (Table 7). The candidate coded independent variables representing possible differences in performance of the identification techniques are $X_{13}L$ and $X_{13}Q$. In the regression analyses, differential performance of the three techniques emerged as statistically significant in two of the equations, 2 and 6 (Table 27). The dependent variable in equation 2 is Y_{12}, natural logarithm of estimated mass concentration of chrysotile fibers on the filter. Independent variables $X_{13}L$ and $X_{13}Q$ are in the equation with negative coefficients. The pattern of effects is that the third technique of fiber identification (morphology in conjunction with both X-ray fluorescence and electron diffraction) tends to result in lower estimates of chrysotile mass concentration than the first two techniques. Note, however, that this effect was not significant when all fibers were assigned to the chemical species on the basis of the available evidence (alternative classification method).

The other equation in which the performance of the identification techniques differs has the dependent variable Y_{13}, which represents the percentage of fibers classified as exceptional. In this equation, No. 6, both $X_{13}L$ and $X_{13}Q$ are included with positive coefficients. The pattern of effects is that the third identification technique (morphology plus X-ray fluorescence plus electron diffraction) results in the highest percentage of exceptional (ambiguous or other) fibers, the second technique (morphology plus electron diffraction) results in the lowest percentage of exceptional fibers, while the first technique (morphology plus X-ray fluorescence) results in an intermediate percentage of exceptional fibers.

Selected Plots

Significant findings from the analysis of the Phase 2 data are illustrated by the confidence-interval plots of Figures 7 through 10. The estimated number

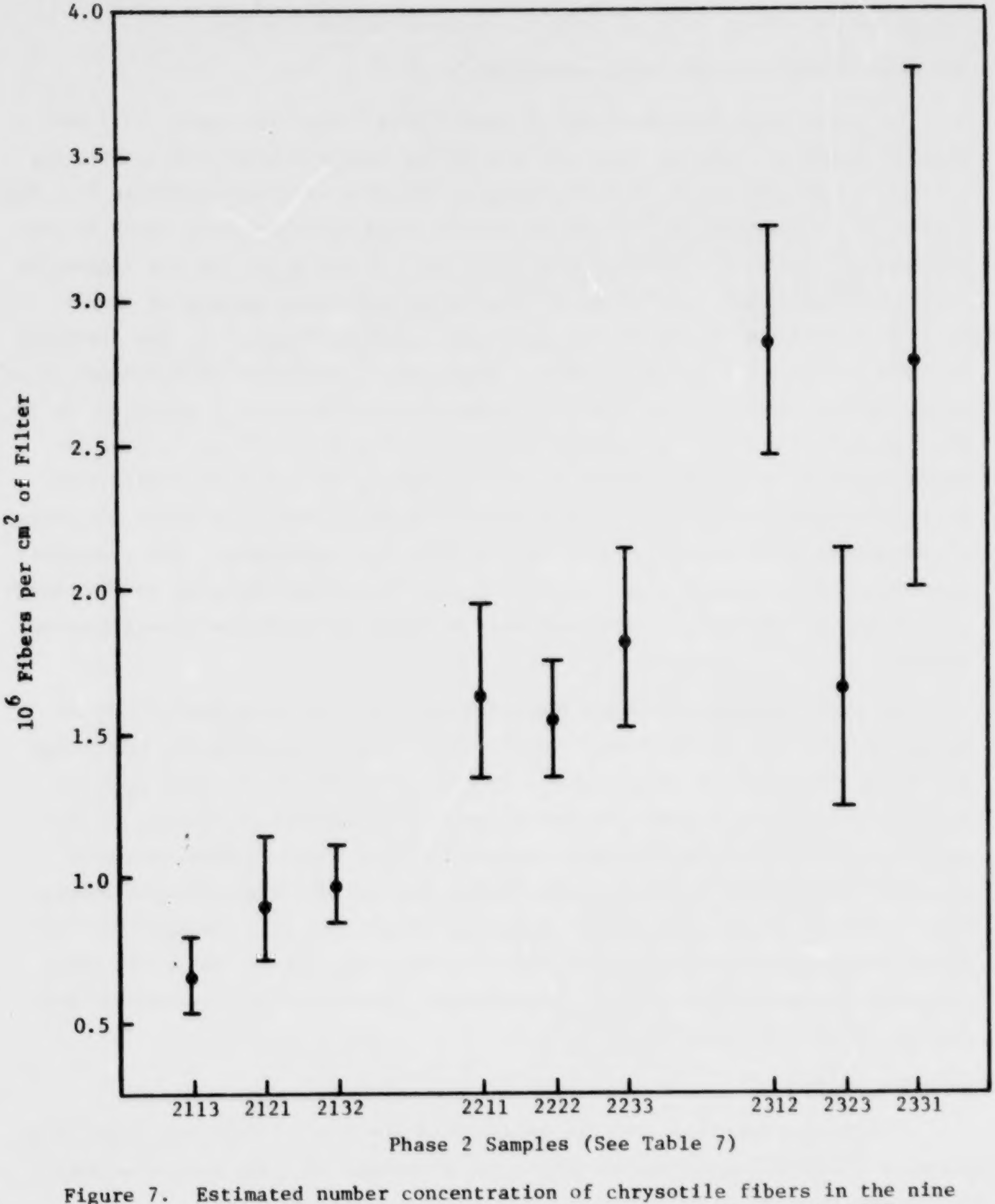

Figure 7. Estimated number concentration of chrysotile fibers in the nine Phase 2 samples (standard classification method), with 95% confidence intervals.

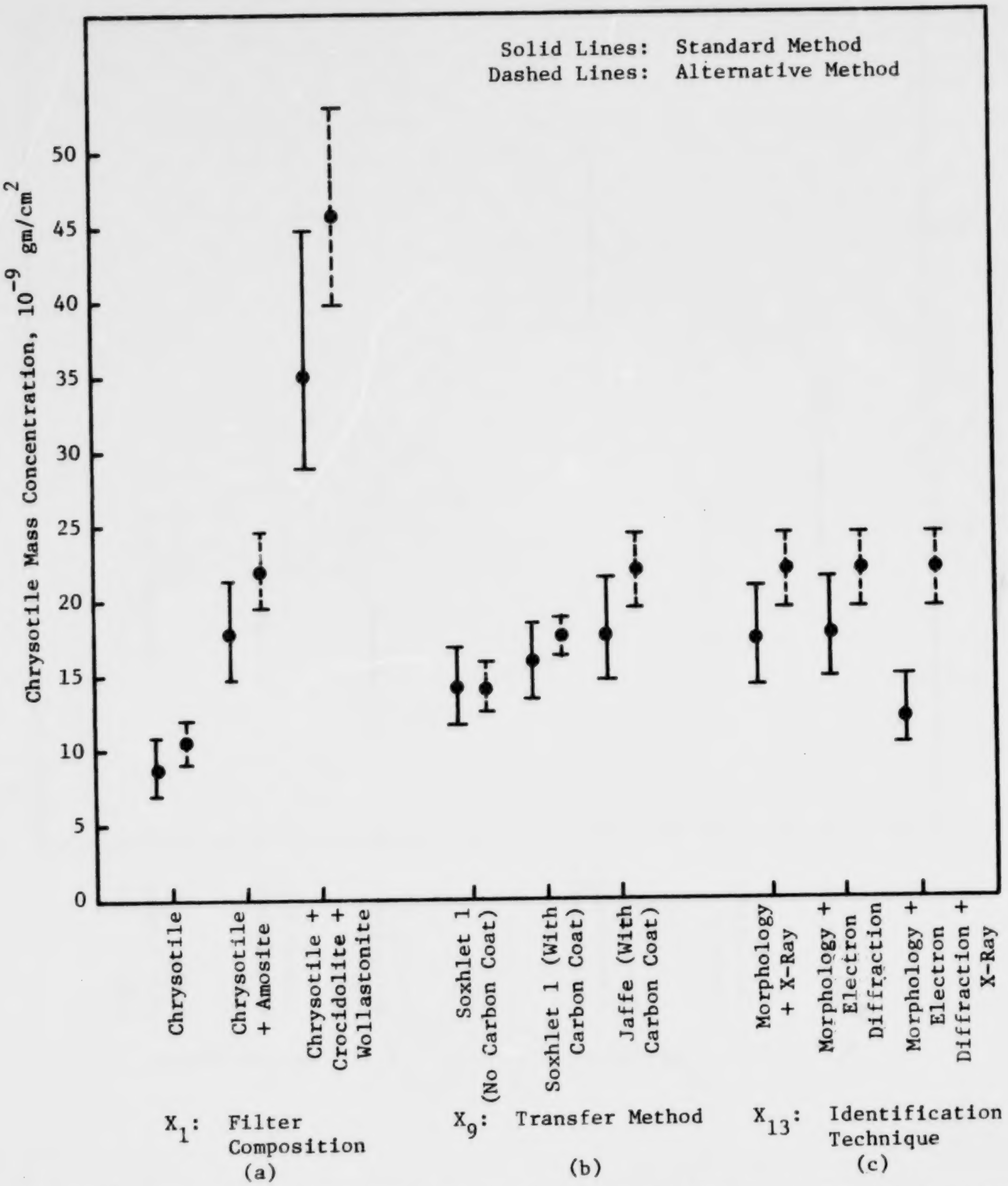

Figure 8. Estimated mass concentration of chrysotile fibers in Phase 2 (standard and alternative classification methods) in relation to filter composition, transfer method, and identification technique, with 90% confidence intervals.

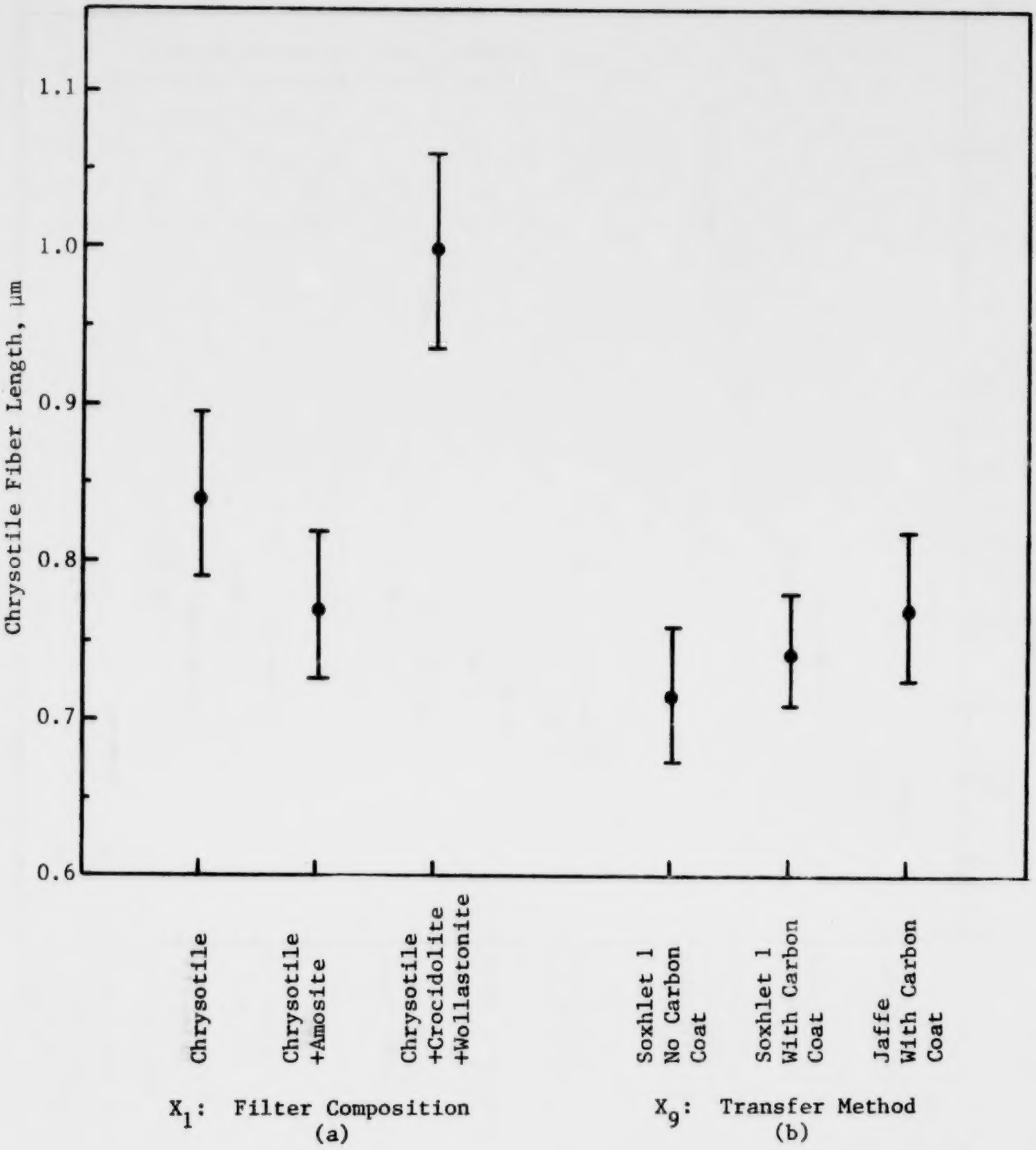

Figure 9. Estimated geometric mean length of chrysotile fibers in Phase 2 (standard classification method) in relation to filter composition and transfer method, with 90% confidence intervals.

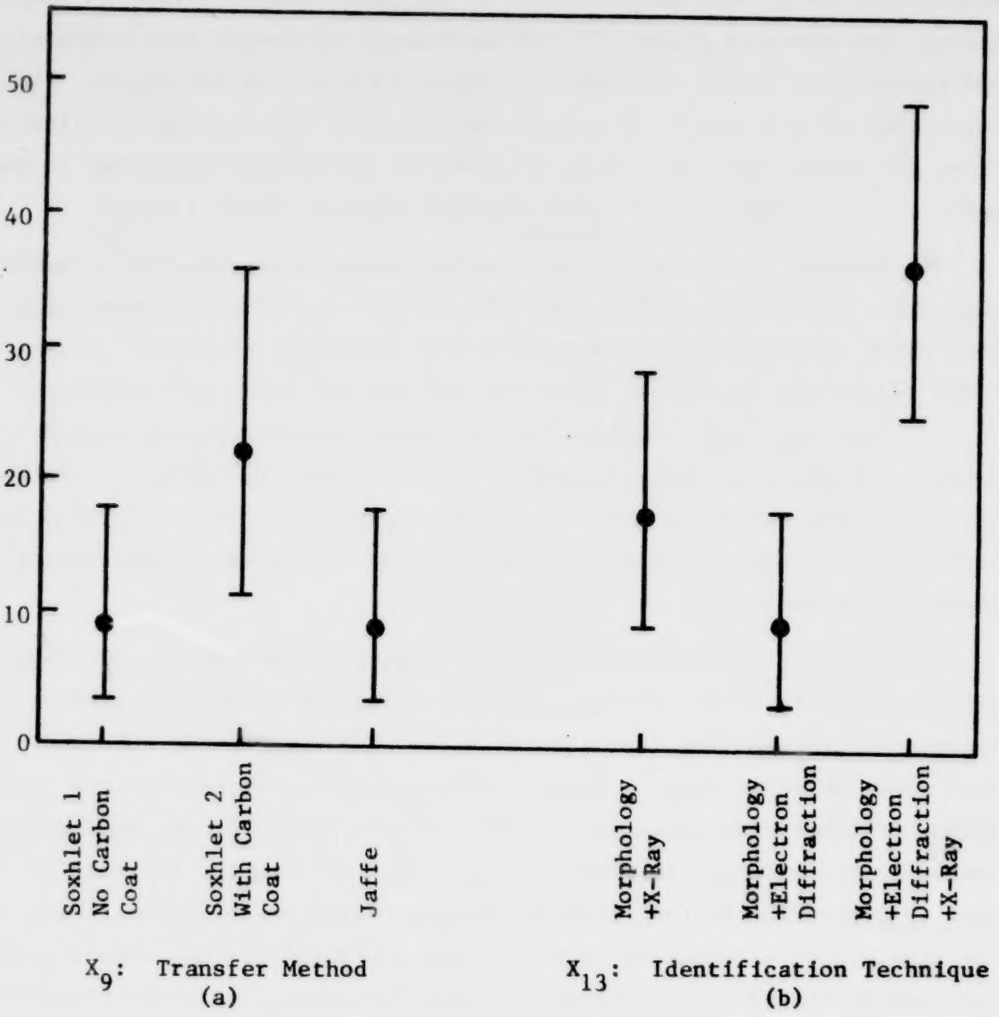

Figure 10. Estimated percent of all Phase 2 fibers that were exceptional (ambiguous or other by the standard classification method) in relation to transfer method and identification technique, with 90% confidence intervals.

concentrations of chrysotile fibers in the nine samples (standard classification method) are shown in Figure 7. The confidence intervals were computed at the 95% probability level, assuming a Poisson distribution of fibers. The increasing number concentration of chrysotile fibers in the successive filter preparations is clearly evident. Also apparent is substantial variation in the estimates of the number concentration between samples within filters.

In Figures 8, 9, and 10, the plotted values were computed from the Phase 2 regression equations, showing the effects of the controlled experimental factors. Each point estimate has an associated 90% confidence interval. First, the point values and confidence limits of the various dependent variables, i.e., Y_{12}, Y_3, and Y_{13}, were computed for specified combinations of values of the independent variables in the equations. Then the computed values of the dependent variables were converted back to customary physical units by inverse transformations, e.g., the exponential transformation of values of the logarithmic dependent variables.

Significant differences in estimated mass concentrations of chrysotile are displayed in Figure 8. Results obtained using the standard method of fiber classification, derived from equation 2, are denoted by the confidence intervals drawn as solid lines. Results obtained using the alternative (forced) method of fiber classification, derived from equation 8, are denoted by the dashed-line confidence intervals. There is a very marked increase in chrysotile mass concentration in the three successive filter preparations, based on either the standard or alternative method of fiber classification. The significant increase in the estimated chrysotile mass concentration as the transfer method is changed from Soxhlet 1 without carbon deposition to Soxhlet 1 with carbon deposition, and finally to Jaffe, is also evident regardless of fiber classification method. With respect to identification technique, the significant contrast is between the third technique (morphology together with both X-ray fluorescence and electron diffraction) versus the other two when the standard classification method is used: under these conditions the requirement of a consensus of morphological, X-ray, and electron evidence understandably tends to result in a lower estimate of the chrysotile mass concentration. The contrast disappears, however, when the exceptional fibers are assigned to the most probable chemical species.

Figure 9 illustrates the significant contrasts that are implicit in equation 3. Geometric mean length of chrysotile fibers was smallest in the second filter preparation, largest in the third. Estimated geometric mean fiber length increased in step with the three qualitative levels of transfer method, with the Jaffe method indicated to result in somewhat the longest fibers.

Factors influencing the percent of all fibers classified as ambiguous or other under the standard classification method, are illustrated in Figure 10, based on equation 6. Considering the three transfer methods tested, Soxhlet 1 with carbon deposition appears to result in a somewhat higher percentage of exceptional fibers than the other two methods. The identification technique of electron diffraction in conjunction with fiber morphology resulted in the lowest percentage of exceptional fibers, the combined technique of both X-ray fluorescence and electron diffraction in conjunction with morphology resulted in the highest percentage.

Summary

The Phase 2 data support the choice of the Jaffe method of transfer of fibers to the EM grid and the choice of electron diffraction plus morphology as the technique for fiber identification.

RESULTS AND DISCUSSION OF PHASE 3

Phase 3 Objectives

Phase 3 evaluated the capabilities of two instruments working in the secondary electron imaging (SEM) mode. Both instruments were capable of analyzing small particles by means of an X-ray fluorescence probe. The instruments were the JEOL JSM 50A, a modern high quality instrument designed primarily for SEM operation; and the JEOL 100C analytical electron microscope. Identical areas on marker grids were observed using the two microscopes. A pseudo-random sequence was used in analyzing samples to avoid biases. The data from Phase 3 are summarized in Table 29.

Discussion of Phase 3 Results

The results from Phase 3 were not subjected to statistical analysis because the information needed from Phase 3 could be obtained by a less rigorous evaluation of the data. Additionally, because of the need for key-punching, computer runs, and statistical analysis, the total analysis becomes very time consuming.

The results from tests 1, 2, 5, and 6 gave the difference in the values obtained for fiber counts when the identical areas were observed using the JEOL 100C and JSM 50A instruments, both in SEM mode. In the two instances where

Table 29

SUMMARY OF PHASE 3 DATA

Test No.	Composition[1]	Identification Method[2]	Instrument Used for SEM	Total Area Examined x 10^{-4} cm^2	Total No. of Fibers	Number of Fibers of Each Type of Fiber				
						Chrysotile	Amosite	Crocidolite	Wollastonite	Ambiguous
1	1	M	100C	2.16*	104	104				
2	1	M+X	50A	2.16*	88	58				
3	1	M	100C	2.16	127	127				
4	2	M+X	100C	1.44	50	23	3			24
5	2	M	100C	1.44**	114	106	8			
6	2	M	50A	1.44**	87	74	13			
7	3	M	50A	0.72	42	31		6	5	
8	3	M	100C	0.72***	126	106		12	8	
9	3	M+X	100C[3]	0.72***	153	58		53	9	33

[1] Mixture Composition

1. Chrysotile
2. Chrysotile and Amosite
3. Chrysotile and Crocidolite and Wollastonite

[2] M = Morphology
X = X-ray Analysis

[3] 100C used in STEM Mode

*,**,*** Identical Areas Examined

a direct comparison was made, the JEOL 100C gave higher number of fibers; 18% higher from tests 1 and 2, and 31% higher from tests 5 and 6. A further comparison was made between the use of the scanning transmission mode (STEM), test 9, and the SEM mode, test 8, both measuring fibers on identical areas using the JEOL 100C instrument. The test showed a significant improvement on the fiber count, 21%, when using the STEM mode. The reason for the increase in the fiber count was observed under the JSM 50A and JEOL 100C using the SEM mode and the JEOL 100C using the STEM mode probably results from the respective resolution capabilities of the instruments. The claimed resolution limits of the JSM 50A and JEOL 100C in SEM mode and the JEOL 100C in STEM mode are claimed to be 7 nm, 4 nm, and 2 nm, respectively. In addition, the STEM mode gives an image on the fluorescent screen with higher contrast and consequently fibers are more obvious. One reason for the improved resolution results from the higher accelerating voltage (100 kv) used with the JEOL 100C as opposed to the 40 kv used with the JSM 50A.

Tests were made to consider the difference in the fiber counts when *different areas* were observed using the same instrument. From tests 1 and 3 using the JEOL 100C, it can be seen that from different areas (openings) of the same grid gave results which varied from 104 fibers in test 1, to 127 fibers for test 3, a difference of 22%.

In *combination*, the results obtained from using *different instruments* and observing *different areas* (openings) of the same grid, the difference in the results can be very large indeed. Tests 2 and 3 compared the results obtained from the JEOL 100C and JSM 50A when different areas (openings) of the same grid were interrogated; test 2 gave 88 fibers while test 3 gave 127 fibers, a difference of 45%. Similarly, test 4 gave 50 fibers while test 5 gave 114 fibers, a difference of 128%. Again, test 7 gave 42 fibers while test 8 gave 126 fibers, a difference of 200%.

It should be noted that in every case, the results from the JSM 50A were lower than when the JEOL 100C was used (see Table 29).

A further test was made to compare the results from the JEOL 100C in STEM mode with those from a different area on the same grid using the SEM mode. The results from tests 9 and 7, respectively, showed a very large, 264%, increase in fiber counts being noted when the STEM mode was used.

Tests 2, 4, and 9 indicate that when X-ray analysis is used for fiber type identification, a substantial proportion, 34%, 48%, and 22%, respectively, of all the fibers cannot be classified. This is because the X-ray yield from the fiber is too low, or is ambiguous. The results do not indicate any trends in terms of the instrument used or the fiber type to be identified. It should be noted, however, that more detailed studies could reveal such trends.

A final test, which was not part of the original Phase 3 effort, was added because of its obvious pertinence to the overall objectives of the study. The test evaluated the performance of the superior SEM instrument, the JEOL 100C, against the same instrument operating in the conventional TEM mode. Six identical grid openings were scanned in both SEM and TEM modes; the results are given in Table 30. Fibers were recognized by morphology alone. It can be seen that the TEM mode gives consistently higher fiber counts (with an average over six grid openings) of plus 79%. Stationary image of the conventional TEM mode is less fatiguing to the eye than a scanning image.

Application of t-test shows that this difference is quite significant (t value of 2.27 is significant at 5% probability for 10 degrees of freedom).

Conclusions from Phase 3

The conclusions drawn from Phase 3 are as follows:

1. In secondary electron imaging mode (SEM), the higher resolution JEOL 100C gave consistently higher values than the JSM 50A.
2. The X-ray probe analysis indicated that approximately one-third of the fibers could not be positively identified even when laboratory prepared samples were utilized. The JSM 50A X-ray probe was easier to use than the JEOL 100C in that it gave higher count rates and could be operated at a lower tilt angle.
3. Higher fiber counts are obtained with higher resolution equipment. When compared with the JEOL 100C, SEM, the counts were improved by 21% when switching to the STEM mode and 79% (average of six) in the conventional TEM mode. Thus, the conventional TEM is the desired mode for asbestos analysis.

PHASE 4 RESULTS

Phase 4 was designed to evaluate parameters of ashing, ultrasonification, and reconstitution of samples.

Table 31 summarizes results from Phase 4 for fiber number concentration and mass concentration. Table 32 summarizes results on dimensions of observed

Table 30

DIFFERENCE IN NUMBER OF CHRYSOTILE FIBERS COUNTED WHEN SAME GRID OPENINGS ARE OBSERVED UNDER SEM AND CONVENTIONAL TEM MODE IN JEOL 100C

Grid Opening No.	SEM[1] No. Fibers	CTEM[2] No. Fibers	% Increase TEM Over SEM
1	48	100	108
2	18	24	33
3	38	62	63
4	31	51	65
5	48	104	116
6	48	72	50
AVERAGE VALUES	38.5	68.8	79
STD. DEVIATIONS	12.23	30.31	
STD. EFFOR OF MEAN	4.99	12.37	

---

[1] SEM 100 kv, 0° tilt, 10,000X (secondary electron mode).

[2] CTEM 100 kv, 0° tilt, 16,000X (conventional transmitted electron image).

Table 31

ESTIMATING CHRYSOTILE ASBESTOS IN PHASE 4 SAMPLES
(ASHING AND SONIFICATION EXPERIMENTS)

Sample Number†	Area Examined 10^{-4} cm^2	Fiber Concentration Estimate, 10^6/cm^2 of Filter	Mass Concentration Estimate, 10^{-9} gm/cm^2 of Filter
1201	3.2	0.4531	2.287
1202	6.4	0.1672	3.471
1203	1.92	0.6719	6.913
1204	1.28	0.7891	7.903
1205	5.12	0.1973	1.829
1206	1.92	0.5573	7.402
1207	1.28	0.8594	14.43
1208	2.56	0.4023	6.693
1209	4.48	0.2857	3.160
1210*	2.56	0.4922	8.712
1211*	2.56	0.3750	17.53

† For explanation of the sample number, please see Tables 9 and 13.

* Unashed.

Table 32

SIZE DISTRIBUTION CHARACTERISTICS OF CHRYSOTILE FIBERS IN PHASE 4 SAMPLES
(ASHING AND SONIFICATION EXPERIMENTS)

	Length µm			Diameter µm			Mass (10^{-14} gm)		
Sample Number†	Mean	Std. Dev.	Mean Ln(Length)	Mean	Std. Dev.	Mean Ln (Dia.)	Mean	Std. Dev.	Mean Ln (Mass)
1201	0.6341	0.3659	-0.5832	0.0556	0.0260	-2.9906	0.5048	0.6670	-33.4816
1202	1.0135	2.2693	-0.4734	0.0552	0.0432	-3.0887	2.076	8.394	-33.5678
1203	0.8819	1.0231	-0.3766	0.0601	0.0391	-2.9847	1.029	2.812	-33.2831
1204	0.9039	1.1187	-0.3483	0.0600	0.0364	-2.9604	1.002	2.413	-33.1862
1205	0.9689	0.6788	-0.2458	0.0588	0.0311	-2.9562	0.9270	1.382	-33.0753
1206	0.9661	1.6861	-0.4686	0.0575	0.0358	-3.0003	1.328	4.402	-33.3863
1207	.9386	0.7594	-0.2776	0.0672	0.0417	-2.8544	1.679	4.031	-32.9035
1208	1.0238	0.8998	-0.2653	0.0663	0.0406	-2.8615	1.663	4.438	-32.9053
1209	0.6818	0.3960	-0.5319	0.0636	0.0411	-2.9089	1.106	3.634	-33.2669
1210*	1.2255	1.2621	-0.1019	0.0430	0.0308	-3.2829	1.770	12.79	-33.5848
1211*	1.6383	2.7305	0.1311	0.0572	0.0417	-3.0089	4.676	36.26	-32.5261

† For explanation of the sample number, please see Tables 9 and 13.

* Unashed.

fibers in Phase 4. Tables 31 and 32 also list results on two initial filters, one polycarbonate and one cellulose acetate, studied without the ashing and reconstitution step.

Dependent Variables in Phase 4

The dependent variables in Phase 4 are as follows.

DEPENDENT VARIABLES, PHASE 4

Variable	Definition
Y_{11}	Square root of estimated number of chrysotile fibers per square centimeter of filter
Y_{12}	Natural log of estimated mass concentration of chrysotile fibers on filter, nanograms per square centimeter
Y_3	Mean of natural log of chrysotile fiber lengths (μm)

Regression Analysis

The dependent variable Y_{11} was subjected to a square root transformation and Y_{12} to a log transformation to normalize the distributions. Similarly, variable Y_3 was chosen as the mean of the natural log of length of the individual fibers.

Regressions were performed on each of the dependent variables using stepwise regression program BMDO2R from the BMD library of statistical programs. The data input to the program included coded values of the independent variables found in Table 9 and the values of dependent variables listed in Table 33.

The mean values and standard deviation of the dependent variables are listed in Table 34. The resulting regression equations are given in Table 35. In any given equation, only those independent variables appear that have coeffients significant at the 20% probability level.

Each of the equations describes a relationship between a dependent variable and the various independent variables.

The net effects and their confidence limits are shown graphically in Figures 11 and 12.

Table 33

VALUES OF DEPENDENT VARIABLES IN PHASE 4

	Fiber Concentration		Mass Concentration		
Sample Number*	10^6 Fibers per cm^2	Square Root of Fiber Concentration Y_{11}	10^{-8} Grams per cm^2	Natural Log of Mass Concentration Y_{12}	Mean Ln (length) Y_3
1201	0.4531	0.6731	0.2287	-1.4753	-0.5832
1202	0.1672	0.4089	0.3471	-1.0581	-0.4734
1203	0.6719	0.8197	0.6913	-0.3692	-0.3966
1204	0.7891	0.8833	0.7903	-0.2353	-0.3483
1205	0.1973	0.4442	0.1829	-1.6988	-0.2458
1206	0.5573	0.7465	0.7402	-0.3008	-0.4686
1207	0.8594	0.9270	1.443	0.3667	-0.2776
1208	0.4023	0.6343	0.6693	-0.4015	-0.2653
1209	0.2857	0.4537	0.3160	-1.1520	-0.5319

* For explanation of the sample number, please see Tables 9 and 13.

Table 34

MEANS AND STANDARD DEVIATIONS OF DEPENDENT VARIABLES IN PHASE 4

Regression Equation	Variable	Mean	Standard Deviation
6	Y_{11} Square root of chrysotile fiber concentration (million fibers/cm^2 filter)	0.6662	0.1966
7	Y_{12} Natural log of mass concentration of chrysotile (10^{-9} gm/cm^2 filter)	-0.7027	0.6748
8	Y_3 Mean log of chrysotile fiber length (micrometers)	-0.399	0.1229

Table 35

REGRESSION EQUATIONS IN PHASE 4

Phase 4

(6) $Y_{11} = 0.6619 - 0.0781(X_{15}L) + 0.0852(X_{15}Q)$

(7) $Y_{12} = - 0.7027$

(8) $Y_3 = - 0.3990 + 0.0478(X_{14}Q) - 0.0354(X_{15}Q)$

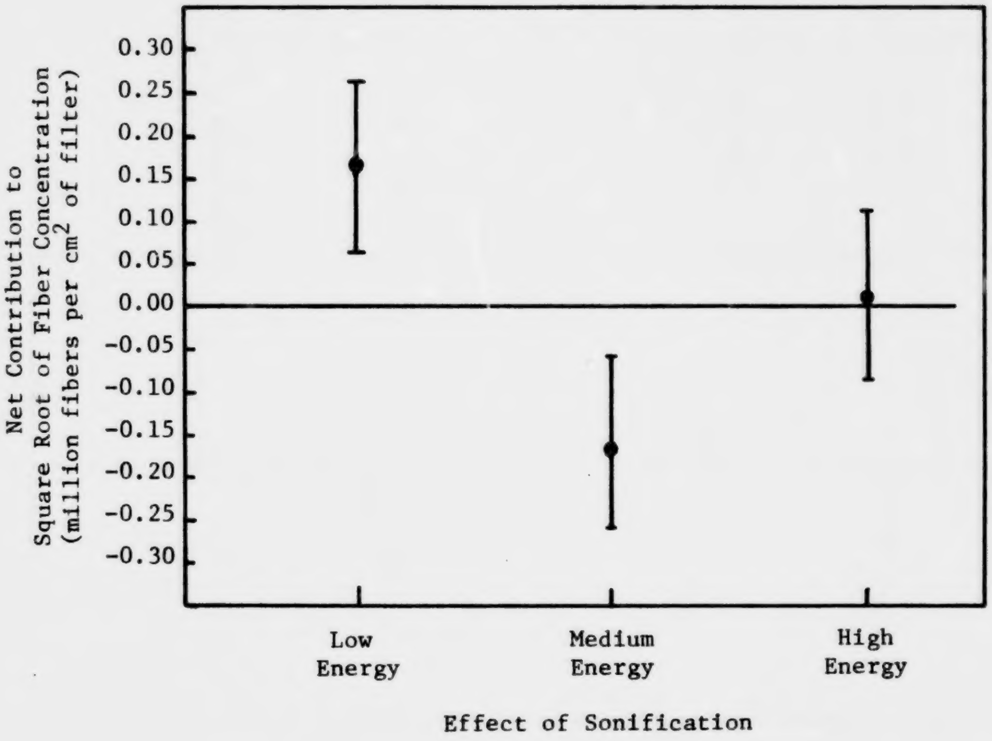

Figure 11. Graphical presentation of performance equation 6 in Phase 4. Net contribution to square root of fiber concentration, $10^6/cm^2$ of filter.

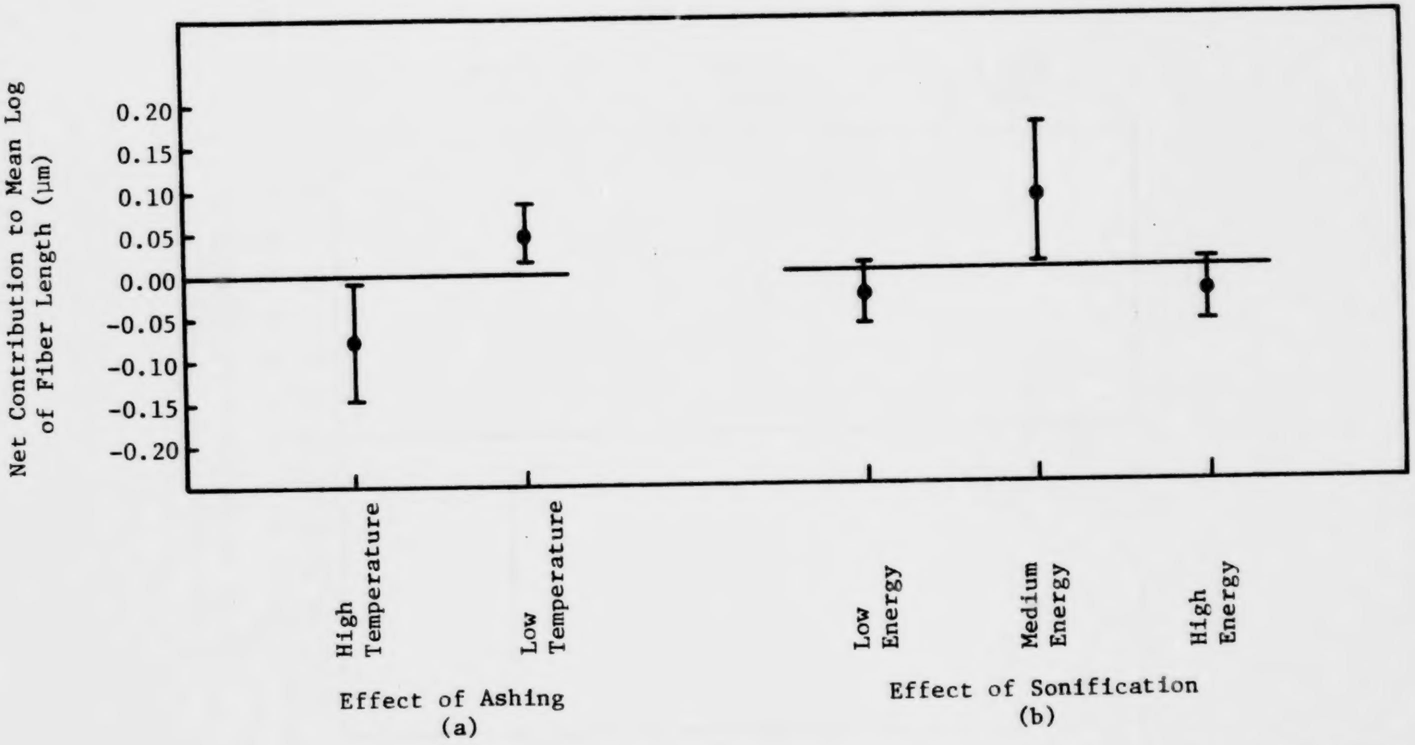

Figure 12. Graphical presentation of performance equation 8 in Phase 4. Net contribution to mean log of fiber length (μm).

Interpretation of Phase 4 Results

Square Root of Fiber Concentration of Chrysotile--

Figure 11 shows that high energy ultrasonification increases the fiber concentration as compared with the medium energy ultrasonification. This is most probably due to the disruption of fibrils into shorter fibrils as evidenced by the decrease in the mean fiber length (see Figure 12).

It is difficult to rationalize why low energy ultrasonification (which is conducted in a different sonifying equipment than the medium and high energy ultrasonification) should give the highest estimate of chrysotile fiber concentration and also the smallest mean fiber length.

Figure 12 shows that high temperature ashing results in shorter fibrils as compared with the low temperature ashing, presumably because of the violent nature of high temperature ashing. This conclusion may be interpreted to mean that low temperature ashing is preferable to the high temperature ashing. Also from Table 32, it is clear that mean fiber length is larger for the unashed samples than that for both low temperature ashing and high temperature ashing. This suggests that ashing may be shortening the fiber length.

Cumulative Size Distributions for Chrysotile Fibers--

The mean fiber length and width are susceptible to a large variation if a few large fibers are present in the group of fibers observed. Hence, a cumulative distribution of length and width for all eleven samples are listed in Tables 36 and 37, respectively.

It is clear that the maximum value of length of fiber in each sample is different, but minimum length is almost constant. The different percentile 10th, 20th, . . . 90th values show that the length is always lower (regardless of which ashing and ultrasonification treatment is employed) than that for the unashed samples. Thus, qualitatively one can conclude that the ashing and ultrasonification treatments chosen in this study lead to a shortening of the length of fibers and hence should be used very cautiously.

From Table 37, it appears that width does not show much change or any consistent trends of alteration.

Number Concentration of Chrysotile Fibers--

In the data, we have nine samples studied with various combinations of ashing and sonification treatment and two samples studied directly (without

Table 36

CHARACTERISTICS OF FIBER LENGTH IN CUMULATIVE DISTRIBUTION IN PHASE 4

Sample Code	1201	1202	1203	1204	1205	1206	1207	1208	1209	1210	1211
Length (μm):											
Minimum	2.0	1.0	2.0	2.0	2.0	1.0	2.0	2.0	1.0	1.0	2.0
Maximum	20.0	175.0	80.0	80.0	30.0	100.0	40.0	40.0	20.0	80.0	200.0
Median	4.129	4.115	4.945	5.018	6.011	3.957	5.143	5.948	4.212	7.543	8.49
Maximum Length for (percentile):											
10th*	2.0	1.966	2.00	2.965	3.011	2.000	2.927	2.000	2.018	2.922	3.925
20th	2.933	2.853	2.987	3.091	3.153	3.036	3.887	2.948	3.001	3.924	4.827
30th	2.99	2.993	3.905	4.000	4.086	3.173	4.005	3.915	3.095	5.035	5.757
40th	4.035	3.869	4.063	4.144	4.973	3.836	4.947	4.999	4.068	5.791	8.125
50th	4.129	4.115	4.945	5.018	6.011	3.957	5.143	5.948	4.212	7.548	8.492
60th	4.865	4.968	5.713	5.685	6.786	4.799	6.073	6.237	4.934	8.020	9.765
70th	5.009	6.153	6.723	6.649	7.994	5.042	8.041	8.214	5.844	10.308	11.532
80th	5.943	8.328	9.486	7.962	11.779	7.329	9.753	10.011	7.800	12.248	14.042
90th	8.171	15.00	12.119	9.982	14.744	11.569	14.445	19.627	8.121	15.019	21.136

* 10th refers to the 10th percentile of the distribution. The numbers in this row refer to the maximum length in each sample, for the 10th percentile.

Table 37

CHARACTERISTICS OF FIBER WIDTH IN CUMULATIVE DISTRIBUTION IN PHASE 4

Sample Code	1201	1202	1203	1204	1205	1206	1207	1208	1209	1210	1211
Width (μm):											
Minimum	0.2	0.1	0.1	0.1	0.2	0.100	0.200	0.200	0.200	0.2	0.2
Maximum	1.0	2.0	2.0	2.0	1.2	2.000	2.000	2.000	2.000	2.0	2.0
Median	0.397	0.305	0.402	0.400	0.399	0.398	0.415	0.411	0.408	0.291	0.30
Maximum Width for (percentile):											
10th*	0.200	0.197	0.197	0.199	0.200	0.199	0.200	0.200	0.200	0.2	0.2
20th	0.295	0.201	0.203	0.295	0.298	0.294	0.291	0.293	0.291	0.2	0.2
30th	0.298	0.295	0.298	0.301	0.302	0.300	0.299	0.299	0.296	0.2	0.2
40th	0.302	0.300	0.306	0.307	0.306	0.306	0.405	0.404	0.302	0.2	0.29
50th	0.397	0.305	0.402	0.400	0.399	0.398	0.415	0.411	0.408	0.291	0.300
60th	0.404	0.311	0.416	0.415	0.406	0.412	0.495	0.484	0.481	0.295	0.408
70th	0.501	0.409	0.491	0.503	0.500	0.482	0.589	0.582	0.581	0.300	0.488
80th	0.604	0.572	0.688	0.603	0.598	0.584	0.801	0.800	0.599	0.408	0.596
90th	0.802	0.976	0.984	0.803	0.804	0.798	0.831	0.833	0.825	0.493	0.971

* 10th refers to the 10th percentile of the distribution. The numbers in this row refer to the maximum length in each sample for the 10th percentile.

ashing). We may compare the chrysotile fiber number concentration in these two groups.

CHRYSOTILE FIBER NUMBER CONCENTRATION $10^6/cm^2$ in
ASHED SAMPLES AND IN UNASHED SAMPLES

	Nine Ashed Samples	Two Unashed Samples
Mean Value of Fiber Number Concentration	0.4870	0.4336
Standard Deviation	0.2510	0.0829
Standard Error of Mean	0.0837	0.0586
Variance	0.00700	0.00343

$$t = \frac{0.4840 - 0.4336}{\sqrt{0.00700 + 0.00343}} = 0.5229$$

This t-value is not statistically significant with 9 degrees of freedom, thus indicating that the slight increase in chrysotile number concentration in the ashed samples compared with the unashed samples is unimportant.

It should be noted here that in preparing these filters, carbon-coating was not used, because some filters were cellulose acetate. Thus, the fibers on the Phase 4 filters were not locked and during the Jaffe wash may have resulted in a variable loss. This possibility may have made the evaluation of ashing and sonification variables difficult.

Although the length distribution data suggest that ashing and ultrasonification treatments tend to decrease the length of fibers, the fiber concentration estimates suggest that the effect of ashing is not significant.

MASS CONCENTRATION OF CHRYSOTILE nanogram/cm^2 IN
ASHED SAMPLES AND UNASHED SAMPLES

	Nine Ashed Samples	Two Unashed Samples
Mean of Mass Concentration, nanogram/cm^2	6.0098	13.121
Standard Deviation	3.9308	6.2353
Standard Error of Mean	1.3103	4.4090
(Standard Error)^2	1.71680	19.43965

$$t = \frac{13.121 - 6.0098}{\sqrt{1.71680 + 19.43965}} = 1.546$$

This t-value for 9 degrees of freedom is significant at a probability between 10 and 20%. It indicates that the average mass concentration of chrysotile in the ashed samples is lower than that in the unashed samples. This suggests some loss of chrysotile during ashing and reconstitution step.

Clearly, more work is required to establish, quantitatively, the effects of ashing and sonification treatment. Redeposition filters should be polycarbonate and these should be coated with evaporated carbon to lock all particulates prior to Jaffe wash.

One possible explanation for the failure to detect strong alteration in fiber characteristics due to ashing subprocedure is that the initial stock solutions had been subjected to high energy ultrasonics to break down the fibers to a small enough stable size. Thus, a subsequent ashing and ultrasonic treatment had only a marginal effect on the fiber dimensions. One needs a sample that has not seen prior ultrasonic treatment.

Another possible area for future work is the effect of diluting the sample (without ashing). This can be done by dissolving the primary filter with particulate matter in a suitable solvent and then to redeposit it, after appropriate dilution, onto a polycarbonate filter.

Phase 4 Conclusions

1. Ashing and ultrasonic treatments should be used only when direct sample preparation and examination are not possible. These cases

include presence of organic matter or high total particle density on primary filter.

2. Since ashing and reconstitution involves elaborate procedure, much care is necessary in handling the products.

STATISTICAL ANALYSIS OF PHASE 5 DATA

The Experiment Design

In Phase 5, two independent variables were used: X_6, the orientation of the droplet during drying (face up or down), and X_{11}, the radial location of the grid opening (position used: center, mid-radius, or periphery). A full factorial experiment was run, with the design indicated in Table 10. The various levels of the independent variables and their codes were also listed in Table 10. The dependent variables considered were: mean Ln liber length and square root of fiber concentration. The values of these in the various cases are given in Table 38, along with their means and standard deviations. These data were based on the results of computer analysis given in Table 39, similar to that used in Phases 2 and 4.

Regression Analysis

As in Phases 2 and 4, the dependent variable, Y_{11}, fiber concentration, was subjected to a square root transformation since it is essentially a count of fibers. The dependent variable Y_3 was chosen as mean Ln fiber length. The Ln transformation was used to "smooth out" the large variations usually found in length measurements and to normalize the distribution.

Regressions were performed on each of the dependent variables using the stepwise regression program BMDO2R from the BMD library of statistical programs [59]. The data input to the program included the coded variables of the independent variables found in Table 10 and the values of the dependent variables from Table 38.

The resulting regression equations are given below.

REGRESSION EQUATIONS - PHASE 5

$$Y_{11} = 0.5024 - 0.11903(X_6) + 0.0514(X_{11}Q)$$

$$Y_3 = - 0.6025$$

Table 38

VALUES OF DEPENDENT VARIABLES IN PHASE 5

	Variables	
Sample Number	$\underline{Y}_1$ Square Root of Fiber Concentrations	$\underline{Y}_3$ Mean Ln Fiber Length
5101	0.6124	-0.6069
5102	0.4815	-0.5058
5103	0.7705	-0.6453
5104	0.4507	-0.8795
5105	0.3176	-0.5469
5106	0.3818	-0.4307
Mean	0.5024	-0.6025
Standard Deviation	0.1648	-0.1553

Table 39

FIBER NUMBER AND MASS CONCENTRATION IN PHASE 5

Input mass: 10.3 x 10^{-9} gm /cm^2

		5101	5102	5103	5104	5105	5106
Fiber Count (fibers)		24	89	76	39	71	84
Fiber Concentration (10^6 fibers per sq. cm.)		0.3750	0.2318	0.5937	0.2031	0.1009	0.1458
Mass Concentration (10^{-9} gm per sq. cm.)		1.963	1.312	2.116	1.318	0.8827	1.073
Length (μm)	Mean	0.7522	0.7209	0.6681	0.5295	0.7417	0.7792
	Standard Deviation	0.7375	0.4562	0.4853	0.4069	0.6876	0.4776
	Mean Ln	-0.6069	-0.5058	-0.6453	-0.8795	-0.5469	-0.4307
	Geom Mean	0.5451	0.6030	0.5243	0.4150	0.5787	0.6501
Diameter (μm)	Mean	0.0368	0.0468	0.0412	0.0549	0.0613	0.0555
	Standard Deviation	0.0208	0.0341	0.0201	0.0301	0.0379	0.0274
	Mean Ln	-3.4201	-3.2123	-3.2794	-3.0318	-2.9408	-3.0010
	Geom Mean	0.0327	0.0403	0.0377	0.6513	0.0528	0.0497
Mass (10^{-14} gm)	Mean	0.5285	0.5659	0.3563	0.6489	0.8752	0.7357
	Standard Deviation	1.078	1.611	0.7563	1.301	2.227	1.242
	Mean Ln	-34.3641	-33.8474	-34.1212	-33.8603	-33.3455	-33.3497
	Geom Mean	0.1191	0.1997	0.1518	0.1971	0.3298	0.3284

In any given equation, only those independent variables appear that have coefficients significant at the 20% probability level. That is, an independent variable did not enter an equation if it was determined that its coefficient value could have occurred with probability 20% or greater due to accidents of sampling. It is worthwhile to note each case which independent variables are in a given equation and which ones are absent.

These net effects and their confidence limits are shown graphically in Figure 13.

The results of the attempted regression of Y_3, mean Ln fiber length, on the independent variables showed no significant effect of any factor at the 80% confidence level. That is, all the variation in mean Ln fiber length would occur by chance with probability at least 20%.

Conclusions from Phase 5

Phase 5 investigated the effect of placing a drop of liquid containing fibers in suspension directly onto an EM grid. The results indicated that surface tension effects tended to move the fibers as the drop dried with the result that an uneven fiber loading was observed on the grid.

In particular, as shown graphically in Figure 13, a grid allowed to dry with the drop facing down gave higher fiber counts than when dried rightside up. Further, a point on the mid-radius of the grid gave lower values than either the periphery of the grid or the center of the grid.

For these reasons, the use of the direct drop method is not recommended.

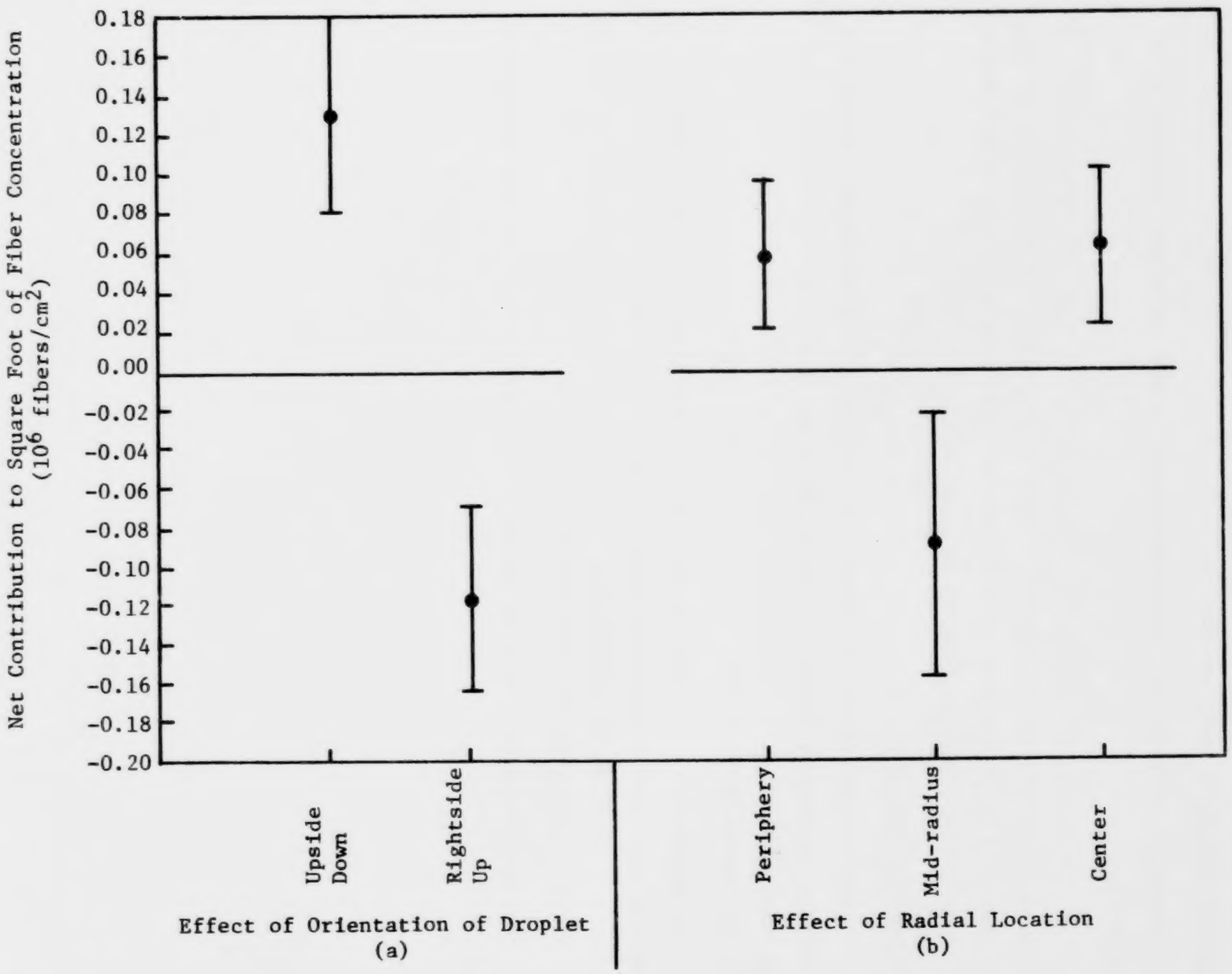

Figure 13. Graphical presentation of performance equation 1 in Phase 5. Net conctribution to square root of fiber concentration (10^6 fibers/cm^2).

SECTION 9

PROVISIONAL OPTIMIZED METHOD AND ROUND-ROBIN TESTING

A provisional method was developed as based on the results of the five-phase program. The subprocedures were adjusted to achieve the best precision (see Table 21). Some adjustments were made to accommodate practical considerations. A brief description of the optimized method is given in Appendix D. Also, procedures or subprocedures which gave inconsistent results or which altered the initial sample were eliminated from the optimized method. The final draft of the detailed manual has been issued separately [64].

ROUND-ROBIN TESTS

In order to determine the ruggedness of the provisional optimized method, a round-robin test was planned. This test was to serve as interlaboratory experience of the method and provide important feed back to further improve the optimized method. Of the several laboratories sought for participation, the following laboratories offered to cooperate.

1. Environmental Protection Agency, Research Triangle Park, NC
2. Environmental Protection Agency, Athens, GA
3. Environmental Protection Agency, Duluth, MN
4. National Institute for Occupational Safety and Health, Cincinnati, OH
5. A.D. Little, Cambridge, MA
6. Ontario Ministry of the Environment, Toronto, Ontario Canada

PREPARING CALIBRATION FILTERS

It would be ideal to prepare filters with known amounts of asbestos, known size distributions of asbestos fibers, and to use these for round-robin tests. This would serve as an independent external absolute calibration for evaluating the absolute accuracy of the electron microscopy method. The concept of a fully known and characterized sample proved elusive, since none of the methods could completely characterize a sample. Non-microscopic methods would not give size distributions, parameters and fiber counts. The most one could expect to achieve was to measure the total mass of asbestos per unit area of the filter.

Even this apparently easy measurement was quite difficult to achieve. Our own repeated attempts at estimating chrysotile mass on filters of Phase 1, by atomic absorption measurements, proved futile because of the very small mass involved.

Being aware of the recent work on neutron activation technique at AERE, Harwell, England, Dr. Morgan was asked to prepare six polycarbonate filters with known small mass concentrations of asbestos. The method consisted of compacting UICC asbestos into a disc, irradiating it with an intense flux of neutrons in a nuclear reactor, then eroding the disc with an air jet and collecting the resulting aerosol on 47 mm diameter polycarbonate filters. The actual mass of the asbestos deposited on the filter was measured by radio-activity measurements of some short-lived isotopes of rare-earth elements present as trace impurities. With some trial and error, Dr. Morgan succeeded in depositing three different levels of mass concentration on these filters.

Our own work on two of these calibration filters showed that the filter dissolution using Jaffe technique required much longer durations. Also, the samples contained a wide size distribution of fibers and several bundles or aggregates of fibers. One more serious problem with these samples was that it was extremely difficult to obtain good electron diffraction patterns even at 100 kv. For these reasons, these calibration samples were discarded from consideration in the round-robin test.

FINAL CHOICE OF SAMPLES FOR ROUND-ROBIN TEST

Following are two air samples we selected for round-robin test.

1. Air sample collected under controlled conditions in our laboratory using aerosol generations in Phase 1. (High-volume samplers, polycarbonate filter, 0.4 μm pore size, 708 liters/min for 13 minutes.) Standard UICC chrysotile mineral was used for obtaining the aerosol cloud.

2. A field air sample collected at the Johns-Manville Plant in Waukegan, Illinois. (High-volume sampler, polycarbonate filter, 0.4 μm pore size, 560 liters/min for one hour.)

The provision for two samples was meant to avoid total failure of the round-robin test, if the field sample posed any unsurmountable problems.

INDEPENDENT ESTIMATE OF CHRYSOTILE MASS CONCENTRATIONS

Neutron Activation Analysis

Segments representing about half the areas of these filters were dispatched to Dr. Morgan at AERE, Harwell, England, to estimate the chrysotile mass using ultrasensitive neutron activation technique. Our letter is appended (see Appendix E). Dr. Morgan's reply explaining the problems, and his inability to estimate the low mass, is also appended (see Appendix E).

Fortunately, it was possible to obtain estimates of the chrysotile mass concentration in the filter deposits by X-ray fluorescence spectrometric analysis for magnesium. Fluorescence intensities above background of the Mg-k_α line were measured with a simultaneous multi-wavelength spectrometer (Siemens MRS-3), adapted for use with thin filter-deposited samples, using procedures described by Wagman [65]. Values for chrysotile were derived from magnesium concentration data, on the basis of the chemical formula $Mg_3Si_2O_5(OH)_4$. Further detailes are given in Appendix F.

The chrysotile mass concentration estimates on the two polycarbonate filters used in the round-robin test, as determined by the X-ray fluorescence method in Dr. Wagmen's X-ray laboratory, are as follows:

Air Sample	Chrysotile Mass Concentration μg/m³	Standard Deviation of Mass Concentration μg/m³	Ratio Standard Error/Mean x 100
Lab Sample 154	2.452	0.096	1.598
Field Sample 661	57.919	1.015	0.715

It is evident that the X-ray fluorescence method gives highly reproducible results. The mass concentration estimate for the laboratory sample should be fairly accurate, inasmuch as it consisted of high purity chrysotile. The estimate for the field sample is likely to be too high because some of the magnesium present is associated with materials other than chrysotile.

The filter segments were carbon-coated at IITRI laboratory tacked to the bottom of disposable petri dishes and mailed to each of the participating laboratories along with specific instructions and with copies of the provisional method.

Dr. Anant Samudra visited the participating laboratories to (1) discuss and demonstrate the fine aspects of the optimized method, (2) to explain the proper use of the electron diffraction capability of the transmission electron microscopes, and (3) to obtain criticism and comments on the provisional method. Most of the electron microscope data were received later in the mail. These data were reorganized using fortran coding forms and transferred to key-punch cards. The data consisted of 54 sets and required 9,000 cards. The statistical descriptors or characterizing parameters were derived for each data set, i.e., for each separate TEM grid examined.

SECTION 10

RESULTS AND DISCUSSION OF ROUND-ROBIN TESTS

The voluminous data from round-robin tests allow several analyses. It is proposed to first check the Poisson distribution test and then to study the summaries of statistical descriptors or characterizing parameters for the two air samples.

POISSON DISTRIBUTION TESTS

Goodness of Fit with Poisson Distribution

This test requires the data about the number of fibers observed in a field of view 0, 1, 2 ... etc., and the corresponding frequency of occurrence. These data were extracted from the basic electron microscope data of the 54 data sets mentioned earlier. The minimum data should consist of 40 fields of view and, when arranged for fiber frequency, should give a minimum of three class intervals.

Following the method outlined in Phase 1 analysis, data from round-robin tests were analyzed by the Poisson 1 program. The results are summarized in Table 40. Of the 54 sets of data, 30 sets are in appropriate form for Poisson distribution tests. Our of the 30 tests, 19 conformed definitely to the Poisson distribution, seven are borderline cases, and only two tests definitely do not conform to the Poisson distribution. In data sets 76 and 77, tests cannot be applied because they had only two class intervals and, hence, no degree of freedom.

The finding that the majority of the sets conform to the Poisson distribution may be interpreted to mean that the differences in sample preparation and sample contamination have not altered (or rearranged) the initial random settling of fibers on the Nuclepore filter.

Confidence Intervals on the Mean Number Concentration

The Poisson distribution model allows computing intervals, for any given degree of confience, on the value of λ, the mean number of fibers per field.

Table 40

TESTS FOR APPLICABILITY OF THE POISSON DISTRIBUTION TO NUMBER OF FIBERS PER FIELD

Data Set No.	Size of Field $cm^2 x10^{-6}$	No. of Fields	No. of Fibers	Mean No. Fibers per Field, λ	Degrees of Freedom	Chi Square	Probability	Good Fit to Poisson	1 Fiber per Field of View Represents so much Fiber Concentration, 10^6 fibers/m^3
1	0.18	58	106	1.83	3	0.61	0.90>P>0.80	*	245.47
2	0.725	28	106	3.79	4	2.03	0.80>P>0.70	*	69.94
3	0.18	40	114	2.85	3	4.47	0.30>P>0.20	*	242.77
4	0.235	40	110	2.75	3	5.73	0.20>P>0.10	*	188.02
5	0.235	62	108	1.74	3	10.3	0.02>P>0.01	(*)	188.02
6	0.235	30	75	2.50	3	1.35	0.80>P>0.70	*	188.02
7	0.235	33	104	3.15	4	1.18	0.90>P>0.80	*	188.02
8	0.235	43	105	2.44	4	8.67	0.10>P>0.05	*	188.02
9	0.235	42	109	2.60	4	7.77	0.20>P>0.10	*	188.02
18	0.309	43	101	2.35	4	6.65	0.20>P>0.10	*	142.99
19	0.309	37	78	2.11	3	8.28	0.05>P>0.02	(*)	142.99
21	0.187	95	141	1.48	3	8.59	0.05>P>0.02	(*)	236.36
22	0.187	93	103	1.11	2	7.77	0.05>P>0.02	(*)	236.36
23	0.187	89	106	1.19	2	1.77	0.50>P>0.30	*	236.36
24	0.187	71	105	1.48	3	2.09	0.70>P>0.50	*	236.36
25	0.187	80	105	1.31	3	10.3	0.02>P>0.01	(*)	236.36
26	0.187	113	104	0.92	2	25.3	0.001>P		236.36
31	0.72	34	154	4.53	4	1.39	0.90>P>0.80	*	61.37
41	0.19	44	98	2.23	4	1.61	0.90>P>0.80	*	232.55
42	0.472	21	101	4.81	2	0.63	0.80>P>0.70	*	93.61
43	0.472	30	100	3.33	4	3.33	0.70>P>0.50	*	93.61
45	0.18	56	102	1.82	3	1.31	0.80>P>0.70	*	245.47
73	0.105†	102	27	0.26	1	6.16	0.02>P>0.01	(*)	1135.63
74	0.105†	100	31	0.31	1	3.40	0.10>P>0.05	*	1135.63
75	0.105†	100	44	0.44	1	3.42	0.10>P>0.05	*	1135.63
76	0.06 †	100	19	0.19	0	0.12	no test		1995.14
77	0.06 †	100	8	0.08	0	0.40	no test		1995.14
86	0.464†	97	107	1.10	2	13.9	0.001>P		257.95
90	0.105†	100	59	0.59	1	4.14	0.05>P>0.02	(*)	1135.63
91	0.105†	100	39	0.39	1	0.30	0.70>P>0.50	*	1135.63

† This takes into account the dilution factor in ashing also.

* Conform to Poisson.

(*) Borderline conformation to Poisson.

In this study we have obtained 90% confidence as well as 95% confidence limits on the mean λ in each set since the size of the field varies from one set to another, we normalized all these values of λ and its confidence interval to give the number concentrations in standard units (namely, 10^6 fibers/m^3). The normalized values are listed in Table 41 and are shown graphically for the laboratory air sample in Figure 14 for a quick comparison.

Precision Measured by Ratio of Standard Error of λ to the Mean Value of λ

Precision can be measured from the ratio of standard error to the mean to the mean value of λ. These ratios, expressed as a percentage, are also listed in Table 41. These values appear quite comparable among different sets, i.e., for different laboratories and operators (with a few exceptions in the case of the field air sample) the precision of the fiber count estimate is about 10%, which is quite good.

GENERAL PROCEDURES

For each of the 54 data sets, statistical descriptors or characterizing parameters were derived using a special fortran program. These characterizing parameters are summarized for the laboratory air sample in Table 42 and for the field air sample studied with ashing in Table 43 and for the field sample studied without ashing in Table 44.

Column 3 lists - number concentration of all fibers, $10^6/m^3$

Columns 4 and 5 list - mean fiber length and mean fiber diameter, μm

Column 6 lists - mean fiber volume, 10^{-15} cm^3

Column 7 lists - volume concentration of all fibers, 10^{-9} cm^3/m^3

Column 8 lists - number concentration of chrysotile fibers, $10^6/m^3$

Columns 9 and 10 list - mean fiber length and mean fiber diameter, μm

Column 11 lists - mean fiber volume, 10^{-15} cm^3

Column 12 lists - chrysotile mass concentration in air, μg/m^3

In Tables 42 through 44, the numerical values in column 3 are slightly lower than the corresponding values listed in Table 41. This is because fibers crossing the perimeter of the field of view have been treated as half fibers in computing fiber concentration in Tables 42 through 44.

Table 41

MEAN VALUES AND LOWER AND UPPER LIMITS OF FIBER CONCENTRATION ESTIMATE ACCORDING TO POISSON DISTRIBUTION

Data Set	Lab	Number Conc. of all Fibers 10^6 Fibers/m^3 Mean	90% Confidence Limits Lower	90% Confidence Limits Upper	95% Confidence Limits Lower	95% Confidence Limits Upper	$\frac{\text{Std. Error}}{\text{Mean}}$ x100
SAMPLE 154							
1	RTP	448.72	379.50	527.27	367.22	542.74	10.26
41	RTP	517.89	434.87	612.54	420.45	631.14	9.67
42	RTP	450.27	379.13	531.15	366.68	547.07	9.48
43	RTP	312.01	262.58	368.46	253.88	379.50	9.47
2	Athens	230.72	195.14	271.14	188.87	279.06	10.47
3	NIOSH	691.90	588.97	808.43	570.76	831.26	7.06
4	IITRI	517.06	438.65	605.80	424.93	623.29	14.60
5	IITRI	327.53	277.52	384.31	268.68	395.41	12.52
6	IITRI	470.05	384.50	569.70	369.65	589.26	11.14
7	IITRI	592.64	500.32	697.37	484.15	718.05	9.07
8	IITRI	459.15	387.88	539.99	375.48	555.79	12.21
9	IITRI	487.91	413.64	572.15	400.67	588.69	10.18
21	IITRI	350.76	303.73	403.47	295.22	413.64	10.67
22	IITRI	261.90	220.76	308.46	213.67	317.43	11.67
23	IITRI	281.51	238.02	330.91	230.45	340.60	11.06
24	IITRI	349.58	295.45	411.04	285.77	423.10	10.41
25	IITRI	310.10	262.12	364.94	253.12	375.58	12.02
26	IITRI	(217.46)	(183.65)	(255.99)	(177.74)	(263.54)	(12.90)
31	Duluth	277.93	242.16	317.76	235.77	325.49	7.75
18	Ontario	355.89	282.84	396.23	273.55	408.10	12.10
19	Ontario	301.43	247.52	363.92	238.23	376.21	13.73
45	ADL	447.00	376.80	527.03	364.52	542.74	11.96
SAMPLE 661							
73	IITRI	300.94	212.36	414.50	197.60	437.22	23.50
74	IITRI	352.04	254.38	474.69	239.62	499.68	21.84
75	IITRI	499.68	382.71	642.76	363.40	671.16	20.52
76	IITRI	(379.08)	(247.40)	(556.64)	(227.45)	(592.56)	(24.47)
77	IITRI	(159.61)	(79.81)	(287.30)	(67.83)	(315.23)	(42.37)
90	IITRI	670.02	533.74	832.41	509.90	864.21	14.07
91	IITRI	442.89	332.74	578.03	314.57	605.29	17.82
86	Ontario	(284.52)	(240.92)	(334.04)	(233.18)	(343.84)	(15.47)

Numbers in brackets are considered tentative, since the data did not conform to Poisson distribution or when the test for conformity could not be applied.

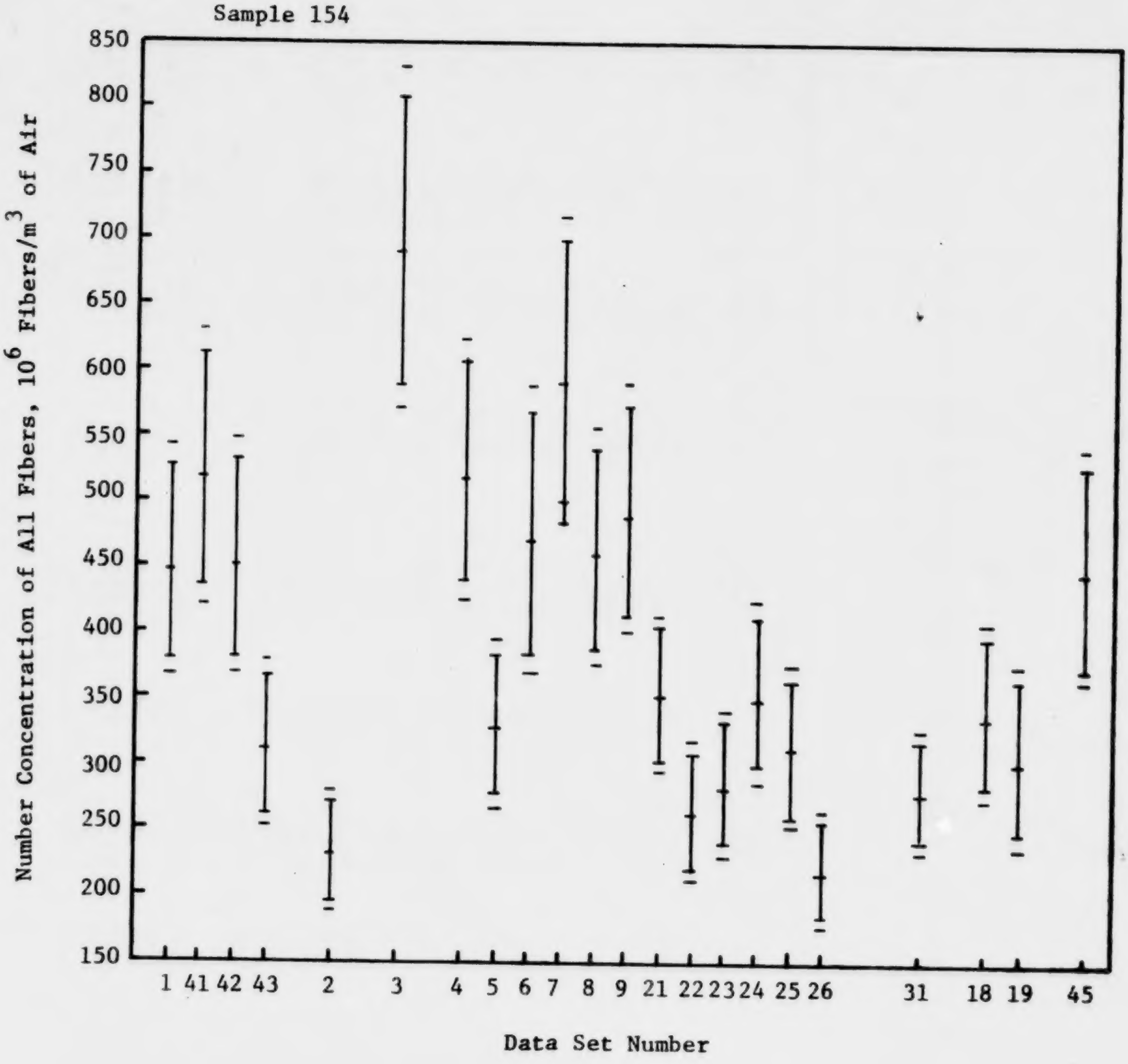

Figure 14. 90% confidence intervals (inner) and 95% confidence intervals on the mean fiber number concentration.

Table 42

SUMMARY OF ROUND-ROBIN TEST RESULTS ON AIR SAMPLE 154

Operator Code	1	2	3	4	5	6	7	8	9	10	11	12
				Size Distribution of All Fibers					Size Distribution of Chrysotile			
	Data Set Code	Filter	Number Concentration of All Fibers, $10^6/m^3$	Mean Length, μm	Mean Diameter, μm	Mean Volume, 10^{-15} cm^3	Volume Concentration of All Fibers, 10^{-9} cm^3/m^3	Number Concentration of Chrysotile, $10^6/m^3$	Mean Length, μm	Mean Diameter, μm	Mean Volume, 10^{-15} cm^3	Chrysotile Mass Concentration in Air, μg/m^3
1	4	154-2	434.8	1.061	0.067	4.301	1870.5	296.1	1.316	0.076	5.769	4.442
1	5	154-8	297.2	0.780	0.059	2.161	642.2	222.9	0.846	0.063	2.574	1.492
1	6	154-6	429.3	0.838	0.067	3.472	1490.5	369.8	0.912	0.069	3.912	3.761
1	7	154-3	547.0	0.770	0.057	2.284	1249.3	421.6	0.874	0.062	2.742	3.006
1	8	154-1-A	432.8	0.714	0.055	2.297	994.1	284.3	0.876	0.063	3.162	2.391
1	9	154-1-B	436.5	0.894	0.061	3.117	1360.6	268.6	1.064	0.072	4.414	3.083
2	21	154-8	328.4	0.995	0.067	4.778	1569.1	108.2	1.318	0.081	9.103	2.561
2	22	154-4	230.3	1.385	0.077	7.520	1729.6	52.2	2.017	0.108	18.978	2.570
2	23	154-5-A	268.3	0.943	0.060	3.320	890.7	103.6	1.091	0.074	5.667	1.526
2	24	154-5-B	329.6	0.934	0.070	5.557	1831.6	136.5	1.161	0.083	10.096	3.584
2	25	154-5-C	289.5	1.062	0.067	4.243	1228.3	141.8	1.291	0.078	6.130	2.260
2	26	154-5-D	199.8	0.987	0.072	5.966	1192.0	92.0	1.035	0.091	8.762	2.097
3	1	154-8	421.1	1.236	0.042	1.638	689.8	412.6	1.251	0.042	1.662	1.783
3	41	154-8-A	486.2	1.151	0.049	2.045	994.3	486.2	1.151	0.049	2.045	2.585
4	42	154-8-B	439.1	0.810	0.049	1.945	885.4	439.1	0.810	0.049	1.948	2.224
4	43	154-8-C	293.3	0.888	0.046	2.020	592.5	145.1	1.067	0.055	3.207	1.210
5+6	31	154-7	266.2	1.384	0.053	3.995	1063.5	140.8	1.569	0.064	6.174	2.270
7	45	154-4-A	447.1	0.873	0.060	3.595	1607.3	355.1*	0.953	0.060	3.890	3.591
8	46A	154-4-B	37.1	1.352	0.053	4.673	173.4					
8	46B	154-4-B	55.1	1.096	0.044	2.043	112.6					
8	47A	154-4	24.23	1.209	0.076	40.33	977.2					
8	47B	154-4 (ashed)	16.15	1.177	0.061	4.19	67.7					
9	2-1	154-6A	209.2	1.739	0.064	6.44	1347.2	170.6	1.879	0.069	7.445	3.303
9	2-2	154-6-B	215.5	1.682	0.068	0.002	1724.4	180.7	1.697	0.070	7.932	3.726
10	3-1	154-3-A	623.5	1.104	0.044	3.590	2238.4	292.4	1.658	0.068	7.210	5.482
10	3-2	154-3-B	570.5	1.025	0.052	3.822	2180.5	242.8	1.794	0.086	8.428	5.320
11	18	154-2-A	310.9	1.032	0.046	3.179	988.3	126.4	1.298	0.056	3.011	0.989
11	19	154-2-B	274.4	1.310	0.040	5.613	1540.2	36.7	1.602	0.038	1.718	0.164

* Morphology alone.

Table 43

SUMMARY OF ROUND-ROBIN TEST RESULTS ON FIELD SAMPLE 661 (ALL SAMPLES ASHED)

Operator Code	1	2	3	4	5	6	7	8	9	10	11	12
				Size Distribution of All Fibers					Size Distribution of Chrysotile			
	Date Set Code	Filter	Number Concentration of All Fibers, $10^6/m^3$	Mean Length, μm	Mean Diameter, μm	Mean Volume, 10^{-15} cm^3	Volume Concentration of All Fibers, 10^{-9} cm^3/m^3	Number Concentration of Chrysotile, $10^6/m^3$	Mean Length, μm	Mean Diameter, μm	Mean Volume, 10^{-15} cm^3	Chrysotile Mass Concentration in Air, μg/m^3
1	73	661-4	278.3	0.846	0.065	5.314	1478.9	116.9	1.206	0.065	9.964	3.029
1	74	661-4	300.9	1.916	0.073	7.345	2210.1	158.9	1.892	0.079	12.18	5.035
1	75	661-4	425.9	1.682	0.085	11.02	4693.4	278.2	2.105	0.093	14.85	10.740
1	76	661-5	349.1	1.223	0.077	8.108	2858.4	139.7	2.320	0.067	9.39	3.411
1	77	661-5	109.7	3.614	0.113	17.09	1874.8	49.9	7.515	0.133	32.47	4.211
1	78	661-5	179.1	1.016	0.073	8.22	1472.2	123.7	1.259	0.065	9.20	2.957
1	79	661-4	415.1	0.895	0.073	63.57	26388.0	137.1	0.974	0.048	2.09	0.746
1	90	661-4	659.6	0.771	0.077	5.571	3674.6	223.7	0.979	0.056	3.026	1.760
1	91	661-4	408.8	0.978	0.106	82.25	33623.8	318.0	1.132	0.119	105.3	87.09
2	69	661-1	92.3	1.323	0.098	21.71	2003.8	41.2	1.644	0.087	21.20	2.267
2	70	661-1	76.6	1.745	0.114	61.23	4690.0	32.6	2.057	0.099	76.91	6.526
3	51-A	661-1	49.8	1.408	0.118	127.1	6329.6	47.3	1.382	0.117	132.5	16.31
3	51-B	661-1	23.3	3.356	0.200	281.2	6551.9	14.9	4.017	0.210	373.1	14.50
3	51-C	661-1	14.9	2.019	0.166	902.0	13439.8	14.1	2.050	0.169	954.1	35.01
4	52-1	661-1	11.1	3.900	0.351	720.5	7997.5	8.8	4.391	0.394	882.5	20.32
4	52-2	661-1	16.3	2.020	0.166	251.2	4094.6	10.24	2.400	0.170	373.3	9.939
4	52-3	661-1	21.6	2.298	0.144	176.5	3812.4	17.16	2.561	0.161	220.2	9.824
5	81-A	661-7	556.5	1.098	0.074	9.22	5130.9	291.5	1.494	0.078	12.19	9.241
5	81-B	661-7	432.8	0.989	0.094	43.31	18744.5	185.5	1.381	0.126	95.92	46.26
6	82-A	661-7	547.6	1.124	0.097	58.13	31831.9	176.7	1.865	0.130	166.1	76.28
6	82-B	661-7	379.8	1.042	0.062	5.89	2237.0	159.0	1.539	0.061	5.18	2.14
8	48-A	661-5	147.2	1.562	0.080	15.91	2341.9	23.0	1.773	0.070	13.82	0.827
8	48-B	661-5	138.0	1.047	0.077	9.36	1291.7	32.2	1.417	0.109	15.85	1.327
8	48-C	661-5	174.8	0.963	0.074	23.53	4113.0	9.2	1.310	0.120	37.11	0.888
9	49-A	661-6	208.5	1.865	0.058	9.05	1886.9	151.2	1.946	0.060	9.81	3.857
9	49-B	661-6	200.3	1.139	0.052	3.99	799.2	134.9	1.337	0.056	4.68	1.642
11	86	661-2	260.6	1.248	0.071	17.52	4565.7	58.5	2.029	0.100	45.69	6.949
11	87	661-2	259.5	1.698	0.068	11.41	2960.9	80.8	2.811	0.084	23.09	4.85

Table 44

SUMMARY OF ROUND-ROBIN TEST RESULTS ON FIELD SAMPLE 661 (ALL SAMPLES ANALYZED WITHOUT ASHING)

Operator Code	1	2	3	4	5	6	7	8	9	10	11	12
			Number Concentration of All Fibers, $10^6/m^3$	Size Distribution of All Fibers			Volume Concentration of All Fibers, 10^{-9} cm^3/m^3	Number Concentration of Chrysotile, $10^6/m^3$	Size Distribution of Chrysotile			Chrysotile Mass Concentration in Air, $\mu g/m^3$
	Data Set Code	Filter		Mean Length, µm	Mean Diameter, µm	Mean Volume, 10^{-15} cm^3			Mean Length, µm	Mean Diameter, µm	Mean Volume 10^{-15} cm^3	
1	71	661-4*	79.7	3.067	0.167	293.0	23352.0	34.0	4.853	0.171	328.1	29.035
1	72	661-4*	78.0	1.490	0.134	53.43	4167.5	47.3	1.589	0.131	63.03	7.755
2	80	661-4*	21.4	2.916	0.178	124.87	2672.0	9.3	3.719	0.145	90.32	2.193
5	83A	661-7*	71.4	1.728	0.138	58.07	4146.2	36.53	2.614	0.170	83.54	7.935
5	83B	661-7*	53.14	2.197	0.119	95.61	5080.7	18.27	4.227	0.163	218.5	10.37
6	84	661-7*	53.1	2.100	0.091	31.90	1693.9	23.3	3.064	0.098	48.53	2.933
4	53	661-1*	23.6	3.519	0.280	1781.0	42031.6	18.6	3.713	0.313	2203.0	106.7
4	54	661-1*	33.2	2.284	0.151	82.55	2740.7	27.6	3.361	0.151	81.53	5.483
10	50	661-3*	43.2	1.551	0.109	53.05	2291.8	11.2	2.25	0.120	62.97	1.827

INTERLABORATORY COMPARISONS

A direct and simple statistical method is follwed here for comparing transmission electron microscope estimates for the two air samples examined in the round-robin test.

Data from the different laboratories were considered in three types of comparisons.

1. Data for the laboratory air sample (unashed) as summarized in Table 42
2. Data for the field air sample with ashing as summarized in Table 43 (ashed only)
3. Data for the field air sample without ashing presented in Table 44

In each case, estimates of the following four parameters can be compared:

1. Number concentrations of all fibers, $10^6/m^3$
2. Volume concentrations of all fibers, $10^{-9}\ cm^3/m^3$
3. Number concentrations of chrysotile fibers, $10^6/m^3$
4. Mass concentrations of chrysotile fibers, $\mu g/m^3$

For each of these parameters, sample means and standard deviations were computed for each operator. Confidence intervals about the mean at the 95% level were calculated and graphed for comparison with the overall mean for each case. These are listed in Tables 45, 46, and 47. The quantities listed in each table are as follows:

Operator Code - 1 to 11

n - Number of observations (or grids examined)

$t\ (\frac{\alpha}{2}, n-1)$ - t-value at 95% confidence ($\alpha = 0.05$) and n-1 degrees of freedom

s - Standard deviation of the observed values

SEm - Standard error of the mean value

t•SEm - Interval for obtaining 95% confidence limits

$\bar{x}$ - Mean value

Lower - Lower limit at 95% confidence, i.e., $\bar{x} - t\cdot(SEm)$

Upper - Upper limit at 95% confidence, i.e., $\bar{x} - t\cdot(SEm)$

Table 45

95% CONFIDENCE INTERVALS ON THE MEAN ESTIMATES FOR INDIVIDUAL OPERATORS IN AIR SAMPLE 154 (SEE TABLE 42)

Operator Code		1	2	3	4	566	7	8	9	10	11	All Operators Combined
	n	6	6	2	2	1	1	2	2	2	2	26
	$t\ (\frac{\alpha}{2}, n-1)$	2.571	2.571	12.706	12.706	--	--	12.706	12.706	12.706	12.706	2.060
Concentration of All Fibers ($10^6/m^3$)	s	79.24	52.42	46.03	103.10	--	--	16.76	4.45	37.48	25.81	143.98
	SEm*	32.35	21.40	32.55	72.90	--	--	11.85	3.15	26.50	18.25	28.24
	t•SEm	83.2	55.0	413.6	926.3	--	--	150.6	40.0	336.7	231.9	58.2
	$\bar{x}$	429.6	274.3	453.6	366.2	266.2	447.1	31.2	212.4	597.0	292.6	332.4
	lower	346.4	219.3	40.0	Negative	--	--	Negative	172.4	260.3	60.7	274.2
	upper	512.8	329.3	867.2	1292.5	--	--	181.8	252.4	933.7	524.5	390.6
Volume Concentration (10^{-9} cm^3/m^3)	s	421.33	362.04	215.31	185.90	--	--	197.21	266.72	40.94	390.25	526.29
	SEm	172.01	147.80	152.25	131.45	--	--	139.45	188.60	28.95	275.95	103.21
	t•SEm	442.2	380.0	1934.5	1670.2	--	--	1771.8	2396.3	367.8	3506.2	212.6
	$\bar{x}$	1267.8	1406.9	842.0	724.0	1063.5	1067.3	292.6	1535.8	2209.4	1264.2	1248.3
	lower	825.6	1026.9	Negative	Negative	--	--	Negative	Negative	1841.6	Negative	1035.7
	upper	1710.0	1786.9	2776.5	2394.2	--	--	2064.4	3932.1	2577.2	4770.4	1460.9
Concentration of Chrysotile ($10^6/m^3$)	s	72.36	32.60	52.04	207.89	--	--	--	7.14	35.07	63.43	131.01
	SEm	29.54	13.31	36.80	147.00	--	--	--	5.05	24.80	44.85	26.74
	t•SEm	75.95	34.2	467.5	1867.8	--	--	--	64.1	315.1	569.9	55.3
	$\bar{x}$	310.6	105.7	449.4	292.1	140.8	355.1	--	175.6	267.6	81.6	230.2
	lower	234.6	7.15	Negative	Negative	--	--	--	111.5	Negative	Negative	174.9
	upper	386.5	139.9	916.9	2159.9	--	--	--	239.7	582.7	651.6	285.5
Chrysotile Mass Concentration ($\mu g/m^3$) in Air	s	1.030	0.682	0.567	0.717	--	--	--	0.299	0.115	0.583	1.291
	SEm	0.420	0.278	0.401	0.507	--	--	--	0.211	0.081	0.412	0.264
	t•SEm	1.081	0.716	5.094	6.442	--	--	--	2.686	1.033	5.238	0.545
	$\bar{x}$	3.029	2.433	2.184	1.717	2.260	3.591	--	3.515	5.401	0.577	2.725
	lower	1.948	1.717	Negative	Negative	--	--	--	0.829	4.368	Negative	2.180
	upper	4.110	3.149	7.278	8.159	--	--	--	6.201	6.434	5.815	3.270

* SEm stands for standard error of the mean.

Table 46

95% CONFIDENCE INTERVALS ON THE MEAN ESTIMATES FOR INDIVIDUAL OPERATORS IN FIELD AIR SAMPLE 661 (SEE TABLE 43) (Ashed Samples Only)

Operator Code		1	2	3	4	5	6	8	9	11	All Operators Combined
	n	9	2	3	3†	2†	2†	3†	2†	2†	28
	t $(\frac{\alpha}{2}, n-1)$	2.306	12.706	4.303	4.303	12.706	12.706	4.303	12.706	12.76	2.052
Concentration of All Fibers ($10^6/m^3$)	s	159.59	11.10	18.22	5.25	87.47	118.65	19.15	5.80	0.78	184.40
	SEm*	53.20	7.85	10.52	3.03	61.86	83.91	11.06	4.10	0.55	34.85
	t•SEm	122.7	99.7	45.3	13.04	785.98	1066.2	47.58	52.09	6.99	71.51
	$\bar{x}$	347.4	84.4	29.3	16.3	494.7	463.7	153.3	204.4	260.1	240.64
	lower	224.7	Negative	Negative	3.26	Negative	Negative	105.72	152.31	253.61	169.13
	upper	470.1	184.1	74.6	29.34	1280.68	1529.9	200.88	256.49	267.59	312.15
Volume Concentration (10^{-9} cm^3/m^3)	s	12260.61	1899.43	3105.37	2339.0	9626.27	20926.7	1425.92	769.12	1134.76	9126.5
	SEm	4086.87	1343.10	1792.89	1350.4	6806.8	14797.5	823.2	543.85	802.40	1724.7
	t•SEm	9424.3	17065.4	7714.8	5811.0	86487.4	188016.9	3542.5	6910.17	10195.3	3539.2
	$\bar{x}$	8697.1	3346.9	11937.3	5301.5	11937.7	17034.5	2582.2	1343.05	3763.3	7253.5
	lower	Negative	Negative	4222.5	Negative	Negative	Negative	Negative	Negative	Negative	3714.3
	upper	18121.4	20413.0	19652.1	11112.5	98425.1	205051.4	6124.7	8253.22	13958.6	10792.7
Concentration of Chrysotile ($10^6/m^3$)	s	85.13	6.08	18.94	4.47	74.95	12.51	11.57	11.52	15.77	92.11
	SEm	28.38	4.30	10.94	2.58	53.00	8.85	6.68	8.15	11.15	17.41
	t•SEm	65.4	54.7	47.1	11.10	673.42	112.45	28.75	103.55	141.67	35.72
	$\bar{x}$	171.88	36.9	25.4	12.07	238.50	167.85	21.47	143.05	69.65	108.39
	lower	106.4	Negative	Negative	0.97	Negative	55.40	Negative	39.50	Negative	72.67
	upper	237.2	91.5	72.5	23.17	931.92	280.30	50.23	46.60	211.32	144.11
Mass Concentration in Air ($\mu g/m^3$)	s	27.846	3.012	7.437	6.027	26.176	52.425	0.273	1.566	1.484	21.859
	SEm	9.282	2.130	4.294	3.480	19.623	37.070	0.157	1.107	1.049	4.131
	t•SEm	21.404	27.061	18.476	14.973	249.325	471.013	0.677	14.072	13.335	8.477
	$\bar{x}$	13.220	4.397	30.140	13.361	27.750	39.210	1.014	2.749	5.877	13.855
	lower	Negative	Negative	11.664	Negative	Negative	Negative	0.337	Negative	Negative	5.378
	upper	34.624	31.458	48.616	28.334	227.075	510.223	1.691	16.821	19.234	22.332

* SEm stands for standard error of the mean.

† The basic data on some TEM grid was split into two or more subsets, based on either one or more grid openings. This was necessary to obtain the variation.

Table 47

95% CONFIDENCE INTERVALS ON THE MEAN ESTIMATES FOR INDIVIDUAL OPERATORS IN FIELD AIR SAMPLE 661 (SEE TABLE 44) (Unashed Samples Only)

Operator Code		1	2	4	5	6	10	All Operators Combined
	n	2	1	2	2†	1	1	9
	t ($\frac{\alpha}{2}$, n-1)	12.706	--	12.706	12.706	--	--	2.306
Concentration of All Fibers ($10^6/m^3$)	s	1.20	--	6.79	12.91	--	--	22.31
	SEm*	0.85	--	4.80	9.13	--	--	7.44
	t·SEm	10.80	--	60.99	116.00	--	--	17.15
	$\bar{x}$	78.85	21.4	28.40	62.27	53.1	43.2	50.75
	lower	68.05	--	Negative	Negative	--	--	33.60
	upper	89.65	--	89.39	178.27	--	--	67.90
Volume Concentration (10^{-9} cm^3/m^3)	s	13565.5	--	27782.9	660.8	--	--	13834.80
	SEm	9592.3	--	19645.5	467.2	--	--	4611.61
	t·SEm	121879.4	--	249615.7	5936.9	--	--	10634.37
	$\bar{x}$	13759.7	2672.0	22386.1	4613.45	1693.9	2291.8	9797.38
	lower	Negative	--	Negative	Negative	--	--	Negative
	upper	135639.1	--	277398.6	10550.35	--	--	20431.75
Concentration of Chrysotile ($10^6/m^3$)	s	9.40	--	6.36	12.91	--	--	12.47
	SEm	6.65	--	4.50	9.13	--	--	4.156
	t·SEm	84.49	--	57.18	116.00	--	--	9.58
	$\bar{x}$	40.65	9.3	23.10	27.40	23.3	11.2	25.12
	lower	Negative	--	Negative	Negative	--	--	15.54
	upper	125.14	--	80.28	143.40	--	--	34.70
Mass Concentration Chrysotile in Air ($\mu g/m^3$)	s	15.047	--	71.571	1.722	--	--	33.787
	SEm	10.65	--	50.608	1.217	--	--	11.262
	t·SEm	135.192	--	643.033	15.469	--	--	25.971
	$\bar{x}$	18.395	2.193	56.091	9.152	2.933	1.827	19.359
	lower	Negative	--	Negative	Negative	--	--	Negative
	upper	153.585	--	699.124	24.621	--	--	45.330

* SEm stands for standard error of the mean.

† Data from same TEM grid was split into two subsets, based on grid opening, in order to obtain variability.

For some operators, there is only one observation. In such a situation, only the value is plotted, but no estimate for standard error is obtainable and the confidence interval is undetermined. These are shown as the point values with no confidence interval, where it should be noted that this represents a confidence interval that is indefinite.

GRAPHICAL REPRESENTATION OF RESULTS

These results are graphed in Figures 15 (a, b, c, and d), 16 (a, b, c, and d), and 17 (a, b, c, and d) for the observed parameters and in cases 1, 2, and 3 previously mentioned.

When the computed lower limit is negative, the confidence interval is truncated at zero. This suggests that Ln-transformation should be used to avoid non-positive values, in better agreement with the physical situation.

The overall mean in each case has been plotted as dashed lines to facilitate direct comparison with estimates of individual operators. Laboratories and operators whose confidence intervals overlap the overall averages can be considered in good agreement. Some operators have narrower confidence intervals due to a larger number of replications.

The results for Tables 43 and 44 (field air sample) showed greater variations than that in laboratory sample, and thus the change in scale for the plots should be noted.

ACCURACY AND PRECISION OF ESTIMATES

Accuracy of TEM Chrysotile Mass Estimates

As described earlier, it is impossible to obtain complete characterization of an asbestos sample by some method independent of electron microscopy. At the most, only the chrysotile mass estimate may be obtained by an independent method. Of the several approaches tried, only high-precision X-ray fluorescence spectrometry appeared useful [65]. The overall chrysotile mass estimates by the electron microscope method on the two round-robin tests are compared below with those by X-ray fluorescence analysis for magnesium content.

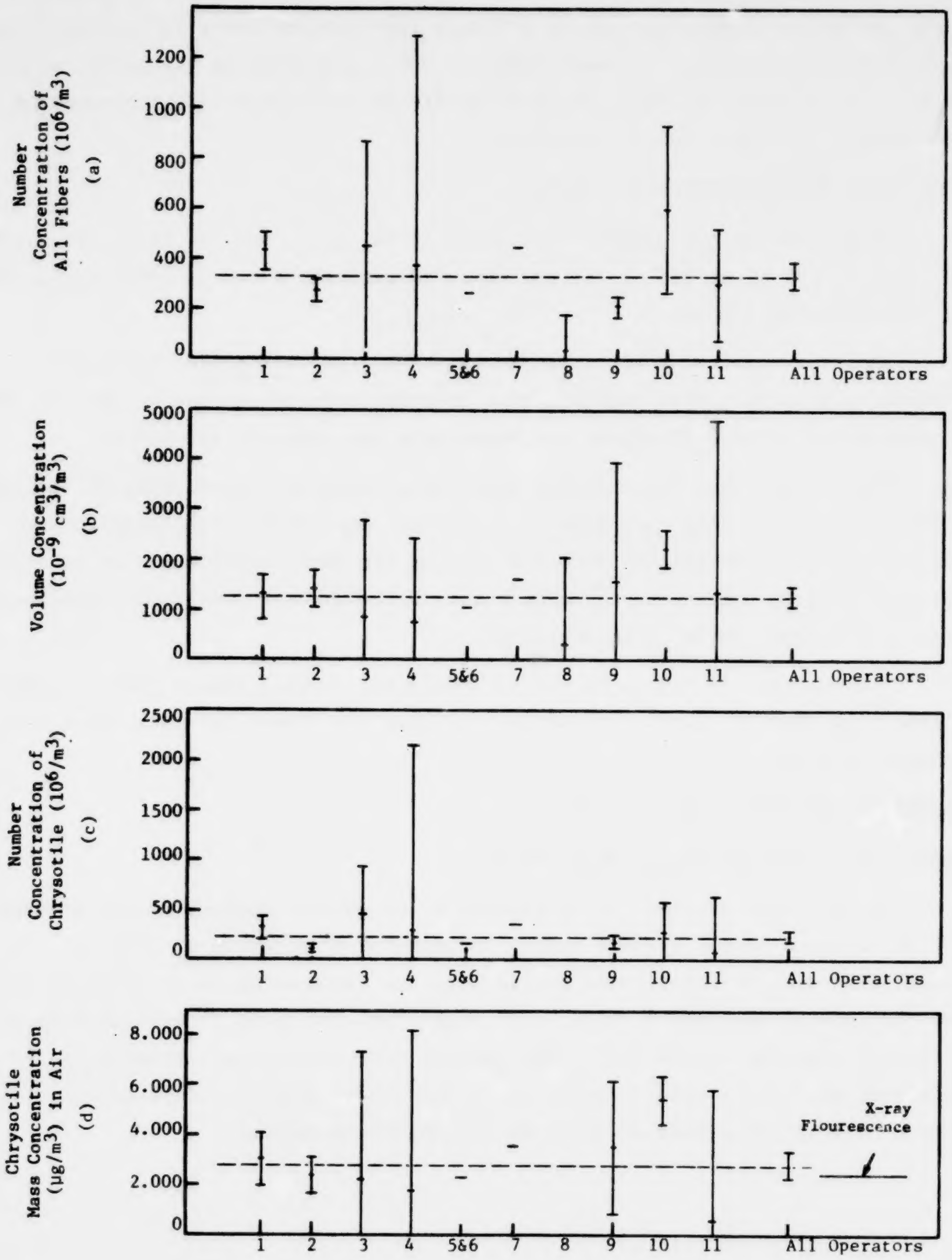

Figure 15. 95% confidence intervals about the means in laboratory air sample 154 (see Tables 42 and 45).

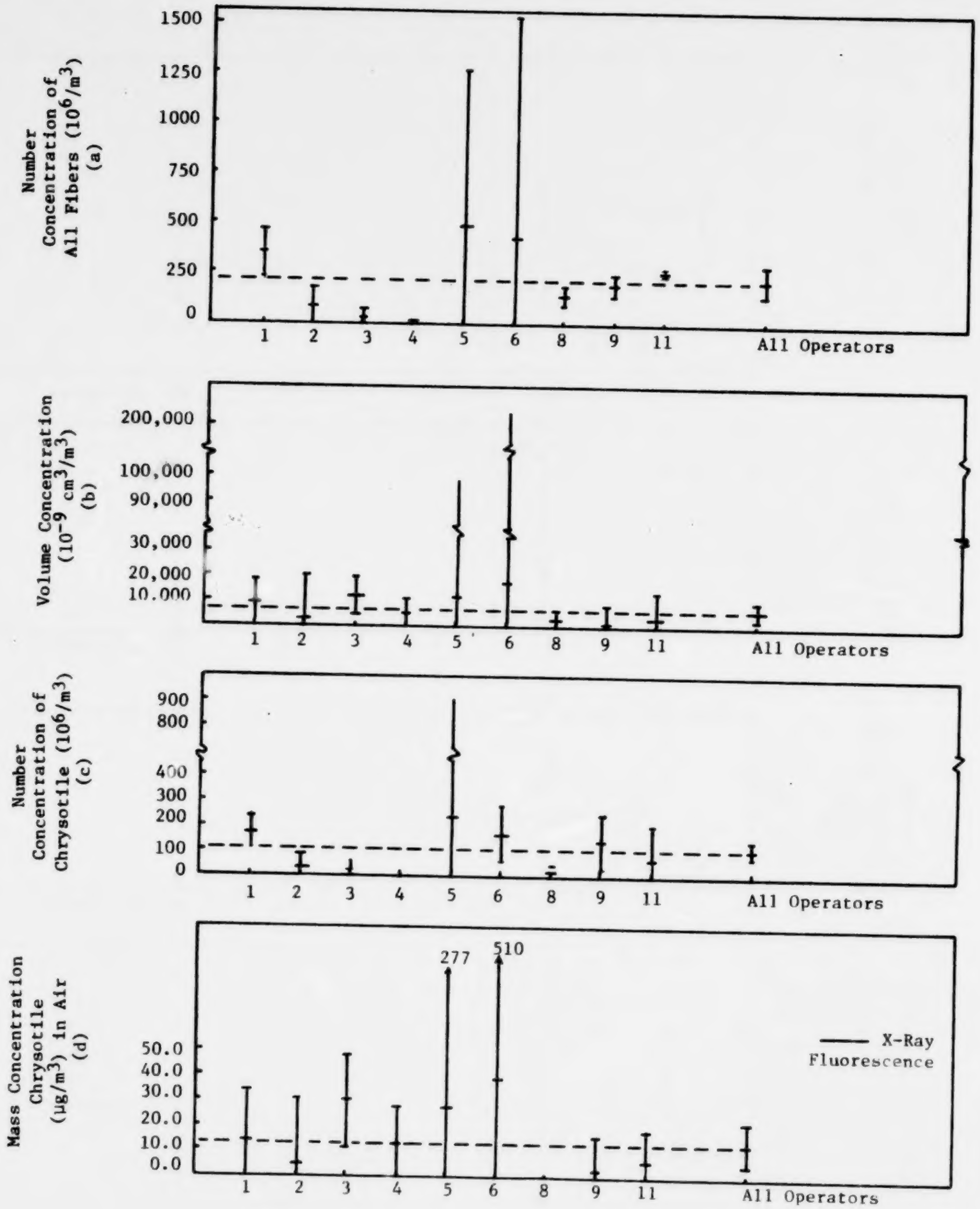

Figure 16. 95% confidence intervals about the means in field air sample 661 (see Tables 43 and 46), ashed samples only.

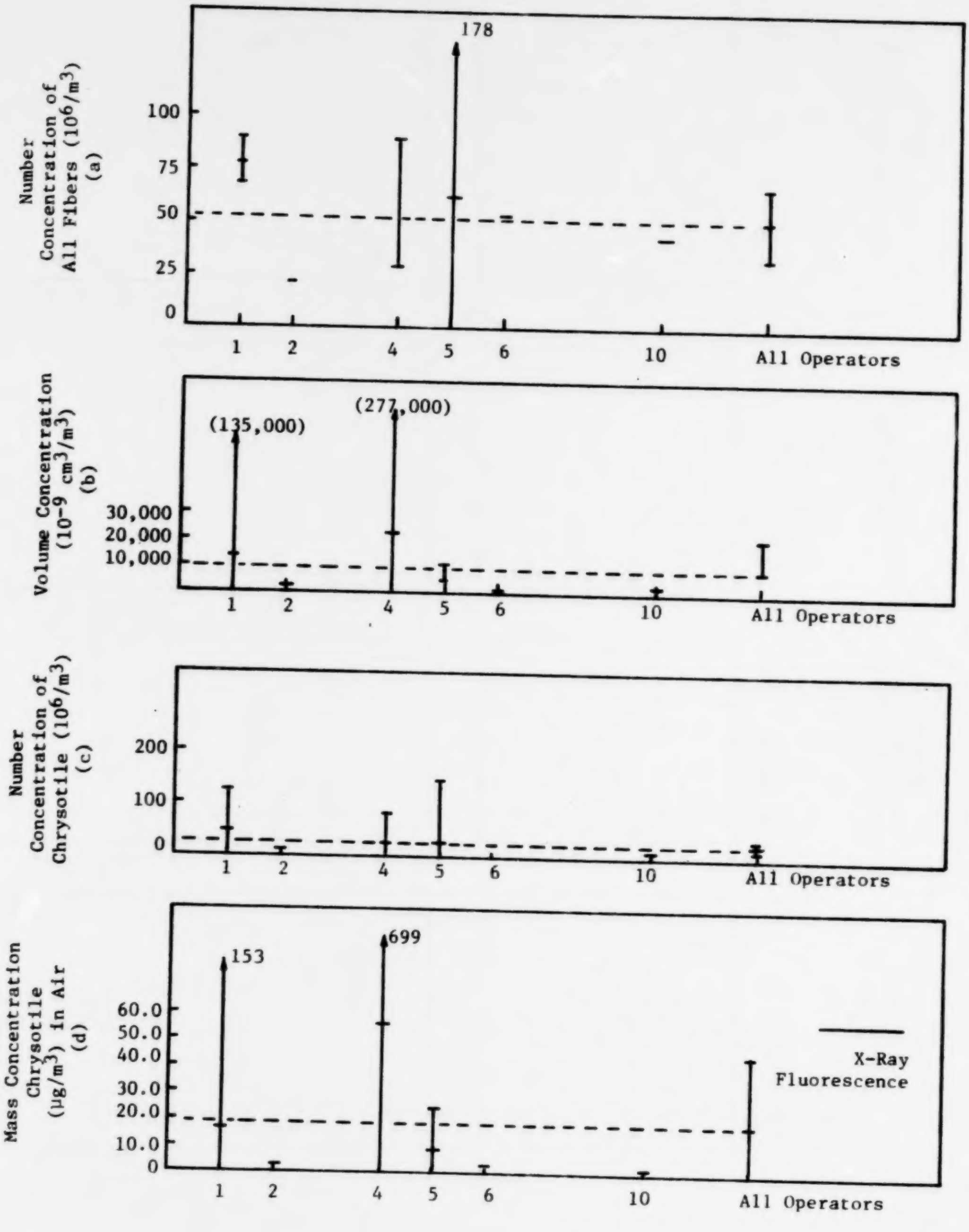

Figure 17. 95% confidence intervals about the means in field air sample 661 (see Tables 44 and 47), unashed samples only.

Air Sample	Electron Microscope Estimate Chrysotile Mass Concentration in Air $\mu g/m^3$	X-ray Fluorescence Chrysotile Mass Concentration in Air $\mu g/m^3$
Lab Sample 154	2.725	2.452
Field Sample 661 (ashed & unashed)	15.396	57.919
Field Sample 661 (ashed samples only)	13.751	57.919

As expected, the agreement is good for the laboratory air sample 154, but poor for the field air sample. Direct comparison of results on field sample is inappropriate because XRF measures all magnesium in chrysotile, non-chrysotile, and even non-fibrous minerals present. For the laboratory air sample, where such interferences are avoided, the EM method is in good agreement with the XRF method. These estimates from X-ray fluorescence method are also included in Figures 15d, 16d, and 17d for direct comparison with estimates of individual TEM operators.

Precision of TEM Estimates in Laboratory Air Sample

One way of comparing precision of individual operators is illustrated in Table 48. Here, the ratio of the standard error to the mean value is expressed as a percentage and used as a measure of precision. Smaller value of this ratio signifies better precision.

From Table 48 the precision appears very good (less than 10%) for operators 1, 2, 3, 9, 10, and 11 for number concentrations of all fibers (see column 5). The precision for operator 11 is poor (55% and 71%) for number concentrations and mass concentrations of chrysotile respectively (see columns 8 and 11). In chrysotile fiber number concentration estimate, operator 11 is the lowest (81.55) and operator 3 the highest (449.4). The mean value of the estimate for all operators is 230.0×10^6 fibers/m^3. In chrysotile mass concentration estimate, operator 11 is the lowest (0.58) and operator 10 the highest (5.4). The mean value of the estimate for all operators is 2.72 $\mu g/m^3$.

Table 48

PRECISION OF FIBER CONCENTRATION ESTIMATES ON LABORATORY AIR SAMPLE 154

1	2	3	4	5	6	7	8	9	10	11	12	13	14
		All Fibers Number Concentration 10^6 Fibers/m^3			Chrysotile Fibers Number Concentration 10^6 Fibers/m^3			Chrysotile Fibers Mass Concentration μg/m^3			Percentage of Fibers Identified by SAED		
Operator Code	No. of Tests	Mean	Std. Error	$\frac{\text{Std. Error}}{\text{Mean}}$ x100	Mean	Std. Error	$\frac{\text{Std. Error}}{\text{Mean}}$ x100	Mean	Std. Error	$\frac{\text{Std. Error}}{\text{Mean}}$ x100	Mean	Std. Error	$\frac{\text{Std. Error}}{\text{Mean}}$ x100
1	6	429.6	32.35	7.53	310.55	29.54	9.51	3.029	0.420	13.88	72.59	3.489	4.81
2	6	274.26	21.42	7.81	105.72	13.31	12.59	2.433	0.278	11.44	39.30	3.953	10.06
3	2	453.65	32.55	7.18	449.4	36.80	8.19	2.184	0.401	18.36	99.00	1.000	1.01
4	2	266.20	72.90	19.91	292.1	147.00	50.32	1.717	0.507	29.53	76.33	23.670	31.00
5&6	1	266.2	--	--	140.8	--	--	2.260	--	--	52.66	--	--
7	1	447.1	--	--	355.1	--	--	3.591	--	--	--	--	--
8	1	43.1	--	--	--	--	--	--	--	--	--	--	--
8*	1	19.4	--	--	--	--	--	--	--	--	--	--	--
9	2	212.35	3.15	1.48	175.65	5.05	2.88	3.515	0.211	6.02	82.70	1.140	1.38
10	2	597.0	26.50	4.44	267.6	24.80	9.27	5.401	0.081	1.50	55.19	6.515	11.81
11	2	292.65	18.25	6.24	81.55	44.85	55.00	0.577	0.412	71.49	27.01	13.630	50.47

* Ashed and reconstituted.

Precision of TEM Estimates in Field Air Sample

Precision as measured by the ratio of standard error to the mean value, expressed as a percentage, on field sample is summarized in Tables 49 and 50.

The precision for chrysotile fiber number concentration in the ashed samples varies from 5.69 to 43 (see column 8 in Table 49), and for chrysotile mass concentration varies from 14.20 to 94.5 (see column 11 in Table 49).

The precision for chrysotile fiber number concentration in unashed samples varies from 16.36 to 33.32 (see column 8 in Table 50), and for chrysotile mass concentration varies from 13.33 to 90.24 (see column 11 in Table 50).

Comparison of Precision in Round-Robin Samples

Table 51 lists the average precision value and its standard deviation for the laboratory sample and the field sample.

It is evident that the mean precision for chrysotile fiber number concentration is almost the same for the laboratory sample and the field sample, ashed as well as unashed. However, the mean precision for chrysotile mass concentration is much better for the laboratory sample (21.74) than that for field sample (44.17 for ashed and 53.81 for unashed). In general, there is no difference in mean values of precision between ashed and unashed field samples.

Ashed Field Sample - (See Table 49)

In chrysotile fiber number concentration, operator 4 is the lowest (12.07) and operator 5 is the highest (238.5). The mean for all operators is 108×10^6 fibers/m^3. In chrysotile mass concentration, operator 8 is the lowest (1.01) and operator 6 is the highest (39.21). The mean for all operators is 13.85 μg/m^3.

Unashed Field Sample - (See Table 50)

In the chrysotile fiber number concentration estimate, operator 2 is the lowest (9.3) and operator 1 is the highest (40.65). The mean value of estimate for all operators is 25.12×10^6 fibers/m^3. In the chrysotile mass concentration estimate, operator 10 is the lowest (1.83) and operator 4 is the highest (56.09). The mean value of the estimate for all operators is 19.36 μg/m^3.

The spread in estimates is much higher in the ashed field sample than in the unashed field sample.

Table 49

PRECISION OF FIBER CONCENTRATION ESTIMATES ON FIELD SAMPLE 661 (ALL SAMPLES ASHED)

1	2	3	4	5	6	7	8	9	10	11	12	13	14
Operator Code	No. of Tests	All Fibers Number Concentration 10^6 Fibers/m^3			Chrysotile Fibers Number Concentration 10^6 Fibers/m^3			Chrysotile Fibers Mass Concentration $\mu g/m^3$			Percentage of Fibers Identified by SAED		
		Mean	Std. Error	$\frac{\text{Std. Error}}{\text{Mean}}$x100	Mean	Std. Error	$\frac{\text{Std. Error}}{\text{Mean}}$x100	Mean	Std. Error	$\frac{\text{Std. Error}}{\text{Mean}}$x100	Mean	Std. Error	$\frac{\text{Std. Error}}{\text{Mean}}$x100
1	9	347.3	53.20	15.31	171.8	28.37	16.52	13.22	9.28	70.20	66.094	4.287	6.48
2	2	84.4	7.85	9.30	36.9	4.30	11.65	4.39	2.13	48.51	50.385	0.385	0.76
3	3	29.3	10.52	35.86	25.4	10.94	43.00	30.15	4.29	14.23	95.873	3.327	3.47
4	1	16.3	3.03	18.59	12.0	2.58	21.37	13.36	3.48	26.05	87.57	7.35	8.39
5	2	494.7	61.86	20.99	238.5	53.0	22.22	27.75	19.62	70.70	49.66	2.72	5.48
6	2	463.8	83.91	18.09	167.8	8.85	5.27	39.21	37.07	94.54	37.06	4.80	12.95
8	3	153.3	11.06	7.21	21.4	6.68	31.11	1.01	0.16	15.34	15.77	5.42	34.38
9	2	204.4	4.10	2.00	143.0	8.15	5.69	2.75	1.11	40.36	69.96	2.60	3.72
11	2	260.1	0.55	0.21	69.6	11.75	16.01	5.90	1.05	17.79	28.24	4.28	18.71

Table 50

PRECISION OF FIBER CONCENTRATION ESTIMATES ON FIELD SAMPLE 661 (UNASHED)

1	2	3	4	5	6	7	8	9	10	11	12	13	14
		All Fibers Number Concentration 10^6 Fibers/m^3			Chrysotile Fibers Number Concentration 10^6 Fibers/m^3			Chrysotile Fibers Mass Concentration $\mu g/m^3$			Percentage of Fibers Identified by SAED		
Operator Code	No. of Tests	Mean	Std. Error	$\frac{\text{Std. Error}}{\text{Mean}} \times 100$	Mean	Std. Error	$\frac{\text{Std. Error}}{\text{Mean}} \times 100$	Mean	Std. Error	$\frac{\text{Std. Error}}{\text{Mean}} \times 100$	Mean	Std. Error	$\frac{\text{Std. Error}}{\text{Mean}} \times 100$
1*	2	78.85	0.85	1.07	40.65	6.65	16.36	18.39	10.64	57.85	70.515	1.365	1.94
2*	1	21.4	--	--	9.3	--	--	2.75	--	--	47.58	--	--
4*	2	28.4	4.80	16.90	23.6	4.50	19.07	56.09	50.61	90.24	95.48	2.521	2.64
5*	2	62.3	9.13	14.65	27.4	9.13	33.32	9.15	1.22	13.33	45.89	5.270	11.48
6*	1	53.1	--	--	23.3	--	--	2.93	--	--	43.75	--	--
10*	1	43.2	--	--	11.2	--	--	1.83	--	--	47.31	--	--

* Unahsed direct transfer.

Table 51

PRECISION OF DIFFERENT MEASUREMENTS IN THE TWO SAMPLES

		Laboratory Sample	Field Sample	
		Unashed	Ashed	Unashed
All Fibers Concentration $10^6/m^3$	Mean Value of Precision*	7.80	14.17	10.87
	Standard Deviation of Precision	5.78	11.00	8.56
Chrysotile Fibers $10^6/m^3$	Mean Value of Precision**	21.11	19.20	22.92
	Standard Deviation of Precision	21.79	12.11	9.11
Chrysotile Mass Concentration $\mu g/m^3$	Mean Value of Precision***	21.74	44.17	53.81
	Standard Deviation of Precision	23.71	28.95	38.61

* Obtained from mean of the values listed in column 5 of Tables 48, 49, and 50, respectively.

** Obtained from mean of the values listed in column 8 of Tables 48, 49, and 50, respectively.

*** Obtained from mean of the values listed in column 11 of Tables 48, 49, and 50, respectively.

Explanation of Large Variation in Field Sample

A large amount of this variation can be attributed to the presence of large bundles or fiber aggregates occasionally found in this sample. Quantitative characterization of samples containing fiber bundles is difficult for the following reasons:

1. One cannot readily estimate the volume of an aggregate of fibers. The current method of assigning some average length and width and assumption of a cylindrical shape results in a gross overestimate of the volume.
2. Fiber bundles generally have a large volume as compared with majority of individual fibers. The presence of fiber bundles makes the fiber distribution bi-modal. A few large bundles can account for a disproportionately large percentage of the total particulate volume and mass.

Table 52 shows that substantially large fractions of total chrysotile mass can be accounted for by a few chrysotile bundles. The contribution of these large bundles (i.e., larger than 1 μm^3 in volume) to the chrysotile number concentration is relatively small.

Characterizing of Fiber Bundles

At present there is no rational method for characterizing fiber bundles. Grouping fiber bundle entities along with individual fibers leads to problems as explained above. Elimination of fiber bundles through high energy ultrasonic treatment should not be undertaken because this may radically alter the initial sample characteristics. A complete disregard of the bundle entities, big and small, would result in biasing the data. In such cases, the following modifications are suggested:

1. Fiber bundles encountered should be reported as bundle entities with tentative average lengths and widths.
2. An arbitrary cut off, for example, bundles with volumes greater than $\simeq 1.0\ \mu m^3$, should be used to separate the large bundles from the other fibers or small bundles.
3. When a few large bundles are encountered during the random scans, we recommend that after collecting data on 100-200 fibers, the sample be searched for large fiber bundles only collecting data on these large bundles (say 20 or 30) by scanning over large areas. A somewhat lower magnification, say 10,000X or 5,000X, would be better for this. This will enable one to obtain more representative distribution of fiber bundles and their number and volume concentrations in the initial sample.

Table 52

EFFECT OF A FEW LARGE BUNDLES ON NUMBER CONCENTRATION AND MASS CONCENTRATION OF CHRYSOTILE IN FIELD SAMPLE 661

1	2	3	4	5	6
Data Set	Number Conc. of all Chrys. $10^6/m^3$	Number Conc. of Chrys. Bundles Greater than 1 μm^3 in Size $10^6/m^3$	Actual Number (counted) of Chrys. Bundles Greater than 1 μm^3	Mass Conc. of all Chrys. $\mu g/m^3$	Mass Conc. of Chrys. Bundles $\mu g/m^3$
73	116.9			3.029	
74	158.9			5.035	
75	278.2			10.740	
76	139.7			3.411	
77	49.9			4.211	
78	123.7			2.957	
79	137.1			0.746	
69	41.2			2.850	
70	32.6			8.204	
90	223.7			1.760	
91	318.0	11.36	1	80.629	63.8840
71*	34.0	1.66	2	29.035	24.2986
72*	47.3			7.755	
80*	9.3			2.757	
81	238.5		2	22.62	15.5115
82	167.8			9.91	
83*	27.4		1	9.153	3.5265
84*	23.3			2.933	
86	58.5			6.949	
51-1	47.3	3.32	4	21.58	15.8360
51-2	14.9	1.65	2	33.83	27.7713
51-3	14.1	0.83	1	35.01	34.3326
52	12.1	1.47	8	13.5	8.3418
53*	18.6	2.35	10	106.7	100.6012
54*	27.6			5.483	
50	11.2			1.827	
48	21.5			1.014	
49	143.1			2.749	

* Unashed.

4. In the analysis of the particulate data, these large bundles should be treated separately from the other fibrous particulates and their number and mass reported separately.

EFFECT OF ASHING, ULTRASONIFICATION, AND RECONSTITUTION

The field sample was studied with the inclusion of an ashing step by nine operators (see Table 43). The same sample was also studied without low temperature ashing, ultrasonification, and reconstitution by six operators (see Table 44).

Effect of Ashing on Number Concentration

One question most commonly asked is whether ashing, ultrasonification, and reconstitution alter the initial sample. To answer this question, one can compare the number concentration estimates and mean fiber length and width dimensions, in the unashed and ashed samples.

Table 53 lists the data for number concentrations of all fibers in the ashed samples (column 2), unashed samples (column 3), and the ratio of the concentration estimates for ashed samples to those for unashed samples. Similar quantities for number concentration for chrysotile fibers are listed in columns 5, 6, and 7, and for mass concentration of chrysotile in columns 8, 9, and 10.

From columns 4 and 7 of Table 53, it is clear that the data from operators 1, 2, 5, and 6 distinctly show an appreciable increase in the reported number of all fibers as well as the chrysotile fibers. This is in contrast to data from operator 4, who reports a net loss of fibers due to the ashing step.

The increase in fiber number concentrations due to ashing step may have two possible explanations:

1. Fiber breakage and breaking of bundles into fibrils.

2. A reduced interference by non-fibrous debris in the ashed sample, thus facilitating unhindered detection of fibers.

If the number of fibers is increased due to breakage, it should decrease the mean fiber length and mean fiber width in the ashed and reconstituted sample. However, this would also result if ashing led to reduced interference with the detection of relatively short and thin fibers.

Effect of Ashing on Mean Length and Mean Diameter of Fibers

The data on mean fiber length for all fibers and for chrysotile fibers are summarized in Table 54. The ratio of the mean fiber length in the ashed sample

Table 53

EFFECT OF LOW TEMPERATURE ASHING AND RECONSTITUTION OF FIBER CONCENTRATION ESTIMATES

1	2	3	4	5	6	7	8	9	10	11
	All Fibers Mean Number Concentration 10^6 Fibers/m^3			Chrysotile Fibers Mean Number Concentration 10^6 Fibers/m^3			Chrysotile Fibers Mean Mass Concentration $\mu g/m^3$			Remarks
Operator Code	Ashed	Unashed	Ratio Ashed/Unashed	Ashed	Unashed	Ratio Ashed/Unashed	Ashed	Unashed	Ratio Ashed/Unashed	Does Ashing Increase the Number of Fibers Counted?
1	347.39	78.85	4.406	171.79	40.65	4.226	13.22	18.39	0.719	Definitely
2	84.45	21.4	3.946	36.9	9.3	3.968	5.52	2.756	2.006	Definitely
3	29.33	--	--	25.43	--	--	30.15	--	--	Not enough data
4	16.3	28.4	0.574	12.1	23.6	0.513	13.50	56.09	0.241	No, there is a definite loss
5	494.7	62.3	7.941	238.5	27.4	8.704	22.62	9.15	2.472	Definitely
6	463.8	53.1	8.734	167.8	23.3	7.202	9.99	2.93	3.410	Definitely
8	153.3	--	--	21.5	--	--	1.01	--	--	Not enough data
9	204.4	--	--	143.1	--	--	2.75	--	--	Not enough data
10	--	43.2	--	--	11.2	--	--	1.83	--	Not enough data
11	260.6	--	--	58.5	--	--	6.95	--	--	Not enough data

Table 54

EFFECT OF LOW TEMPERATURE ASHING AND RECONSTITUTION OF MEAN FIBER DIMENSIONS

1	2	3	4	5	6	7	8	9	10	11	12	13	14	
	All Fibers - Characteristic Dimensions						Chrysotile Fibers - Characteristic Dimensions							
	Mean Fiber Length µm			Mean Fiber Diameter µm			Mean Fiber Length µm			Mean Fiber Diameter µm				
Operator Code	Ashed	Unashed	Ratio Ashed / Unashed	Ashed	Unashed	Ratio Ashed / Unashed	Ashed	Unashed	Ratio Ashed / Unashed	Ashed	Unashed	Ratio Ashed / Unashed	Does Ashing Reduce Observed Mean Fiber Length?	Does Ashing Reduce Observed Mean Fiber Diameter?
1	1.358	2.279	0.60	0.082	0.051	0.54	2.154	3.221	0.67	0.081	0.151	0.54	Definitely	Definitely
2	1.534	2.915	0.53	0.106	0.178	0.60	1.851	3.719	0.50	0.093	0.145	0.64	Definitely	Definitely
3	2.258	--	--	0.198	--	--	2.483	--	--	0.217	--	--	No Test Possible	
4	2.568	2.902	0.88	0.206	0.216	0.95	2.963	3.037	0.98	0.231	0.232	1.00	N.S.*	N.S.
5	1.075	1.928	0.56	0.079	0.126	0.63	1.450	3.152	0.46	0.093	0.168	0.55	Definitely	Definitely
6	1.005	2.100	0.48	0.082	0.091	0.90	1.474	3.064	0.48	0.097	0.098	0.99	Definitely	N.S.
8	1.180	--	--	0.077	--	--	1.529	--	--	0.097	--	--	No Test Possible	
9	1.510	--	--	0.055	--	--	1.659	--	--	0.058	--	--	No Test Possible	
10	--	1.551	--	--	0.109	--	--	2.255	--	--	0.120	--	No Test Possible	
11	1.248	--	--	0.071	--	--	2.029	--	--	0.100	--	--	No Test Possible	

* N.S. stands for not significant.

to that in the unashed sample is listed in column 4 for all fibers, and in column 10 for chrysotile fibers, Similar quantities for mean fiber diameter are listed in column 7 for all fibers and in column 13 for chrysotile fibers. Data from operators 1, 2, 5, and 6 support the contention that more fibers are being generated in ashing step due to fiber breakage. The data from operator 4 are inconclusive.

The second explanation may also be simultaneously correct, but it is difficult to verify. Operators 2, 5, and 6 have reported increased chrysotile mass estimates in ashed samples (see Table 53). This seems to suggest the second explanation.

The reported low number concentration in ashing step by operator 4 may be explained in two ways:

1. All fibers are not retained during the ashing and reconstitution.
2. Agglomeration occurs in the ashing step.

If the first explanation was valid, the mass concentration of chrysotile would be reduced after ashing. Table 53, column 10, does show that there was a substantial loss (75%) of chrysotile mass concentration.

If the second explanation was valid, the mean fiber dimensions should increase. Table 54 shows a slight decrease for mean fiber length for all fibers and practically no increase in mean length and mean diameter of chrysotile fibers. Hence, we may conclude that this is a real possibility of a true loss of fibers because of the several transfer steps in the ashing and reconstitution of samples.

We had used the mean fiber length and mean width for assessing the effect of ashing and sonification step. An alternative method would be to consider the entire length distribution. Table 55 lists the length distribution of fibers for unashed and ashed samples for operator 2. Tables 56, 57, and 58 show the length distributions reported by operations 4, 5, and 6, respectively. Frequencies have been expressed as percent frequencies for a direct comparison between ashed and unashed samples.

In all four cases, it appears that the largest fibers reported in unashed samples were longer than those for the ashed sample. Also, there were fewer long fibers in ashed sample as compared with the unashed sample.

Table 55

LENGTH DISTRIBUTION IN ASHED AND UNASHED SAMPLES, DATA FROM OPERATOR NUMBER 2

Ashed (Data Set 70) % Frequency		Length, μm		Unashed (Data Set 80) % Frequency
		15.15		1.92
		14.54		1.92
1.85		10.61		
		7.57		3.84
1.85		7.27		
1.85		6.97		
		6.67		1.92
1.85		6.36		1.92
		5.76		1.92
		5.15		1.92
1.85		4.85		5.77
		4.54		1.92
1.85		3.94		3.84
		3.64		7.69
		3.33		1.92
3.70		3.03		1.92
		2.75		7.69
7.41		2.42	←Median→	5.77
3.70		2.12		7.69
1.85		2.06		
3.70		1.82		7.69
1.85		1.57		
7.41		1.51		1.92
1.85		1.45		
1.85	←Median→	1.33		
1.85		1.21		5.77
5.55		1.09		
		0.97		1.92
3.70		0.91		11.51
11.11		0.73		3.84
20.37		0.61		5.77
5.55		0.48		1.92
1.85		0.36		
100.00				100.00

Table 56

LENGTH DISTRIBUTION IN ASHED AND UNASHED SAMPLES, DATA FROM OPERATOR NUMBER 4

Ashed (Data Set 52) % Frequency		Length, μm		Unashed (Data Set 53) % Frequency
		31.0		1.0
		27.0		1.0
		19.5		1.0
1.08		16.0		
1.08		14.0		
		11.5		2.0
		11.0		1.0
2.17		10.0		1.0
1.08		9.0		
		8.0		1.0
		7.75		1.0
		7.50		4.0
		7.00		1.0
		6.00		2.0
2.17		5.00		
		4.75		1.0
		4.50		1.0
1.08		4.25		1.0
2.17		4.00		6.0
1.08		3.75		
1.08		3.50		1.0
9.78		3.00		7.0
6.52		2.50		6.0
3.26		2.25		9.0
		2.17	←Median→	1.0
10.86		2.00		6.0
1.08		1.75		1.0
4.35	←Median→	1.50		9.0
5.43		1.25		5.0
		1.10		1.0
20.65		1.00		8.0
5.43		0.75		2.0
		0.70		3.0
1.08		0.65		
2.17		0.60		3.0
9.78		0.50		4.0
		0.45		3.0
		0.40		3.0
1.08		0.35		2.0
1.08		0.30		
3.25		0.25		
100.00				100.0

Table 57

LENGTH DISTRIBUTION IN ASHED AND UNASHED SAMPLES, DATA FROM OPERATOR NUMBER 5

Ashed (Data Set 81) % Frequency		Length, µm		Unashed (Data Set 83) % Frequency
		13.0		1.33
0.89		12.8		
		8.8		1.33
		8.5		1.33
		7.0		1.33
0.89		4.5		
		4.2		1.33
0.89		4.0		
		3.9		1.33
		3.7		1.33
0.89		3.5		2.67
		3.3		1.33
0.89		3.1		
0.89		3.0		1.33
0.89		2.9		
		2.8		2.67
0.89		2.7		
0.89		2.6		2.67
0.89		2.5		5.33
		2.4		1.33
2.68		2.3		
		2.2		5.33
0.89		2.0		5.33
0.89		1.8		1.33
3.57		1.7		1.33
2.68		1.5		5.33
1.78		1.4	←Median→	4.00
2.68		1.3		5.33
0.89		1.2		1.33
0.89		1.1		
7.14		1.0		6.67
1.78		0.9		
2.68		0.8		4.00
8.93	←Median→	0.7		5.33
16.07		0.6		12.00
16.96		0.5		5.33
12.50		0.4		5.33
8.03		0.3		4.00
100.00				100.00

Table 58

LENGTH DISTRIBUTION IN ASHED AND UNASHED SAMPLES, DATA FROM OPERATOR NUMBER 6

Ashed (Data Set 82) % Frequency		Length, μm		Unashed (Data Set 84) % Frequency
		0.30		3.12
		9.00		3.12
0.95		6.00		
0.95		4.50		
0.95		4.30		
0.95		4.00		9.38
		3.10		3.12
0.95		3.00		12.50
0.95		2.80		
0.95		2.50		
0.95		2.30		3.12
0.95		2.10		
1.90		2.00		
0.95		1.90		6.25
0.95		1.80		
0.95		1.70		
0.95		1.60		3.12
0.95		1.50		
0.95		1.40	←Median→	3.12
0.95		1.30		
2.86		1.20		
2.86		1.10		3.12
9.52		1.00		9.38
7.62		0.90		6.25
8.57	←Median→	0.80		9.38
10.47		0.70		6.25
5.71		0.60		3.12
19.05		0.50		12.50
11.43		0.40		3.12
3.81		0.30		
0.95		0.20		
100.00				100.00

The tendency for the distribution to shift towards the small length after ashing is quite evident.

With the limited data from this study, we tentatively conclude that ashing and sonification can significantly alter the measured sample characteristics. The exact mechanism of this difference remains obscure.

In this study of ashing and reconstitution, aerosol O.T. solution was used for resuspending the ash. There is a possibility that aerosol O.T. may have contributed to some breakage of chrysotile fibers and obscured the effects of actual ashing and ultrasonic treatment. So, further work is needed to evaluate the effects of ashing, dilution and reconstitution on the asbestos sample.

A full-scale study is also needed to evaluate the effect of dilution, without the ashing step. This could be done by dissolving the initial filter in a suitable solvent and then redepositing the solids onto a new polycarbonate filter after appropriate dilution.

CONCLUSIONS

This round-robin test was carried out with very little opportunity for most of the participants to become familiar with the provisional procedure. Much better results should be expected if such a test were repeated after participants obtained more experience with the procedure.

From the round-robin test, the following conclusions can be reached.

1. It is difficult to determine absolute accuracy of the electron microscope estimates. The overall mean estimate for chrysotile mass concentration according to the electron microscope method is 2.72 $\mu g/m^3$ in the laboratory air sample. This may be compared to a chrysotile concentration of 2.45 $\mu g/m^3$ for the same sample as determined independently by X-ray fluorescence spectrometric analysis of magnesium. Thus, the EM estimate of chrysotile mass concentration differs by only 10% with that by the X-ray fluorescence method.

2. In laboratory sample, the ratio of spread between 95% confidence limits to the mean value was 0.48 for chrysotile fiber concentration and about 0.40 for chrysotile mass concentration.

3. In the field air sample, studied with ashing, the ratio of the spread between 95% confidence limits to the mean value was about 0.49 for chrysotile fiber concentration and about 1.57 for chrysotile mass concentration. In the same sample, studied without ashing, the corresponding values are 0.62 for chrysotile fiber concentration and about 2.34 for chrysotile mass concentration.

4. Presence of a few large fibers or fiber bundles strongly influence the mass concentration estimates and mean values of length, width, and volume of fibers, but does not significantly affect the number concentration of fibers.

5. The following modifications are suggested to mitigate the adverse effects of fiber aggregates on sample characterization.

   a. Bundles or aggregates of fibers larger than 1 μm^3 (as judged by mean length, diameter, and cylindrical shape assumption) should be counted as single entities.

   b. Bundle entities should be treated separately and reported separately from other single fibers in the statistical analysis of fiber characteristics.

   c. Representative data on bundles can be collected by scanning the sample at a lower magnification (e.g., 5,000 X).

6. In any air sample, the precision of the estimates can be improved by studying at least three or four TEM grids.

REFERENCES

1. Thomson, J.G., R.O.C. Kaschula, and R.R. McDonald. Asbestosis as a Modern Urban Hazard. S. African Med. J., 37: 77, 1963.

2. Thomson, J.G. Asbestos and the Urban Dweller. Ann. N.Y. Acad. Sci., 132: 196, 1965.

3. Selikoff, I.J., J. Chrug and E.C. Hammond. The Occurrence of Asbestosis Among Insulation Workers in the United States. Ann. N.Y. Acad. Sci., 132: 139, 1965.

4. Hourihane, D.O. The Pathology of Mesotheliomata and Analysis of Their Association With Asbestos Exposure. Thorax, 19: 268-278, 1964.

5. Owen, W.G. Mesothelial Tumors and Exposure to Asbestos Dust. Ann. N.Y. Acad. Sci., 132: 674, 1965.

6. Newhouse, M.L. and H. Thompson. Mesothelioma of Pleura and Peritoneum Following Exposure to Asbestos in the London Area. Brit. J. Ind. Med., 22: 261, 1965.

7. Whipple, H.E. Biological Effects of Asbestos. Ann. N.Y. Acad. Sci., 132: 766, 1965.

8. Knox, J.F., R.S. Doll and I.D. Hill. Cohort Analysis of Changes in Incidence of Bronchial Carcinoma in a Textile Factory. Ann. N.Y. Acad. Sci., 132: 526, 1965.

9. Harington, J.S., et. al. Studies of the Mode of Action of Asbestos As a Carcinogen. S. African Med. J. 41(32): 800-804, 1967.

10. Tabershaw, I.R. Asbestos as an Environmental Hazard. J. Occup. Med., 16: 32, 1968.

11. McDonald, A.D., et. al. Epidemiology at Primary Malignant Mesothelial Tumors in Canada. Cancer, 26(4): 914-919, 1970.

12. Bader, M.E., et. al. Pulmonary Function and Radiographic Changes in 598 Workers with Varying Duration of Exposure to Asbestos. Mt. Sinai J. Med. 37(4): 492-500, 1970.

13. Gross, P., et. al. The Pulmonary Response to Fibrous Dusts of Diverse Compositions. Amer. Ind. Hyg. Assoc. J. 31(2): 25-32, 1970.

14. Reeves, A.L., et. al. Experimental Asbestos Carcinogenesis. Environ. Res. 4(6): 495-511, 1971.

15. Langer, A.M., I.J. Selikoff and A. Sastre. Chrysotile Asbestos in the Lungs of Persons in New York City. Arch. Environ. Health., 22: 348-361, 1971.

16. Selikoff, I.J., et. al. Asbestos Air Pollution. Arch. Environ. Health, 25(1): 1-13, 1972.

17. Selikoff, I.J., W.J. Nicholson and A.M. Langer. Carcinogenicity of Amosite Asbestos. Arch. Environ. Health, 25(3): 183-188, 1972.

18. Gilson, J.C., Health Hazards of Asbestos. Composites, 3: 59, 1972.

19. Sherrill, R. Asbestos - The Saver of Lives has a Deadly Side. N.Y. Times Magazine, January 21, 12 pp., 1973.

20. Asbestos Health Question Perplexes Experts. Chem. Eng. News. 51(50): 18, 1973.

21. Timbrell, V. Inhalation and Biological Effects of Asbestos. In: Assessment of Airborne Particles. Ed. T.T. Mercer et. al. Charles C. Thomas Publ., p. 429, 1972.

22. Stanton, M.F. and C. Wrench. Mechanism of Mesothelioma Induction with Asbestos and Fiber Glass. J. National Cancer Inst., 48: 797, 1972.

23. Report of the Advisory Committee on Asbestos Cancers to the Director of the International Agency for Research on Cancer. In: Biological Effects of Asbestos. International Conference, Lyon, France, International Agency for Research on Cancer, IARC Scient. Publ. 8: 341, 1973.

24. National Emission Standards for Hazardous Air Pollutants - Asbestos, Beryllium, Mercury. Fed. Register. 38(66): pp. 8820-8850, 1973.

25. Wagner, C. Disputes on the Safety of Asbestos. New Scientist, 61(888): 606, 1974.

26. Wagner, J.C. Current Opinions on the Asbestos Cancer Problem. Ann. Occup. Hyg., 15: 61-64, 1972.

27. Background Documentation on Evaluation of Occupational Exposure to Airborne Asbestos. Joint ACGIH-AIHA Aerosol Hazards Evaluation Committee. Amer. Ind. Hyg. Assoc., 36(2): 91-103, 1975.

28. Keenan, R.G. and J.R. Lynch. Techniques for the Detection, Identification and Analysis of Fibers. Amer. Ind. Hyg. Assoc. J., 31:587, 1970.

29. Mumpton, F.A. Characterization of Chrysotile Asbestos and Other Members of the Serpentine Group of Minerals. Siemens Review, XLI, 75, 1974.

30. Kramer, J.R., O. Mudroch and S. Tihor. Asbestos in the Environment. McMaster University, Report submitted to Research Advisory Board, International Joint Commission and Environment Canada, 1974.

31. Richards, A.L. Estimation of Trace Amounts of Chrysotile Asbestos by X-ray Diffraction. Anal. Chem. 44: 1872, 1972.

32. Birks, L.S. Quantitative Analysis of Airborne Asbestos by X-ray Diffraction. Naval Res. Labs., Final Report, EPA-650/2-75-004, 1975.

33. Crable, J.V., and M.J. Knott. Application of X-ray Diffraction to the Determination of Chrysotile in Bulk and Settled Dust Samples. Amer. Ind. Hyg. J., 27: 382-385, 1966

34. Crable, J.V., and M.J. Knott. Quantitative X-ray Diffraction Analysis of Crocidolite and Amosite in Bulk or Settled Dust Samples. Amer. Ind. Hyg. J., 27:449-453, 1966.

35. Cook, P.M., J.B. Rubin, C.J. Maggiore, and W.J. Nicholson. X-ray Diffraction and Electron Beam Analysis of Asbestiform Minerals in Lake Superior Waters. Proc. Intern. Conf. on Environmental Sensing and Assessment, Pub. by IEEE, Piscataway, NJ, #$(2): 1-9, 1976.

36. Schelz, J.P. The Detection of Chrysotile Asbestos in Low Levels of Talc by Differential Thermal Analysis. Termochem. Acta., 8: 197-203, 1974.

37. Taylor, D.G., C.M. Nenadic, and J.V. Crable. Infrared Spectra for Mineral Identification. Amer. Ind. Hyg. Assoc. J., 31: 100, 1970.

38. Bagioni, R.P. Separation of Chrysotile Asbestos from Minerals that Interfere with Its Infrared Analysis. Environ. Sci. and Tech., 9: 262, 1965.

39. Gadsden, J.A., J. Parker, and W.L. Smith. Determination of Chrysotile in Airbone Asbestos by an Infrared Spectrometric Technique. Atmos. Env., 4: 667, 1970.

40. Heffelfinger, R.E., C.W. Melton, D.L. Kiefer, and W.M. Henry. Development of a Rapid Survey Method of Sampling and Analysis for Asbestos in Ambient Air. Battelle Columbus Labs, Ohio, Final Report APTD-0965, EPA Contract No. CPA-22-69-110, 46 p., 1972.

41. Richards, A.L. Estimation of Submicrogram Quantities of Chrysotile Asbestos by Electron Microscopy. Anal. Chem., 45: 809, 1973.

42. Beckett, S.T. The Evaluation of Airborne Asbestos Fibers Using a Scanning Electron Microscope. Ann. Occ. Hyg., 16: 405, 1973.

43. Pattnaik, A., and J.D. Meakin. Development of Scanning Electron Microscopy for Measurement of Airborne Asbestos Concentrations. Final Report, Franklin Inst. Res. Lab., Philadelphia, PA, EOA 650/2-75-209, 84 p., National Tech. Inf. Service, Springfield, VA, 1975.

44. Ruud, C.O., C.S. Barrett, P.A. Russell, and R.L. Clark. Selected Area Electron Diffraction and Energy Dispersive X-ray Analysis for the Identification of Asbestos Fibers, A Comparison. Micron, 7: 115-132, 1976.

45. Mueller, P.K., A.E. Alcoer, R.Y. Stanley, and G.R. Smith. Asbestos Fiber Atlas. U.S. EPA Publication No. EPA-650/2-75-036, National Tech. Inf. Service, Springfield, VA, 1975.

46. Gerber, R.M., and R.C. Rossi. Evaluation of Electron Microscopy for Process Control in the Asbestos Industry. The Aerospace Corporation, Los Angeles, CA, Final Report, EPA-600/2-77-059, 55 p., National Tech. Inf. Service, Springfield, VA, 1975.

47. Millette, J.R., and E.F. McFarren. EDS of Waterborne Asbestos Fibers in TEM, SEM, and STEM. Proc. of IITRI Symposium on SET/1976/I, 451-460, 1976.

48. Beamon, D.R., and D.M. File. Quantitative Determination of Asbestos Fiber Concentrations. Anal. Chem., 48(1): 101-110, 1976.

49. Maggiore, C.J., and I.B. Rubin. Optimization of an SEM X-ray Spectrometer System for the Identification and Characterization of Ultramicroscopic Particles. Proc. of IITRI Symposium on SEM/1973, 129-136, 1973.

50. Cochran, W.G., and G.M. Cox. Experimental Designs. Wiley, 1950.

51. Youden, W.J. The Collaborative Test. Journal of the Association of Official Agricultural Chemists, 46(1): 55-62, 1963.

52. Cramer, H. Mathematical Methods of Statistics. Princeton University Press, 1946.

53. Fisher, R.A. Statistical Methods for Research Workers. Oliver and Boyd, 10th Ed., 1946.

54. Davies. O.L. (Ed.). The Design and Analysis of Industrial Experiments. Oliver and Boyd, 1954.

55. Fisher, R.A., and F. Yates. Statistical Tables. Oliver and Boyd, 1948.

56. Bartlett, M.S. The Use of Transformations. Biometrics, 3(1): 39-52, 1947.

57. Herdan, G. Small Particle Statistics. Butterworth & Co., 2nd Ed., 1960.

58. Daniel, C., F.S. Wood. Fitting Equations to Data. Wiley-Interscience, 1971.

59. Dixon, W.J. (Ed.). BMD Biomedical Computer Programs. University of California Press, 1977.

60. Draper, N.R., and Smith, H. Applied Regression Analysis. Wiley, 1966.

61. Tentative Method of Analysis for Suspended Particulate Matter in the Atmosphere (High-Volume Method) 11101-01-70T. Methods of Air Sampling and Analysis, Intersociety Committee, Amer. Public Health Assoc., 1015 18th St., N.W., Washington, DC, 1972.

62. Recommended Procedures for Sampling and Counting Asbestos Fibers; Joint AIHA-ACGIH Aerosol Hazards Evaluation Committee, Amer. Ind. Hygi. Assoc. J., 36(2): 83-90, 1975.

63. Jaffe, M.A. Handling and Washing Fragile Replicas. Proc. of EMSA, Toronto, September 1948. J. Appl. Phys., 19(12): 1189, 1948.

64. Samudra, A.V., and C.F. Harwood. Electron Microscope Measurement of Airborne Asbestos Concentrations - A Provisional Methodology Manual. U.S. Environmental Protection Agency, Publication No. EPA-600/2-77-178, 55 p., National Tech. Inf. Service, Springfield, VA, August 1977.

65. Wagman, J. Chemical Composition of Atmospheric Aerosol Pollutants by High Resolution X-ray Fluorescence Spectrometry. In Colloid and Interface Science, Vol. II. M. Kerker (Ed.), Academic Press, 1976.

APPENDIX A

THE EXPERIMENT DESIGN FOR PHASE 1

The design of the fractional factorial experiment for studying 12 variables is shown in compact form in Table A-1, where X_1 through X_{12} represent the 12 variables, or subprocedures, listed in Table A-2. The indices 1, 2, and 3 represent the variable levels as defined in Table A-2.

In order to evaluate the 12 independent variables, the variable levels were orthogonally coded as shown in Table A-2. Each three-level variable has one linear and one quadratic component, denoted by L and Q respectively, while each two-level factor has one quadratic component. The coding scheme shown in Table A-3 is chosen to satisfy three conditions:

1. The sum of linear components for each variable is zero (8 linear components).
2. The sum of quadratic components for each variable is zero (12 quadratic components).
3. The sum of the cross products of each pair of components is zero (190 pairs of components).

This is illustrated by considering the variable X1.

Level	Linear Comp. Code	Quadratic Comp. Code	Cross Product
1	-1	1	-1
2	1	1	1
3	0	-2	0
	Total 0	Total 0	Total 0

Thus, it satisfies all the three conditions specified above. This coding scheme ensures the orthogonality, i.e., independence and non-correlation of the variables considered, and helps to bring out even relatively small effects of the 12 controlled factors.

Table A-1

PHASE 1 EXPERIMENT DESIGN

Combination	Factor											
	X_1	X_2	X_3	X_4	X_5	X_6	X_7	X_8	X_9	X_{10}	X_{11}	X_{12}
1	1	1	2	2	1	1	3	2	1	2	2	1
2	1	1	2	2	2	1	1	2	2	1	1	3
3	1	1	2	2	3	2	2	1	3	3	3	2
4	1	2	1	1	1	1	1	2	3	2	3	2
5	1	2	1	1	2	1	2	1	1	1	2	1
6	1	2	1	1	3	2	3	2	2	3	1	3
7	1	3	2	2	1	1	2	1	2	2	1	3
8	1	3	2	2	2	1	3	2	3	1	3	2
9	1	3	2	2	3	2	1	2	1	3	2	1
10	2	1	1	2	1	1	3	2	2	3	2	2
11	2	1	1	2	2	2	1	1	3	2	1	1
12	2	1	1	2	3	1	2	2	1	1	3	3
13	2	2	2	2	1	1	1	1	1	3	3	3
14	2	2	2	2	2	2	2	2	2	2	2	2
15	2	2	2	2	3	1	3	2	3	1	1	1
16	2	3	2	1	1	1	2	2	3	3	1	1
17	2	3	2	1	2	2	3	2	1	2	3	3
18	2	3	2	1	3	1	1	1	2	1	2	2
19	3	1	2	1	1	2	3	1	3	1	2	3
20	3	1	2	1	2	1	1	2	1	3	1	2
21	3	1	2	1	3	1	2	2	2	2	3	1
22	3	2	2	2	1	2	1	2	2	1	3	1
23	3	2	2	2	2	1	2	2	3	3	2	3
24	3	2	2	2	3	1	3	1	1	2	1	2
25	3	2	1	2	1	2	2	2	1	1	1	2
26	3	3	1	2	2	1	3	1	2	3	3	1
27	3	3	1	2	3	1	1	2	3	2	2	3

Table A-2

INDEPENDENT VARIABLES, PHASE 1

Variable		Levels and Codes			
INDEPENDENT VARIABLES OF FILTER LOADING					
X_1	Composition of Sample in Aerosol Chamber	(1)	100% Chrysotile	$X_1L=-1$	$X_1Q=1$
		(2)	60% Chrysotile + 40% Amphibole	$X_1L=1$	$X_1Q=1$
		(3)	70% Chrysotile + 20% Amphibole + 10% Non-Asbestos Fiber	$X_1L=0$	$X_1Q=-2$
X_2	Concentration of Sample on Filter	(1)	Light	$X_2L=-1$	$X_2Q=1$
		(2)	Medium	$X_2L=0$	$X_2Q=-2$
		(3)	Heavy	$X_2L=1$	$X_2Q=1$
X_3	Sampling Instrument	(1)	High Volume	$X_3Q=-2$	
		(2)	Personal	$X_3Q=1$	
X_4	Filter Type	(1)	Nuclepore	$X_4Q=-2$	
		(2)	Millipore	$X_4Q=1$	
X_5	Pore Size, nominal	(1)	0.2 μm	$X_5L=-1$	$X_5Q=1$
		(2)	0.4 μm	$X_5L=0$	$X_5Q=-2$
		(3)	0.8 μm	$X_5L=1$	$X_5Q=1$
INDEPENDENT VARIABLES OF TEM GRID PREPARATION					
X_6	Filter Side	(1)	Particle side down	$X_6Q=1$	
		(2)	Particle side up	$X_6Q=-2$	
X_7	2.3 mm Portion Location	(1)	Periphery	$X_7L=-1$	$X_7Q=1$
		(2)	Mid-radius	$X_7L=0$	$X_7Q=-2$
		(3)	Center	$X_7L=1$	$X_7Q=1$
X_8	Use of Carbon Coating	(1)	Yes	$X_8Q=-2$	
		(2)	No	$X_8Q=1$	
X_9	Transfer Method	(1)	Soxhlet Extraction 1 (short)	$X_9L=-1$	$X_9Q=1$
		(2)	Soxhlet Extraction 2 (long)	$X_9L=1$	$X_9Q=1$
		(3)	Jaffe Method	$X_9L=0$	$X_9Q=-2$
INDEPENDENT VARIABLES OF TEM EXAMINATION					
X_{10}	Magnification, nominal*	(1)	5,000X (screen mag. 4,000X)	$X_{10}L=-1$	$X_{10}Q=1$
		(2)	10,000X (screen mag. 8,000X)	$X_{10}L=0$	$X_{10}Q=-2$
		(3)	20,000X (screen mag. 16,000X)	$X_{10}L=1$	$X_{10}Q=1$
X_{11}	Grid Opening Location	(1)	Periphery	$X_{11}L=-1$	$X_{11}Q=1$
		(2)	Mid-radius	$X_{11}L=0$	$X_{11}Q=-2$
		(3)	Center	$X_{11}L=1$	$X_{11}Q=1$
X_{12}	Choice of Fields	(1)	Random choice of small fields	$X_{12}L=-1$	$X_{12}Q=1$
		(2)	Small fields, consecutive	$X_{12}L=1$	$X_{12}Q=1$
		(3)	Entire grid opening as a field	$X_{12}L=0$	$X_{12}Q=-2$

---

*The actual magnification at the fluorescent screen is somewhat smaller than the nominal or camera magnification, depending upon the design geometry of each transmission electron microscope.

Table A-3

VALUES OF CODED INDEPENDENT VARIABLES, PHASE 1 COMBINATIONS

	X1		X2		X3	X4	X5		X6	X7		X8	X9		X10		X11		X12	
Comb.	L	Q	L	Q	Q	Q	L	Q	Q	L	Q	Q	L	Q	L	Q	L	Q	L	Q
1	-1	1	-1	1	1	1	-1	1	1	1	1	1	-1	1	0	-2	0	-2	-1	1
2	-1	1	-1	1	1	1	0	-2	1	-1	1	1	1	1	-1	1	-1	1	0	-2
3	-1	1	-1	1	1	1	1	1	-2	0	-2	-2	0	-2	1	1	1	1	1	1
4	-1	1	0	-2	-2	-2	-1	1	1	-1	1	1	0	-2	0	-2	1	1	1	1
5	-1	1	0	-2	-2	-2	0	-2	1	0	-2	-2	-1	1	-1	1	0	-2	-1	1
6	-1	1	0	-2	-2	-2	1	1	-2	1	1	1	1	1	1	1	-1	1	0	-2
7	-1	1	1	1	1	1	-1	1	1	0	-2	-2	1	1	0	-2	-1	1	0	-2
8	-1	1	1	1	1	1	0	-2	1	1	1	1	0	-2	-1	1	1	1	1	1
9	-1	1	1	1	1	1	1	1	-2	-1	1	1	-1	1	1	1	0	-2	-1	1
10	1	1	-1	1	-2	1	-1	1	1	1	1	1	1	1	1	1	0	-2	1	1
11	1	1	-1	1	-2	1	0	-2	-2	-1	1	-2	0	-2	0	-2	-1	1	-1	1
12	1	1	-1	1	-2	1	1	1	1	0	-2	1	-1	1	-1	1	1	1	0	-2
13	1	1	0	-2	1	1	-1	1	1	-1	1	-2	-1	1	1	1	1	1	0	-2
14	1	1	0	-2	1	1	0	-2	-2	0	-2	1	1	1	0	-2	0	-2	1	1
15	1	1	0	-2	1	1	1	1	1	1	1	1	0	-2	-1	1	-1	1	-1	1
16	1	1	1	1	1	-2	-1	1	1	0	-2	1	0	-2	1	1	-1	1	-1	1
17	1	1	1	1	1	-2	0	-2	-2	1	1	1	-1	1	0	-2	1	1	0	-2
18	1	1	1	1	1	-2	1	1	1	-1	1	-2	1	1	-1	1	0	-2	1	1
19	0	-2	-1	1	1	-2	-1	1	-2	1	1	-2	0	-2	-1	1	0	-2	0	-2
20	0	-2	-1	1	1	-2	0	-2	1	-1	1	1	-1	1	1	1	-1	1	1	1
21	0	-2	-1	1	1	-2	1	1	1	0	-2	1	1	1	0	-2	1	1	-1	1
22	0	-2	0	-2	1	1	-1	1	-2	-1	1	1	1	1	-1	1	1	1	-1	1
23	0	-2	0	-2	1	1	0	-2	1	0	-2	1	0	-2	1	1	0	-2	0	-2
24	0	-2	0	-2	1	1	1	1	1	1	1	-2	-1	1	0	-2	-1	1	1	1
25	0	-2	1	1	-2	1	-1	1	-2	0	-2	1	-1	1	-1	1	-1	1	1	1
26	0	-2	1	1	-2	1	0	-2	1	1	1	-2	1	1	1	1	1	1	-1	1
27	0	-2	1	1	-2	1	1	1	1	-1	1	1	0	-2	0	-2	0	-2	0	-2

Table A-4

STATISTICS OF FIBER CHARACTERISTICS BY SAMPLE
SAMPLE 1

	Total	Mean	S.D.	S.E.	Var.	Min.	Max.
Volume $(\mu m)^3$ (over all fibers)	0.382780	0.0026582	0.0047790	0.0003982	0.0000228	0.0000614	0.0359526
LN Width (μm) (over all fibers)	-433.108917	-3.0077009	0.5166071	0.0430506	0.2668829	-3.6888795	-1.6739764
LN Length (μm) (contained fibers)	-95.527122	-0.7405204	0.6529610	0.0574900	0.4263580	-2.0794415	0.8109303
LN Ashed Ratio (contained fibers)	291.630096	2.2606983	0.6369779	0.0560828	0.4057407	1.3862944	4.0943446
LN Volume $(\mu m)^3$ (contained fibers)	-901.003296	-6.9845219	1.4403129	0.1268125	2.0745010	-9.6987667	-3.3255527

The total number of fibers observed = 144

The number of fibers contained within their field = 129

APPENDIX B

REGRESSION ANALYSIS

The experimental data resulting from execution of the design presented can be best analyzed by multiple regression methods, i.e., find values of the regression coefficients of a model equation that provide the best fit, taking account of the magnitude of the experimental error. A stepwise fitting procedure will be applied making use of the computer program BMD02R from the BMD library of statistical programs [59].

The stepwise method of fitting is preferred because it selects only those candidate terms for inclusion in the regression equation that contribute significantly to the prediction of values of the dependent variable. The regression coefficients enter into the equation as multipliers to compute the values of the dependent variable on the basis of values of the significant independent variables and covariates.

In the stepwise multiple regression analysis, intermediate response equations are obtained through the insertion, at each step, of the candidate term that makes the greatest contribution to the reduction in the residual sum of squared deviations or, alternatively, the deletion of a variable whose contribution falls below a specific threshold significance level. This contribution is measured by the F-value (square of the t value, which is the regression coefficient divided by its standard error). At each step of computation, the regression coefficient and the F-value associated with each variable in the equation are given, together with the potential F-value for each variable not in the equation. The threshold F-values for inclusion and deletion of terms, set by the analyst, at the 20% level determine at what point the fitting process terminates. The candidate variables need not be all the independent variables and covariates together. These variables can be separated into blocks to investigate the relationships among the independent variables and covariates separately as well as in combination.

In the stepwise fitting procedure it is often found that some (perhaps many) of the candidate regression coefficients have estimated values that are not significantly above the "noise level;" hence, those terms should be excluded from the regression equation for the sake of simplicity and predictive accuracy. The sum of squares and degrees of freedom associated with these excluded terms can, in many instances, be pooled to refine the variance estimate.

The final values of the regression coefficients are computed together with their standard errors and levels of statistical significance (F or t values). For each observation, the value of e (difference between observed and predicted value of the dependent variable) is computed as a check on possible out-liers in the data.

In the regression equations for each dependent variable, only those terms were retained having coefficients significant at the 20% probability level. That is, a term was dropped if it was determined that its coefficient value could occur by chance 20% or more of the time due merely to accidents of sampling.

Table B-1 gives the full information on regression equation 9 for dependent variable Y_9, the square root of the estimated fiber count per ml of air. The equation contains 14 terms, the other candidates having been dropped because of their statistical non-significance. The equation is of the form

$$\begin{aligned} Y_9 = {} & B_0(X_0) + B_1(X_1L) + B_2(X_1Q) + B_3(X_2L) + B_4(X_2Q) + B_5(X_3Q) \\ & + B_6(X_6Q) + B_7(X_8Q) + B_8(X_9L) + B_9(X_9Q) + B_{10}(X_{10}L) \\ & + B_{11}(X_{10}Q) + B_{12}(X_{11}Q) + B_{13}(X_{12}Q) \qquad [1] \end{aligned}$$

Since 27 tests were run, there remain 13 degrees of freedom (i.e., 27-14) for estimating the magnitude of the residual variation. The residual standard deviation was calculated to be 1.9012. The degree of determination, R^2, was found to be 96%, i.e., 96% of the variation in the values of Y_9 is accounted for by the independent variables in the equation. For each term in the equation, the values found for the regression coefficients, B_0 through B_{13}, are listed along with their standard errors and variance ratios (which indicate their relative significance). The least-squares fit for equation Y_9 was found to be

$$\begin{aligned} Y_9 = {} & 12.300 + 0.781(X_1L) + 0.489(X_1Q) - 1.714(X_2L) + 0.426(X_2Q) \\ & + 0.811(X_3Q) + 1.001(X_6Q) - 1.601(X_8Q) - 1.590(X_9L) \\ & - 1.796(X_9Q) + 4.265(X_{10}L) + 0.821(X_{10}Q) \\ & + 0.936(X_{11}Q) + 1.358(X_{12}Q) \qquad [2] \end{aligned}$$

Table B-1

PERFORMANCE EQUATION NO. 9

Dependent Variable: Y_9 = Square root (estimated no. of fibers per cm^3 of air)

Number of Tests: 27

Number of Terms in Equation: 14

Residual Degrees of Freedom: 13

Residual Standard Deviation: 1.9012

Degree of Determination, R^2: 96%

Independent Variable	Regression Coefficient b	Standard Error s_b	Variance Ratio F
Constant term			
$X_0 = 1$	12.300		
Composition of sample			
X_1L (Coded -1, 1, 0)	0.781	0.448	3.04
X_1Q (Coded 1, 1, -2)	0.489	0.259	3.57
Concentration on filter			
X_2L (Coded -1, 0, 1)	-1.714	0.448	14.64
X_2Q (Coded 1, -2, 1)	0.426	0.259	2.71
Sampler type			
X_3Q (Coded -2, 1)	0.811	0.259	9.82
Filter side			
X_6Q (Coded 1, -2)	1.001	0.259	14.96
Carbon coating			
X_8Q (Coded -2, 1)	-1.601	0.259	38.30
Transfer method			
X_9L (Coded -1, 1, 0)	-1.590	0.448	12.59
X_9Q (Coded 1, 1, -2)	-1.769	0.259	46.77
Magnification			
$X_{10}L$ (Coded -1, 0, 1)	4.265	0.448	90.61
$X_{10}Q$ (Coded 1, -2, 1)	0.821	0.259	10.07
Grid opening location			
$X_{11}Q$ (Coded 1, -2, 1)	0.936	0.259	13.07
Choice of fields			
$X_{12}Q$ (Coded 1, 1, -2)	1.358	0.259	27.55

Thus, given particular levels for each of the factors X_1 through X_{12}, a corresponding estimate for Y_9 may be found by using the appropriate coded values for X_1L through $X_{12}Q$ defined in Table A-2. For example, for combination 1, the estimated value for Y_9 is found in the following way. Table A-1 gives the levels of the factors X_1 through X_{12} used in combination 1, and for each of these, Table A-2 shows the appropriate coded values of the variable X_1L through $X_{12}Q$. Thus, for combination 1, the coded values of the terms involved in the equation for Y_9 are given by:

Variable	Coded Value	Variable	Coded Value	Variable	Coded Value	Variable	Coded Value
X_1L	-1	X_3Q	1	X_9L	-1	$X_{10}Q$	-2
X_1Q	1	X_6Q	1	X_9Q	1	$X_{11}Q$	-2
X_2L	-1	X_8Q	1	$X_{10}L$	0	$X_{12}Q$	1
X_2Q	1						

so that the estimated value for Y_9 is found to be

$$\begin{aligned} Y_9 \text{ (combination 1)} &= 12.30 + 0.781(-1) + 0.489(1) \\ &-1.714(-1) + 0.426(1) + 0.811(1) + 1.001(1) \\ &- 1.601(1) - 1.590(-1) - 1.769(1) + 4.265(0) \\ &+ 0.821(-2) + 0.936(-2) + 1.358(1) = 12.024 \end{aligned}$$

Equation 2 can be rewritten, grouping together the terms associated with the separate factors

$$\begin{aligned} Y_9 = 12.30 &+ [0.781(X_1L) + 0.489(X_1Q] \\ &+ [-1.714(X_2L) + 0.426(X_2Q)] \\ &+ [0.811(X_3Q)] + [1.001(X_6Q)] \\ &+ [-1.601(X_8Q)] + [-1.590(X_9L) - 1.769(X_9Q)] \\ &+ [4.265(X_{10}L) + 0.821(X_{10}Q)] \\ &+ [0.936(X_{11}Q)] + [1.358(X_{12}Q)] \end{aligned} \quad [3]$$

In this form Y_9, is seen to equal its mean value (12.300) plus or minus the net effect contributed by each factor taken at its specified level. These net effects are listed in Table A-2 for each level of each factor. For example, at level 2 of factor X_1, that is, for a sample composition of 60% chrysotile and 40% amphibole, since the coded values corresponding to this level are given by $X_1L = +1$, $X_1Q = +1$, the corresponding net contribution factor X_1 at this level is found to be

$$[0.781(+1) + 0.489(+1)] = 1.270$$

The standard error of the net effect is found from the standard error of each term by the formula

$$SE = \sqrt{(S_L X_L)^2 + (S_Q X_Q)^2}$$

where X_L, X_Q are the coded values for the appropriate level of the linear and quadratic components, respectively, and S_L and S_Q the standard errors of the linear and quadratic components, respectively. For example, for level 2 of factor X_1

$$SE = \sqrt{(1 \times 0.488)^2 + (1 \times 0.259)^2} = 0.518$$

In the case that the linear component of some factor is missing, the corresponding term is dropped from the formula and $SE = \sqrt{(S_Q X_Q)^2}$; similarly, if the quadractic component is missing, $SE = S_L$.

The 80% confidence limits for each relative effect were found using student's t with 13 degrees of freedom, t = 1.350. Thus, for example, for level 2 of X1, the lower limit of the 80% confidence interval is found to be

$$1.270 - (1.350 \times 0.518) = 0.572$$

and the upper limit

$$1.270 + (1.350 \times 0.518) = 1.968$$

That is, with at least 80% certainty, the net effect of choosing level 2 of X1 would be to raise the estimated mean value of Y_9 by an amount lying in the 80% confidence interval between 0.572 and 1.968. The confidence limits for the various net effects are given in Table B-2 and are presented graphically in Figures 3 and 4 of the main report.

A similar analysis is presented for Y_{10} (the natural log of the estimated concentration of the fibers in the atmosphere) in Tables B-3 and B-4 and Figures 5 and 6 of the main report. From Table B-3 it is seen that the number of terms in the regression equation for Y_{10} was 11, leaving 16 degrees of freedom; the residual standard deviation was 0.6683, and the degree of determination $R^2 = 81\%$.

Table B-2

EFFECTS OF EM PROCEDURAL FACTORS ON SQUARE ROOT OF ESTIMATED NUMBER OF FIBERS PER CUBIC CENTIMETER OF AIR, FROM EQUATION 9

Factor	Level	Relative Effect	Standard Error	80% Confidence Limits	
				Lower	Upper
X_1 Composition of Sample	100% Chrysotile	-0.292	0.518	-0.990	0.406
	60% C + 40% Amphibole	1.270	0.518	0.572	1.968
	70% C + 20% Amphibole + 10% Fiberglass	-0.978	0.518	-1.677	-0.279
X_2 Concentration on Filter	Light	2.140	0.518	1.442	2.838
	Medium	-0.852	0.518	-1.551	-0.153
	Heavy	-1.288	0.518	-1.987	-0.589
X_3 Sampler Type	High volume	-1.622	0.518	-2.321	-0.923
	Personal	0.811	0.259	0.461	1.161
X_6 Filter Side	Particle side down	1.001	0.259	0.651	1.351
	Particle side up	-2.002	0.518	-2.701	-1.303
X_8 Carbon Coating	Yes	3.202	0.518	2.503	3.901
	No	-1.601	0.259	-1.951	-1.251
X_9 Transfer Method	Soxhlet 1	-0.179	0.518	-0.877	0.519
	Soxhlet 2	-3.359	0.518	-4.057	-2.661
	Jaffe	3.538	0.518	2.839	4.237
X_{10} Magnification	5,000X	-3.444	0.518	-4.142	-2.746
	10,000X	-1.642	0.518	-2.341	-0.943
	20,000X	5.086	0.518	4.388	5.784
X_{11} Grid Opening Location	Periphery	0.936	0.259	0.586	1.286
	Mid-radius	-1.872	0.518	-2.571	-1.173
	Center	0.936	0.259	0.586	1.286
X_{12} Choice of Fields	Random, small	1.358	0.259	1.008	1.708
	Consecutive, small	1.358	0.259	1.008	1.708
	Entire grid opening	-2.716	0.518	-3.415	-2.017

Table B-3

PERFORMANCE EQUATION NO. 10

Dependent Variable: Y_{10} = Log_e (estimated mass concentration of fiber micrograms per cubic meter)

Number of Tests: 27

Number of Terms in Equation: 11

Residual Degrees of Freedom: 16

Residual Standard Deviation: 0.6683

Degree of Determination, R^2: 81%

Independent Variable	Regression Coefficient b	Standard Error s_b	Variance Ratio F
Constant term			
$X_0 = 1$	0.286		
Composition of sample			
X_1L (Coded -1, 1, 0)	0.331	0.158	4.41
Concentration on filter			
X_2L (Coded -1, 0, 1)	-0.466	0.158	8.73
Filter type			
X_4Q (Coded -2, 1)	0.184	0.091	4.11
Pore size			
X_5Q (Coded 1, -2, 1)	-0.121	0.091	1.77
3 mm Portion Location			
X_7L (Coded -1, 0, 1)	-0.215	0.158	1.87
Carbon coating			
X_8Q (Coded -2, 1)	-0.351	0.091	14.93
Transfer method			
X_9Q (Coded 1, 1, -2)	-0.450	0.091	24.51
Magnification			
$X_{10}L$ (Coded -1, 0, 1)	0.283	0.158	3.23
$X_{10}Q$ (Coded 1, -2, 1)	-0.159	0.091	3.04
Choice of fields			
$X_{12}Q$ (Coded 1, 1, -2)	0.134	0.091	2.18

The various coefficients of the equation are listed along with their standard errors and variance ratios.

Table B-4 then presents the net effects of the different levels of the various factors on Y_{10} together with their standard errors and 80% confidence limits. The confidence intervals are presented graphically in Figures 5 and 6 of the main report.

Table B-4

EFFECTS OF EM PROCEDURAL FACTORS ON NATURAL LOGARITHM OF ESTIMATED MASS CONCENTRATION OF FIBERS (MICROGRAMS PER CUBIC METER), FROM EQUATION 10

Factor		Level	Relative Effect	Standard Error	80% Confidence Limits	
					Lower	Upper
X_1	Composition of Sample	100% Chrysotile	-0.331	0.158	-0.542	-0.120
		60% C + 40% Amphibole	+0.331	0.158	0.120	0.542
		70% C + 20% Amphibole + 10% Fiberglass	0	0.158	-0.211	0.211
X_2	Concentration on Filter	Light	+0.466	0.158	0.255	0.677
		Medium	0	0.158	-0.211	0.211
		Heavy	-0.466	0.158	-0.677	-0.255
X_4	Filter Type	Nuclepore	-0.368	0.182	-0.611	-0.125
		Millipore	+0.184	0.091	0.062	0.306
X_5	Pore Size	0.22 μm	-0.121	0.091	-0.243	0.001
		0.45 μm	+0.242	0.182	-0.001	0.485
		0.80 μm	-0.121	0.091	-0.243	0.001
X_7	3 mm Position Location	Periphery	+0.215	0.158	0.004	0.426
		Mid-radius	0	0.158	-0.211	0.211
		Center	-0.215	0.158	-0.426	-0.004
X_8	Carbon Coating	Yes	+0.702	0.182	0.459	0.945
		No	-0.351	0.091	-0.473	-0.229
X_9	Transfer Method	Soxhlet 1	-0.450	0.091	-0.572	-0.328
		Soxhlet 2	-0.450	0.091	-0.572	-0.328
		Jaffe	+0.900	0.182	0.657	1.143
X_{10}	Magnification	5,000X	-0.442	0.182	-0.685	-0.199
		10,000X	+0.318	0.182	0.075	0.561
		20,000X	+0.124	0.182	-0.119	0.367
X_{12}	Choice of Fields	Random, small	+0.134	0.091	0.012	0.256
		Consecutive, small	+0.134	0.091	0.012	0.256
		Entire grid opening	-0.268	0.182	-0.511	-0.025

APPENDIX C

POISSON DISTRIBUTION TESTS

LISTING OF COMPUTER PROGRAM POISSON-1 FOR CHECKING CONFORMITY WITH THE POISSON DISTRIBUTION

```
C PROGRAM POISSON1 TO COMPARE OBSERVED AND CALCULATED EVENT DISTRIBUTIONS
C AND DETERMINE THE GOODNESS OF FIT OF THE POISSON MODEL TO THE DATA.
C WRITTEN BY F C BOCK, IIT RESEARCH INSTITUTE.
      REAL M,ML
      DIMENSION VO(99),FO(99),F1(99),F2(99),TEMP(12)
C--NO IS THE NUMBER OF PAIRS OF VALUES OF VO AND FO TO BE READ IN
C--N1 IS THE NUMBER OF CELL FREQUENCIES TO BE CALCULATED, FOR 0 TO N1-1 EVENTS
C--VO(I) IS A SPECIFIED NUMBER OF EVENTS PER CELL, I=1,...,NO
C--FO(I) IS THE OBSERVED NUMBER OF CELLS WITH VO(I) EVENTS PER CELL
C--F1 IS THE COMPLETE ARRAY OF OBSERVED CELL FREQUENCIES INCLUDING ZEROS
C--F2 IS THE COMPLETE ARRAY OF CALCULATED CELL FREQUENCIES
109   READ(5,111) NO,N1,TEMP
111   FORMAT(2I4,12A6)
      WRITE(6,113) TEMP
113   FORMAT(1H1,12A6//)
      IF(NO.EQ.9999) STOP
      READ(5,115) (VO(I),FO(I),I=1,NO)
115   FORMAT(8(F4.0,F6.0))
      F=0.
      TOT=0.
      TOT2=0.
      DO 117 J=1,N1
      F1(J)=0.
117   F2(J)=0.
      DO 119 I=1,NO
      J=IFIX(VO(I))+1
      F1(J)=FO(I)
      F=F+FO(I)
      TOT=TOT+VO(I)*FO(I)
119   TOT2=TOT2+VO(I)*VO(I)*FO(I)
      IF(F.LT.2.) GOTO 109
      M=TOT/F
      DF=F-1
      SS=TOT2-TOT*TOT/F
      VAR=SS/DF
      SD=0.
      IF(VAR.GT.0.) SD=SQRT(VAR)
      SEM=SD/SQRT(F)
      ML=ALOG(M)
      COEF=EXP(-M)*F
      COEFL=ALOG(COEF)
      POWERL=0.
      FACTL=0.
      FF=0.
      CTOT=0.
      WRITE(6,123)
123  0 FORMAT(1X,'NO. EVENTS  OBSERVED    CALCULATED  DIFFERENCE'/
     1        1X,' PER CELL   NO. CELLS   NO. CELLS      O-C     (O-C)**
     22/C'/)
      DO 128 J=1,N1
      J1=J-1
      F2(J)=EXP(COEFL+PO*ERL-FACTL)
      FF=FF+F2(J)
      CTOT=CTOT+J1*F2(J)
      D=F1(J)-F2(J)
      CHI2=99999999.
      IF(F2(J).LE.0.) GOTO 125
      CHI2=D**2/F2(J)
125   WRITE(6,127) J1,F1(J),F2(J),D,CHI2
127   FORMAT(1X,I6,F12.0,F15.4,2F12.4)
      PO*ERL=PO*ERL+ML
128   FACTL=FACTL+ALOG(FLOAT(J))
129   WRITE(6,131) F,FF,TOT,CTOT,M,SS,DF,VAR,SD,SEM
131   FORMAT(/1X,'TOTAL OBSERVED CELLS =          ',F10.4,
     $         /1X,'TOTAL CALCULATED CELLS =        ',F10.4,
     $         /1X,'TOTAL OBSERVED EVENTS =         ',F10.4,
     $         /1X,'TOTAL CALCULATED EVENTS =       ',F10.4,
     $ //1X, 'STATISTICS APPLYING TO NO. EVENTS PER CELL',/
     $         /1X,'MEAN EVENTS PER CELL =          ',F10.4,
     $         /1X,'SUM OF SQUARED DEVIATIONS =     ',F10.4
     $         /1X,'DEGREES OF FREEDOM =            ',F10.4
     $         /1X,'VARIANCE =                      ',F10.4
     $         /1X,'STANDARD DEVIATION =            ',F10.4
     $         /1X,'STANDARD ERROR OF MEAN =        ',F10.4)
      WRITE(6,133)
133  0 FORMAT('1OVERALL CHI-SQUARE TEST FOR GOODNESS OF FIT, WITH CATEGO
     1RIES (NO. EVENTS PER CELL) COMBINED'/' SO THAT NO COMPUTED CELL FR
     2EQUENCY IS LESS THAN 3.0'//'  RANGE OF'/
     3         1X,'NO. EVENTS  OBSERVED    CALCULATED  DIFFERENCE'/
     4         1X,' PER CELL   NO. CELLS   NO. CELLS      O-C      (O-C)**
     52/C'/)
      K=0
      MARK=0
      J1=0
      J11=0
      J22=0
      RF1=0.
      RF2=0.
      RF11=0.
      RF22=0.
      TCHI2=0.
      DO 139 J=1,N1
      J2=J-1
      RF1=RF1+F1(J)
      RF2=RF2+F2(J)
      IF(J.LT.N1) GOTO 135
      IF(RF2.GE.3.0) GOTO 137
      J22=J2
      RF11=RF11+RF1
      RF22=RF22+RF2
      MARK=1
      GOTO 1375
135   IF(RF2.LT.3.0) GOTO 139
137   K=K+1
      IF(K.EQ.1) GOTO 1385
1375  D=RF11-RF22
      CHI2=D**2/RF22
```

```
        TCHI2=TCHI2+CHI2
        WRITE(6,138) J11,J22,RF11,RF22,D,CHI2
138     FORMAT(1X,I4,'-',I3,F10.0,F15.4,2F12.4)
1385    J11=J1
        J22=J2
        RF11=RF1
        RF22=RF2
        J1=J
        RF1=0.
        RF2=0.
        IF(J.LT.N1.OR.MARK,EQ,1) GOTO 139
        MARK=1
        GOTO 1375
139     CONTINUE
        NDF=K-2
        WRITE(6,141) K,NDF,TCHI2
141   0 FORMAT(/'0NO. CLASSES AFTER GROUPING ='I4/
      1          ' DEGREES OF FREEDOM =         'I4/
      2          ' TOTAL CHI-SQUARE =          'F10.4)
        GOTO 109
        END
@XQT
   7  20  TEST 1, RTP
   0     11   1     15   2     16   3      9   4      4   5      2   6      1
   8  20  TEST 2, ATHENS
   1      3   2      5   3      8   4      3   5      4   6      1   7      1   8      3
   6  20  TEST 3, NIOSH
   1      6   2     10   3     14   4      5   5      4   6      1
9999      THIS GROUP IS DONE, PROJECT C6351
```

The computer printouts from program POISSON-1 for two typical cases are given in Tables C-1 and C-2. In the top segment of each printout, the possible numbers of fibers per field (labeled "events per cell") are listed at the left: 0, 1, 2, 3, etc. The succeeding columns are: the observed numbers of fields having the specified numbers of fibers in them, the corresponding calculated numbers of fields based on an assumed Poisson distribution, and the differences between the observed and calculated numbers of fields.

The next segment of the computer output provides the following overall items of information on the sample. (1) The total number of fields observed (F). (2) Th total calculated number of fields assuming that the Poisson distribution applies; this is made equal to the observed number. (3) The total number of fibers observed including those crossing the field perimeter as well as those lying entirely within their field. (4) The total calculated number of fibers; this is made equal to the observed number. (5) The mean number of fibers per field; this is the sample value of the Poisson parameter λ. (6) The sum of squared deviations around the mean. (7) The degrees of freedom, one less than the number of fields. (8) The variance. (9) The standard deviation, i.e., the square root of the variance. (10) The standard error of the mean. Items (6) through (10) are the usual sample statistics, computed by treating each field as a unit of observation without reference to the Poisson distribution.

The final segment of each printout gives the results of the goodness-of-fit test for the Poisson distribution. The classes defined by the number of fibers per field are grouped to the extent necessary for each of the calculated numbers of fields to be no smaller than 3.0 so that the Chi-square values are not unduly inflated. For example, in sample 1 the classes after grouping are: 0 fibers per field, 1 fiber per field, 2 fibers per field, and 3 or more fibers per field. The smallest calculated number of fields is 7.32 for the last grouped class, and the corresponding observed number is 17.

The succeeding columns are the observed numbers of fibers in the classes after grouping the calculated numbers, the differences between the observed and calculated numbers, i.e. O-C, and the contributions to Chi-square, i.e. $(O-C)^2/C$.

The final items of information are the number of classes after grouping, the degrees of freedom associated with the total Chi-square value, and the total Chi-square value itself. The number of degrees of freedom is two less than the number

Table C-1

PRINTOUT OF RESULTS FROM POISSON-1 PROGRAM

```
SAMPLE 1 (Case of poor agreement with Poisson model)

 NO. EVENTS  OBSERVED     CALCULATED  DIFFERENCE
  PER CELL   NO. CELLS    NO. CELLS      O-C

      0         120.        97.3504     22.6496
      1          41.        70.0923    -29.0923
      2          22.        25.2332     -3.2332
      3          12.         6.0560      5.9440
      4           4.         1.0901      2.9099
      5           0.          .1570      -.1570
      6           0.          .0188      -.0188
      7           1.          .0019       .9981
      8           0.          .0002      -.0002
      9           0.          .0000      -.0000



 (1) TOTAL OBSERVED CELLS =          200.0000
 (2) TOTAL CALCULATED CELLS =        200.0000
 (3) TOTAL OBSERVED EVENTS =         144.0000
 (4) TOTAL CALCULATED EVENTS =       144.0000

     STATISTICS APPLYING TO NO. EVENTS PER CELL

 (5) MEAN EVENTS PER CELL =             .7200
 (6) SUM OF SQUARED DEVIATIONS =     246.3200
 (7) DEGREES OF FREEDOM =            199.0000
 (8) VARIANCE =                        1.2378
 (9) STANDARD DEVIATION =              1.1126
(10) STANDARD ERROR OF MEAN =           .0787



  ANGE OF
 NO. EVENTS  OBSERVED    CALCULATED  DIFFERENCE
  PER CELL   NO. CELLS   NO. CELLS      O-C       (O-C)**2/C

   0-  0        120.       97.3504     22.6496       5.2696
   1-  1         41.       70.0923    -29.0923      12.0750
   2-  2         22.       25.2332     -3.2332        .4143
   3-            17.        7.3240      9.6760      12.7834

 NO. CLASSES AFTER GROUPING =     4
 DEGREES OF FREEDOM =             2
 TOTAL CHI-SQUARE =            30.5423
```

Table C-2

PRINTOUT OF RESULTS FROM POISSON-1 PROGRAM

SAMPLE 26 (case of good agreement with Poisson Model)

```
NO. EVENTS  OBSERVED    CALCULATED  DIFFERENCE
 PER CELL   NO. CELLS   NO. CELLS      O-C

     0         38.       32.3740      5.6260
     1         42.       47.4048     -5.4048
     2         32.       34.7071     -2.7071
     3         16.       16.9404      -.9404
     4         11.        6.2014      4.7986
     5          0.        1.8161     -1.8161
     6          0.         .4432      -.4432
     7          1.         .0927       .9073
     8          0.         .0170      -.0170
     9          0.         .0028      -.0028
    10          0.         .0004      -.0004
    11          0.         .0001      -.0001
    12          0.         .0000      -.0000


 (1)TOTAL OBSERVED CELLS =          140.0000
 (2)TOTAL CALCULATED CELLS =        140.0000
 (3)TOTAL OBSERVED EVENTS =         205.0000
 (4)TOTAL CALCULATED EVENTS =       205.0000

    STATISTICS APPLYING TO NO. EVENTS PER CELL

 (5)MEAN EVENTS PER CELL =            1.4643
 (6)SUM OF SQUARED DEVIATIONS =     238.8214
 (7)DEGREES OF FREEDOM =            139.0000
 (8)VARIANCE =                        1.7181
 (9)STANDARD DEVIATION =              1.3108
(10)STANDARD ERROR OF MEAN =           .1108


  RANGE OF
 NO. EVENTS  OBSERVED   CALCULATED  DIFFERENCE
  PER CELL   NO. CELLS  NO. CELLS      O-C      (O-C)**2/C

   0-  0        38.      32.3740      5.6260         .9777
   1-  1        42.      47.4048     -5.4048         .6162
   2-  2        32.      34.7071     -2.7071         .2112
   3-  3        16.      16.9404      -.9404         .0522
   4-           12.       8.5736      3.4264        1.3693

 NO. CLASSES AFTER GROUPING =   5
 DEGREES OF FREEDOM =           3
 TOTAL CHI-SQUARE =             3.2266
```

of classes because two constraints based on the data were imposed in computing the Poisson sequence, i.e., equality of the observed and computed number of fields and equality of the observed and computed number of fibers. Or, in other words, the two parameters F and λ were evaluated from the sample data.

Sample 1 is an illustrative case in which there is poor agreement between the actual data and the Poisson model ($P < .001$). On the other hand, sample 26 is a case in which there is good agreement ($.5 > P > .3$). Inspection of the observed and calculated numbers of fibers per cell for sample 1 after pooling (bottom segment of the computer printout) reveals the pattern of departures from the Poisson frequencies: there is an excess of observed fields with no fibers, and also an excess of observed fields with three or more fibers, as compared with the calculated frequencies; these excesses are of course balanced by deficiencies in the observed fields with one or two fibers in them. This is the general pattern to be expected if there is a tendency for fibers to aggregate beyond that would occur simply by chance settling. In all cases in which there was a poor fit of the Poisson distribution the same type of pattern occurred in the departures of the observed frequencies from the calculated.

LISTING OF COMPUTER PROGRAM POISSON-2 FOR OBTAINING PERCENT CONFIDENCE LIMITS ON THE MEAN OF A POISSON VARIABLE

```
C PROGRAM POISSON2 TO COMPUTE CONFIDENCE LIMITS FOR THE EXPECTED VALUE
C OF A POISSON RANDOM VARIABLE IN A SPACE OF THE SIZE EXAMINED (THE
C SAMPLE SPACE) AND IN THE REFERENCE SPACE, WHICH MAY DIFFER IN SIZE
C FROM THE SAMPLE SPACE.
C WRITTEN BY F C BOCK, IIT RESEARCH INSTITUTE.
C PCCONF IS THE CONFIDENCE LEVEL, I. E., THE PERCENT PROBABILITY THAT THE
C EXPECTED VALUE OF THE POISSON VARIABLE LIES WITHIN THE COMPUTED
C CONFIDENCE INTERVAL
C SIZE1 IS THE NUMBER OF SPATIAL UNITS IN THE SAMPLE SPACE
C SIZE2 IS THE NUMBER OF SPATIAL UNITS IN THE REFERENCE SPACE
C C IS THE OBSERVED NUMBER OF OCCURRENCES (COUNT) IN THE SAMPLE SPACE
C RMEAN IS THE OBSERVED NUMBER OF OCCURRENCES TRANSLATED TO THE REFERENCE SPACE
C LCL1 IS THE LOWER CONFIDENCE LIMIT FOR THE EXPECTED VALUE OF C
C UCL1 IS THE UPPER CONFIDENCE LIMIT FOR THE EXPECTED VALUE OF C
C LCL2 IS THE LOWER CONFIDENCE LIMIT FOR THE EXPECTED VALUE OF RMEAN
C UCL2 IS THE UPPER CONFIDENCE LIMIT FOR THE EXPECTED VALUE OF RMEAN
      REAL LCL1,LCL2
      DIMENSION LABEL(6)
      WRITE(6,101)
101   FORMAT('1CONFIDENCE LIMITS FOR THE EXPECTED VALUE OF A POISSON VAR
     $IABLE IN A SPACE OF THE SIZE EXAMINED (THE SAMPLE SPACE)'/
     $ ' AND ALSO IN THE REFERENCE SPACE')
      WRITE(6,103)
103   FORMAT('0 CONFIDENCE',3X'SIZE OF',3X'OBSERVED',4X'LIMITS ON THE',
     $ 7X'SIZE OF',3X'REFERENCE',4X'LIMITS ON THE'/' PROBABILITY',4X
     $ 'SAMPLE',2X'FREQUENCY',3X'EXPECTATION OF C',4X'REFERENCE',2X
     $ 'FREQUENCY',3X'EXPECTATION OF M'/3X'PERCENT',6X'SPACE',7X'C',8X
     $ 'LOWER',4X'UPPER',7X'SPACE',8X'M',8X'LOWER',4X'UPPER',3X
     $ 'CASE DESCRIPTION'/)
111   READ(5,113) PCCONF,C,SIZE1,SIZE2,LABEL
113   FORMAT(4F5.0,6A6)
      IF(PCCONF.GE.99999.) STOP
      ALPHA=(100-PCCONF)/200
      RNU=2*C
      LCL1=CHIOFP(1-ALPHA,RNU)/2
      RNU=2*(C+1)
      UCL1=CHIOFP(ALPHA,RNU)/2
      FACTOR=SIZE2/SIZE1
      RMEAN=FACTOR*C
      LCL2=FACTOR*LCL1
      UCL2=FACTOR*UCL1
      WRITE(6,121) PCCONF,SIZE1,C,LCL1,UCL1,SIZE2,RMEAN,LCL2,UCL2,LABEL
121   FORMAT(4XF5.2,4XF8.2,2XF9.3,2X,2(F8.3,1X),3XF8.2,3XF9.3,2X,
     $ 2(F8.3,1X),6A6)
      GOTO 111
      REAL FUNCTION CHIOFP(P,RNU)
C CHIOFP COMPUTES AN APPROXIMATE VALUE OF CHI-SQUARE FOR GIVEN PROBABILITY
C P (INTEGRAL FROM CHISQUARE TO INFINITY) AND DEGREES OF FREEDOM RNU.
C RNU SHOULD NOT BE LESS THAN 30. FROM HANDBOOK OF MATHEMATICAL FUNCTIONS,
C NBS APPLIED MATH. SERIES 55, 26.4.17
```

```
      CHIOFP=-1.
      IF(P.LE.0.OR.P.GE.1) RETURN
      CHIOFP=RNU*(1-2/(9*RNU)+XOFP(P)*SQRT(2/(9*RNU)))**3
      RETURN
      REAL FUNCTION XOFP(P)
C XOF P COMPUTES AN APPROXIMATE VALUE OF THE STANDARDIZED NORMAL DEVIATE
C X AS A FUNCTION OF THE PROBABILITY P (0 LT P LE 0.5 AND P IS THE AREA
C UNDER THE NORMAL DENSITY CURVE TO THE RIGHT OF X), FROM HANDBOOK OF
C MATHEMATICAL FUNCTIONS, NBS APPLIED MATH, SERIES 55, 26.2.23 (HASTINGS)
      XOFP=999.
      IF(P.LE.0.OR.P.GE.1) RETURN
      P1=P
      IF(P.GT.0.5) P1=1-P
      T=SQRT(ALOG(1/(P1*P1)))
      XOFP=T-((2.515517+.802853*T+.010328*T*T)/(1+1.432788*T+.189269*T*T
     $ +.001308*T*T*T))
      IF(P.GT.0.5) XOFP=-XOFP
      RETURN
      END
*XQT
95.  93.  1.44 1.   CHRYSO, 2113, STAND
95.  64.  .72  1.   CHRYSO, 2121, STAND
95.  209. 2.16 1.   CHRYSO, 2132, STAND
99999
```

APPENDIX D

OPTIMIZED METHOD FOR MEASUREMENT OF AIRBORNE ASBESTOS CONCENTRATIONS

PROVISIONAL METHODOLOGY

Short Form

(1) Collect an air sample on a Nuclepore filter, pore size 0.4 µm, using a high-volume or personal samplers.

(2) Coat filter portion with about 40 nm thick carbon film using a vacuum evaporator.

(3) A 60 or 100 mesh stainless steel mesh is placed on top of a filter paper stack or form sponge contained in a petri dish. Chloroform is carefully poured into the petri dish until the level is just touching the stainless steel mesh. A 2.3 mm diameter (or 1 mm x 2 mm) portion of carbon coated filter is put particle side down on a 200 mesh carbon coated copper electron microscope grid and this pair placed on the steel mesh. The 2.3 mm diameter (or 1 mm x 2 mm) portion is wetted with a 5 µℓ drop of chloroform. The Nuclepore will be dissolved away in 24 to 48 hours. Chloroform may be added to maintain the level in the petri dish.

(4) Examine the EM grid under low magnification TEM to determine its suitability for high magnification examination. Assertain that the loading is suitable and is uniform, that a high number of grid openings are intact, and that the sample is not contaminated.

(5) Systematically scan the EM grid at a magnification of 20,000X (screen magnification 16,000X). Record the length and breadth of all particles observed if they have an aspect ratio of 3:1 or greater and substantially parallel sides. Observe the morphology of the fiber using the 10X binocular and note whether a tubular structure characteristic of chrysotile asbestos is present. Switch into SAED mode and observe the diffraction pattern. Note whether the pattern is typical of chrysotile or amphibole asbestos, or whether it is ambiguous, or neither chrysotile or amphibole.

(6) Count 100 fibers in several grids squares, or alternatively count all fibers in at least 10 grid squares. If more than 300 fibers are observed in one grid square, then a more lightly loaded filter sample should be used. If no other filter sample can be obtained, the available sample should be transferred onto a 400 mesh grid. Processing of the sample using ashing and sonification techniques should be avoided wherever possible.

(7) Fiber number concentration is calculated from the following

$$\text{Fibers/m}^3 = \frac{\text{Fiber Count}}{\text{No. Fields Counted}} \cdot \frac{\text{Total Filter Area}}{\text{Area of a Field}} \cdot \frac{1}{\text{Volume of Air Sampled}}$$

Fiber mass for each type of asbestos is calculated by assuming that the breadth measurement is a diameter, thus the mass can be calculated from

$$\text{Mass }(\mu\text{m}) = \frac{\pi}{4}\text{ length }(\mu\text{m}) \cdot [\text{diameter }(\mu\text{m})]^2 \cdot \text{density }(\text{g/cm}^3)\ 10^{-6}$$

The density of chrysotile is assumed to be 2.6 g/cm^3, amphibole 3.0. The mass concentration for each type of asbestos is then

$$\begin{array}{l}\text{Mass Concentration}\\ (\mu\text{g/m}^3)\text{ of a Particular}\\ \text{Type of Asbestos}\end{array} = \frac{\text{Total Mass of All Fibers of That Type }(\mu\text{g})}{\text{Volume of Air Sampled }(\text{m}^3)}$$

(8) Other parameters characterizing the asbestos fibers are:

(a) Length and width distributions of chrysotile fibers.

(b) Volume distribution of chrysotile fibers.

(c) Fiber concentration of other types of asbestos species.

(d) Relative proportion of chrysotile fibers with respect to total number of fibers.

APPENDIX E

ESTIMATING CHRYSOTILE MASS ON AIR FILTERS USING NEUTRON ACTIVATION TECHNIQUE

IITRI
IIT Research Institute
10 West 35 Street, Chicago, Illinois 60616
312/567-4000

March 22, 1977

Dr. Arthur Morgan
Environmental and Medical Sciences Div.
Building 551
AERE Harwell, Oxfordshire
OX11 ORA
England

Dear Dr. Morgan:

Pursuing the telephone conversation of Dr. Harwood with you on 18 March, I have prepared a few Nuclepore membranes for analyzing chrysotile by neutron activation. The samples are as follows:

Sample No.	Area of Membrane
142	4-1/4" x 6"
154	4-1/4" x 4-3/4"
2	8" x 10" (Blank)
4	8" x 10" (Blank)

Transmission electron microscopic study of sample 142 gave us an estimate of about 0.07 μg/cm^2. Since I am providing 4-1/4" x 6" area of this membrane, I hope there is enough mass of chrysotile for an accurate measurement by neutron activation. I am also enclosing a sample of asbestos used for preparing the membrane samples.

Please analyze these samples at your earliest and bill us.

Yours very truly,

AVSamudra

Anant V. Samudra
Research Scientist

AVS/eb
encl.

HARWELL

Environmental and Medical Sciences Division, B551
AERE Harwell, Oxfordshire
OX11 0RA
Tel: Abingdon (0235) 24141 Ext. 4622
Telegrams: Aten, Abingdon
Telex 83135

Date 31st May 1977

AS
c635 file

Dr C F Harwood
IIT Research Institute
10 West 35 Street
Chicago
Illinois
USA

Dear Colin

We have attempted to assess the amount of chrysotile on the membrane filter samples you sent using neutron activation analysis. Unfortunately, however, the amount of chromium on the blank filters is sufficient to prevent an accurate determination of fibre at the level required, using the $^{50}Cr(n\gamma)^{51}Cr$ reaction. I have discussed the possibility of using infra-red analysis with people in our analytical group and they do not feel that measurements can be made at the level required using this technique either.

There will of course be no charge for this work but I should point out that £600 is still outstanding for our work on the fibre loaded filters. I understand that Dr Hearsey of our Marketing and Sales Department has written to you about this.

With best regards

Yours sincerely

A Morgan

APPENDIX F

X-RAY FLUORESCENCE ANALYSIS OF STANDARD SAMPLES OF CHRYSOTILE

An independent means for measuring the mass concentration of asbestos in filter-deposited samples is needed if such samples are to be useful in determining the accuracy of mass concentration estimates made by electron microscopy.

Air sample 154, used in the inter-laboratory comparisons of the provisional optimal procedure, consisted of high purity chrysotile deposited on Nuclepore filters in an aerosol chamber. X-ray fluorescence (XRF) analysis of these deposits for Mg provided a convenient, independent and non-destructive means for determining the mass concentrations of chrysotile on these filters.

The XRF measurements were carried out at the EPA Environmental Sciences Research Laboratory (Research Triangle Park, North Carolina) with a simultaneous multiwavelength spectrometer (Siemens MRS-3) adapted for air pollution samples using procedures described by Wagman [65]. Fluorescence intensities above background of the Mg K_α line were measured using 1000-second counting intervals. The calibration standard consisted of a vacuum-evaporated film of Mg deposited at a concentration of 47 $\mu g/cm^2$ on mylar film. The Mg K_α sensitivity was 70.73 cps per $\mu g/cm^2$ and the minimum detectable limit for a 1000-second count, on the basis of 3σ above background, was 1 ng/cm^2.

Precision analysis of a series of XRF measurements of chrysotile deposits indicated a relative standard deviation of less than 4 percent. Particle size and other fluorescence attenuation correction factors were not needed because EM examination of chrysotile deposits showed that all fibers had diameters under 0.1 μm with only rare instances of fiber overlap. The method of computation is illustrated as follows.

SAMPLE CALCULATION METHOD

Method: Measurement of Mg by XRF using Siemens MRS-3

Chrysotile Concentration = 3.8 x Mg Concentration

Magnesium: Standard Vacuum evaporated Mg on Mylar and uniform Mg conc. of 47 μg/cm^2

S_{Mg} (Mg sensitivity) = 70.7315 counts/sec/μg/cm^2

N_B (Nuclepore background) = 640 counts/1000 seconds

$$\text{Minimum Detection Limit for 1000 sec counting} = \frac{3\sqrt{N_B}}{S_{Mg} \times 1000}$$

$$= 0.00107\ \mu g/cm^2$$

MEASUREMENTS ON NUCLEPORE FILTER 154

Measurement	Counts/sec-blank	μg Mg/cm^2
1	0.980	0.0139
2	1.022	0.0144
3	1.019	0.0144
4	1.076	0.0152
5	1.017	0.0144
6	1.090	0.0154

Mean = 0.0146 μg Mg/cm^2

Standard Deviation = 0.00057 μg Mg/cm^2

Relative Std. Dev. = 100 x (Std. Dev)/Mean = 3.9%

Particle size correction factor, $(1 + ab)^2$, is very small (within Std. Dev.) and hence neglected.

Assuming all Mg is in chrysotile form, and that Chrysotile Mass Concentration = 3.8 x Mg Concentration

Chrysotile Mass Conc. = 3.8 x (0.0146 $\pm$ 0.00057) μg/cm^2

= 0.0555 $\pm$ 0.0022 μg/cm^2

Total Volume of Air Sampled = 9.2 m^3

Total Filter Area = 406.5 cm^2

Air Volume/cm^2 of Filter = 0.02263 m^3/cm^2

$$\text{Chrysotile Mass Conc. in Air Sampled} = \frac{0.0555 \pm 0.0022}{0.02263}$$

$$= (2.452 \pm 0.096)\ \mu g/m^3$$

The X-ray fluorescence measurements of chrysotile are summarized in Table F-1.

Table F-1

MEASUREMENT OF CHRYSOTILE MASS
CONCENTRATIONS BY XRF
ANALYSIS FOR MAGNESIUM

	Mg Conc.	Chrysotile Conc.*	
Sample No.	$\mu g/cm^2$	$\mu g/cm^2$	$\mu g/m^3$
154	0.0146	0.0555	2.452
142 C	0.0117	0.0445	1.966
154 A	0.0111	0.0422	1.865
154 B	0.0108	0.0410	1.812
168 D	0.0120	0.0456	2.015

* A chrysotile/Mg factor of 3.8 was used. The aerosol volume sampled per unit filter area was 0.02263 m^3/cm^2.